



National Library
of Canada

Acquisitions and
Bibliographic Services Branch

395 Wellington Street
Ottawa, Ontario
K1A 0N4

Bibliothèque nationale
du Canada

Direction des acquisitions et
des services bibliographiques

395, rue Wellington
Ottawa (Ontario)
K1A 0N4

Number: 1-800-953-6666

Quelle: Notre référence

NOTICE

The quality of this microform is heavily dependent upon the quality of the original thesis submitted for microfilming. Every effort has been made to ensure the highest quality of reproduction possible.

If pages are missing, contact the university which granted the degree.

Some pages may have indistinct print especially if the original pages were typed with a poor typewriter ribbon or if the university sent us an inferior photocopy.

Reproduction in full or in part of this microform is governed by the Canadian Copyright Act, R.S.C. 1970, c. C-30, and subsequent amendments.

AVIS

La qualité de cette microforme dépend grandement de la qualité de la thèse soumise au microfilmage. Nous avons tout fait pour assurer une qualité supérieure de reproduction.

S'il manque des pages, veuillez communiquer avec l'université qui a conféré le grade.

La qualité d'impression de certaines pages peut laisser à désirer, surtout si les pages originales ont été dactylographiées à l'aide d'un ruban usé ou si l'université nous a fait parvenir une photocopie de qualité inférieure.

La reproduction, même partielle, de cette microforme est soumise à la Loi canadienne sur le droit d'auteur, SRC 1970, c. C-30, et ses amendements subséquents.

Canada

THE UNIVERSITY OF ALBERTA

Numerical Modeling of Seismic Waves in 2D inhomogeneous
Structures Using Asymptotic Ray theory

by

Hu-shun Zhou



A thesis submitted to the Faculty of Graduate studies and Research in partial
fulfillment of the requirements for the degree of Master of Science.

in

Geophysics

Department of Physics

Edmonton, Alberta

Spring 1996



National Library
of Canada

Acquisitions and
Bibliographic Services Branch

395 Wellington Street
Ottawa, Ontario
K1A 0N4

Bibliothèque nationale
du Canada

Direction des acquisitions et
des services bibliographiques

395, rue Wellington
Ottawa (Ontario)
K1A 0N4

Your file *Votre référence*

Our file *Notre référence*

The author has granted an irrevocable non-exclusive licence allowing the National Library of Canada to reproduce, loan, distribute or sell copies of his/her thesis by any means and in any form or format, making this thesis available to interested persons.

L'auteur a accordé une licence irrévocable et non exclusive permettant à la Bibliothèque nationale du Canada de reproduire, prêter, distribuer ou vendre des copies de sa thèse de quelque manière et sous quelque forme que ce soit pour mettre des exemplaires de cette thèse à la disposition des personnes intéressées.

The author retains ownership of the copyright in his/her thesis. Neither the thesis nor substantial extracts from it may be printed or otherwise reproduced without his/her permission.

L'auteur conserve la propriété du droit d'auteur qui protège sa thèse. Ni la thèse ni des extraits substantiels de celle-ci ne doivent être imprimés ou autrement reproduits sans son autorisation.

ISBN 0-612-10774-4

Canada

THE UNIVERSITY OF ALBERTA

LIBRARY RELEASE FORM

Name of Author: Hu-shun Zhou

Title of Thesis: Numerical Modeling of Seismic Waves in 2D inhomogeneous Structures
Using Asymptotic Ray Theory

Degree: Master of Science

Year of this Degree Granted: 1996

Permission is hereby granted to the University of Alberta Library to reproduce single copies of this thesis and to lend or sell such copies for private, scholarly, or scientific research purposes only.

The author reserves all other publication and other rights in association with the copyright in the thesis, and except as hereinbefore provided, neither the thesis nor any substantial portion thereof may be printed or otherwise reproduced in any material form whatever without the author's prior written permission.

Hu-shun Zhou

Permanent Address:

No 3, 9722-104 Street

Edmonton, Alberta

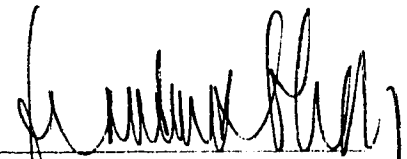
Canada, T5K 0Y7

Dated: April 10, 1996

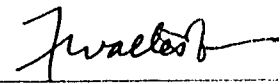
THE UNIVERSITY OF ALBERTA

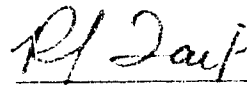
FACULTY OF GRADUATE STUDIES AND RESEARCH


The undersigned certify that they have read, and recommend to the Faculty of Graduate Studies and Research for acceptance, a thesis entitled Numerical Modeling of Seismic Waves in 2D Inhomogeneous Structures Using Asymptotic Ray Theory submitted by Hu-shun Zhou in partial fulfillment of the requirements for the degree of Master of Science in Geophysics.



Supervisor







Date: November 28, 1995

Acknowledgments

I wish to thank sincerely Dr. F. Hron for his suggestion of these topics and for his guidance and advice throughout the work. I appreciate the fact that he allowed me to use and modify some of his computer program and some of his student: Mr. Albert Choi and Dr. Larry W. Marks' research work.

I am grateful to Mr. Jeremy Gallop for helpful discussion and for providing some suggestion of editing the thesis.

The author was supported by University of Alberta during the course of this research.

Abstract

The seismic wave propagation in laterally inhomogeneous media is most important in current geophysical community. To provide the low cost of computation and the ability to associate individual events on synthetic seismograms with particular paths of energy propagation (ray paths), asymptotic ray theory is well suited for this purpose.

However, the asymptotic ray theory has its limitations. It is not applicable in the vicinity of singular points such as caustics and critical points.

The aim of this thesis is to develop a fast and accurate ray tracing method applicable to numerical modelling of seismic body waves in laterally inhomogeneous media with curved interfaces and to extend the applicability of asymptotic ray theory to include the effects of caustics. The travel time, amplitude—distance curves are computed for several complex models.

TABLE OF CONTENTS

CHAPTER	PAGE
1. GENERAL INTRODUCTION	1
2. RAY TRACING BY CIRCULAR APPROXIMATION	4
2.1 Introduction	4
2.2 Ray tracing by circular approximation without interfaces	5
2.3 The effect of an interface	11
2.4 Conclusions: Accuracy and Stability	15
3. RAY AMPLITUDE	21
3.1 Introduction	21
3.2 Differential equation solution for ray amplitudes	21
3.3 Computation of geometrical spreading by dynamic ray tracing	26
3.4 The behavior of an interface	29
3.5 Ray amplitude by circular approximation	33
3.6 Numerical tests	38
4. RAY AMPLITUDE IN THE VICINITY OF A CAUSTIC	41
4.1 Introduction	41
4.2 Airy approximation	41
4.3 Modified airy approximation	46
5. NUMERICAL RESULTS	54
5.1 Introduction	54
5.2 Cerveny's model	54

5.3 A laterally inhomogeneous medium	59
5.4 Bohemian Massif	67
5.4 Conclusions	82
REFERENCE	83
Appendix A Approximation of interfaces by a parabolic spline	88
Appendix B Ray amplitudes using the wave method	91

LIST OF TABLES

TABLE		PAGE
2.1	Results of ray tracing and the analytical solution for $V(z)=6.+0.1z$	17
2.2	Results for general inhomogeneous media from different methods	17
3.1	Geometrical spreading calculated by DRT and the analytical method	28
3.2	The amplitude for converted waves calculated by different methods	38
5.1	The second derivative at a caustic calculated by different methods	54
5.2	The comparsion of P rays computed by different methods	67
5.3	Rays in Bohemian Massif divided by different cell sizes	68

LIST OF FIGURES

FIGURE	PAGE
2.1 Labeling of points used in two-dimensional interpolation	6
2.2 Symbols and geometry used to compute raypaths by circular approximation	9
2.3 Approximation of interfaces using parabolic spline	12
2.4 Approximation of interfaces using cubic spline (de Boor)	13
2.5 Approximation of interfaces using cubic spline (Forsythe)	14
2.6 a Ray diagram with cell size 10×5 km for model $v(z)=6+0.1z$	16
2.6 b Ray diagram with cell size 0.25×0.25 km for model $v(z)=6+0.1z$	16
2.7 Rays in a generally inhomogeneous medium	19
2.8 Ray diagram with buried source	20
3.1 Elementary ray tube between wave fronts at $\tau = t_0$ and τ .	23
3.2 Explanation of various symbols for a ray in a medium with an arbitrary number of interfaces which may not be plane. The ray paths may be curved.	31
3.3 Geometry of the ray tube at source and receiver.	34
3.4 Numerical and analytical geometrical spreading for model $v(z)=6. +0.1z$	37
3.5 Ray diagram of wave S1P2P2S2S2S2P2P2S2P2S1	39
4.1 Ray character of a vertically inhomogeneous medium	42
4.2 A graph of Airy function	47
4.3 Poles, branch cuts, saddle points and contours on the s-plane for the integral 4.14	49
4.4 The focusing point of the wave P1P1 generated by a circle interface	52
4.5 The focusing point of the wave P1S1 generated by a circle interface	53

5.1	Cerveny's model to investigate a caustic at surface	56
5.2	Ray diagram and travel time–distance curve for Cerveny's model	57
5.3	Amplitude–distance curves calculated by different methods	58
5.4	Amplitude–distance curves calculated by different methods	59
5.5	Ray diagram for medium with curved interface and homogeneous layers	61
5.6	A laterally inhomogeneous model	62
5.7	Ray diagram for this laterally inhomogeneous medium	63
5.8	Travel time–distance curve	64
5.9	Ray amplitude of vertical component calculated by the ray method	65
5.10	Ray amplitude of vertical component calculated by the modified Airy approximation	66
5.11	P-wave isovelocity contour of the Bohemian Massif	69
5.12	Ray diagram of reflected and refracted P wave with source at 155.2 km	70
5.13	a) Ray diagram with cell size $0.5 \times 0.25 Km$ b) Ray diagram with size $4 \times 1 Km$	71
5.14	Travel time -distance curve	72
5.15	Ray amplitudes calculated by ray method	73
5.16	Ray amplitude near caustics calculated by the modified Airy approximation	74
5.17	One ray branch with negative $\partial^2 r / \partial p^2$ for one of the caustics	75
5.18	Another ray branch with positive $\partial^2 r / \partial p^2$ for the caustic	76
5.19	Travel time - distance curve of the caustic	77
5.20	Amplitude - distance curve calculated by the ray method and the modified Airy approximation	78
5.21	Ray diagram with the take-off angle ranging from 74.60° to 81°	79
5.22	Travel time -distance curve for ray between 74.60° to 81°	80
5.23	Amplitude - distance curve calculated by our ray method	81

Chapter 1 General Introduction

One of the basic problems of theoretical seismology and seismic prospecting is the computation of seismograms for inhomogeneous media. At present, various methods can be used to compute the seismograms.

It is fair to say that the elementary theory of those methods falls into two groups. One is a direct computational solution of the elastodynamic equation (the so called full-wave method). The other is based on a ray approach.

For the full wave theory, there are three main computational methods. The first is the Cagniard inversion and its extension by Chapman (1976) in the time domain. The second includes double integration over real slowness and real frequency. It includes the reflectivity method (Fuchs and Muller, 1971) that is directed toward the computation of waves within a medium composed of very many homogeneous layers. It is based on the matrix method (Haskell, 1953) for homogeneous layers and extended by Gilbert and Backus (1966) for continuously varying media. The third also uses double integration but the integration is over real or complex slowness and real frequency. In its high frequency domain, approximate method called WKBJ seismogram can be derived by this method although the WKBJ can be considered a ray-based method. In this thesis, it will be used to derive the amplitude in the vicinity of a caustic. The other method was proposed by Alekseev and Mikhailenko (1980) and could produce highly accurate seismogram for vertical inhomogeneous media. If properly applied, these methods can give a total solution including reflected, refracted, diffracted and head waves. However, when using the above methods to calculate the wave amplitude for complex media, a numerical method must be employed since an analytical solution to the equations is unknown and hence vast amounts of CPU time are needed. Furthermore, no identification of particular phase can be made on the resulting synthetic seismograms. For this purpose, one can use ray theory.

The single most successful method for modelling seismic waves to investigate the Earth's internal structure is ray theory, which interprets the short-period body-waves (Aki and Richards 1980). The basic tenets of ray theory were developed by Babich and Alekseev (1958) in the Soviet Union and Karal and Keller (1959) in America. This ray theory is powerful in that it can be applied to the elastodynamic equation in general inhomogeneous media. Attempts to use ray theory for the calculation of the amplitude of body-wave arrivals have been made by many researchers. These include asymptotic methods ranging in complexity and accuracy (Wesson 1970, Hron and Kanasevich 1971, Chapman 1971, Cerveny, Molotkov and Psencik 1977, Cerveny and Hron 1980, Clarke 1993) through WKBJ (Chapman 1978) and Maslov (Chapman and Drummond 1982) to the highly accurate generalized ray method (Hemburg and Harkrider 1979). Using those methods, the ray amplitude can be obtained successfully. However, these papers show that the geometrical spreading function can be an exceedingly sensitive function of the velocity gradients. It is at this stage that one clearly recognizes the limitations in applying the ray theory to the interpretation of seismic data. The problem is a breakdown of the ray theory itself at a caustic where the geometrical spreading tends to zero, and also in shadow zones where rays can not penetrate according to Snell's law. In those areas, the classical ray theory is no longer applicable and some other methods must be employed.

The classical theories of computing ray paths for seismic energy fall into one of two categories. One of these consists of a variational approach of Fermat's Principle (i.e. the so called Bending Method by Julian and Gubbins 1977). Another method consists of numerically solving a system of first order differential equations. Various authors (Chen and Ludwig 1972, Psencik 1972, Green 1976 and White 1978) have used different approaches to arrive at these equations. But all of the above methods cannot avoid the disadvantages stated above.

Recently, to overcome the inability to handle the missing of some raypaths in complicated velocity structure, Marks and Hron (1978) changed the cell model into a model

consisting of grids with constant velocity gradients by smoothing the velocity of the cell model. Vidale (1988). Asakawa et al (1993) made use of the finite difference method to solve the eikonal equation which started a new era of ray tracing. Morse (1989, 1991) and Saito (1989) proposed a ray tracing method based on Huygens' principle. However, most of those methods assume a constant velocity in each cell and have difficulty producing curved raypaths. Also, many of them cannot handle the model which the velocity gradient changes sharply.

In this thesis, some techniques and numerical results related to asymptotic ray theory are presented. A ray tracing method (Marks and Hron 1978) is proposed in Chapter 2. Some improvement of this method enable it to trace rays more efficiently and accurately. Similar techniques were developed independently by Gebrande (1976), Aric and Gutdeutsch (1978) and Marks (1980). All of these techniques require the approximation of the isovelocity lines of the medium.

To find geometrical spreading, and hence the ray amplitude, one must solve a set of differential equations (Cerverny et al 1974). However, this requires vast amounts of computer time and furthermore, as stated above, the ray theory is not applicable in the vicinity of a caustic. Chapter 3 will propose an analytical method (personal communication with Dr. Hron) and a numerical method to calculate the ray amplitude based on our ray tracing scheme. To calculate the amplitude in the vicinity of a caustic, a method called the modified Airy approximation will be used and incorporated into our ray tracing program.

In Chapter 5, some numerical and real models are investigated by our ray tracing scheme. The accuracy and stability of this method are also discussed by comparing its results with analytical solution or other reliable methods.

Chapter 2 RAY TRACING BY CIRCULAR APPROXIMATION

2.1. Introduction

As described in Chapter 1, there are many ray tracing methods for two-dimensional media with curvilinear boundaries. The following will briefly introduce the differential equation method and propose an efficient approximation.

Ray paths for seismic energy may be computed by solving a system of first order differential equations. In two-dimensional media with a point source, three differential equations must be solved for the coordinates of the endpoint of the ray, $(x(t), z(t))$, and the angle that the rays makes with the vertical, $\theta(t)$, as a function of ray travel time t . Following Psencik (1972), these may be written as,

$$\frac{d}{dt} \begin{bmatrix} x \\ z \\ \theta \end{bmatrix} = \begin{bmatrix} V \sin(\theta) \\ V \cos(\theta) \\ V_z \sin(\theta) - V_x \cos(\theta) \end{bmatrix} \quad 0 \leq \theta < 2\pi \quad (2.1)$$

Where $V(x,z)$ is the velocity (P or S wave) at the point (x,z) . V_x , V_z are its spatial derivatives.

The initial conditions:

$$x(0)=x_0, \quad z(0)=z_0, \quad \theta(0) = \theta_0$$

are necessary to solve above equations. Here (x_0, z_0) is the source location and θ_0 is the take-off angle. Note that the positive z axis is generally taken to point into the Earth from the free surface and θ is measured counter-clockwise from negative z axis to the tangent of the ray path.

To solve equation (2.1), the velocity field and its spatial derivatives must be known everywhere of the medium . However, due to the difficulty in finding a function which reasonably approximate the true velocity-position relationships in complex media, the input velocities are often specified on a rectangular grid rather than as analytical expressions. So, some numerical interpolation methods (such as linear interpolation and cubic interpolation) are needed to determine the velocity and its derivatives within any rectangular cell of the grid, although this might introduce some errors.

One must take into account the effect of geological curvilinear interfaces where the ray directions change discontinuously, when solving equation (2.1). It will be further discussed later.

Generally, solving matrix equation (2.1) will give us ray paths which can be considered to be correct; however, it has one serious drawback. This is the extremely large amount of CPU time needed to solve the differential equations within a reasonable degree of accuracy. The severity of this will be worsen when one computes synthetic seismograms for which very many rays are needed. Seeing that, an efficient and fast ray tracing method was originally proposed by Marks & Hron (1980), and has been now improved by the author.

2.2 Ray Tracing By Circular Approximation without interface

In this section, a ray tracing method(Marks and Hron, 1978) is proposed. Some improvements have been made that enable it to trace rays more efficiently and accurately. It also has the potential to extend to three dimensions. The difference between the original and new one will be discussed later in this chapter.

This method is formulated for a 2D rectangular block method specified in an Cartesian coordinate system with x oriented horizontally and z vertically downward and calculation of traveltimes and ray paths are carried out on the rectangle boundaries (the

calculation of the inner points of the block is also easily performed). The ray paths within the rectangle are straight lines for a homogeneous block and circular arcs for an inhomogeneous block. It implies that if the velocity field $V(x,z)$ within one small rectangular region of the model is approximated by

$$V(x,z) = V_0(x_0,z_0) + \nabla V \cdot d\vec{r} \quad (2.2)$$

where V_0 and ∇V are constant in this small region, then the ray endpoint location on the block boundaries can be found as a function of travel time.

Considering an elastic isotropic medium whose velocity field $V(x,z)$ is specified by velocities given on the nodal points of a rectangular grid. A point source of harmonic waves is placed somewhere within the medium, say at (x_s, z_s) . Another set of coordinate axes parallel to the original global coordinates and with the origin at the source is defined as local coordinates. Employing the velocities at the four corner points of the block $V_i, i = 1, 2, 3, 4$ (Figure 2.1), one can compute a linear mapping

$$V(x,z) = Ax + Bz + C \quad (2.3)$$

by making use of two dimensional interpolation.

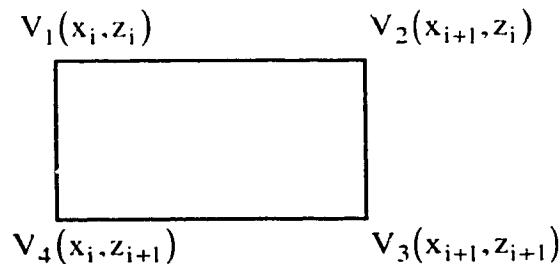


Fig. 2.1 Labeling of points used in the two-dimensional interpolation

The simplest interpolation in two dimensions is bilinear interpolation on the grid square (Numerical Recipes, 1992). Its formulae are

$$\begin{aligned}
v &\equiv (x - x_i)/(x_{i+1} - x_i) \\
u &\equiv (z - z_i)/(z_{i+1} - z_i)
\end{aligned}
\tag{2.4}$$

(so that v and u each lie between 0 and 1), and

$$V(x, y) = (1 - v)(1 - u)V_1 + v(1 - u)V_2 + vuV_3 + (1 - v)uV_4
\tag{2.5}$$

To find (2.2) at the center (x_c, z_c) of the block, we have

$$\begin{aligned}
x_c &= (x_3 - x_1)/2 \\
z_c &= (z_3 - z_1)/2
\end{aligned}$$

and

$$\begin{aligned}
A &= \left. \frac{\partial V(x, z)}{\partial x} \right|_{(x=x_c, z_c)} \\
B &= \left. \frac{\partial V(x, z)}{\partial z} \right|_{(x=x_c, z_c)} \\
C &= V(x_c, z_c) - Ax_c - Bz_c
\end{aligned}
\tag{2.6}$$

For each block, the local coordinate origin is set at the ray entry point.

As the interpolating point moves from grid square to grid square, the interpolation function value changes continuously.

After obtaining the local velocity field given by (2.2), we rotate the axes through an angle ϕ to get velocity which depends on z' only,

$$\phi = -\tan^{-1}\left(\frac{A}{B}\right)
\tag{2.7}$$

Then we can define a set of local, rotated coordinates (x', z') such that

$$\begin{bmatrix} x' \\ z' \end{bmatrix} = \begin{bmatrix} \cos(\phi) & \sin(\phi) \\ -\sin(\phi) & \cos(\phi) \end{bmatrix} \begin{bmatrix} x \\ z \end{bmatrix} \quad (2.8)$$

In Figure 2.2, note that ϕ is positive when measured in the clockwise direction.

In the coordinates (x', z') , the velocity field is given by

$$V(x', z') = V(0, 0) + (A^2 + B^2)^{1/2} z' \quad (2.9)$$

Clearly, it is depth - dependent only.

The analytical expression of seismic raypaths for a medium whose velocity medium is $V(z) = V_0 + kz$ was derived by Nettleton in 1940. Essentially, these ray paths are circular arcs in the (x', z') plane and are defined by

$$\left(x' - \frac{V_0}{k \tan(\theta_0)} \right)^2 + \left(z' + \frac{V_0}{k} \right)^2 = \left(\frac{V_0}{k \sin(\theta_0)} \right)^2 \quad (2.10)$$

where θ_0 is the angle made by the tangent to the ray with the gradient at $(x' = 0, z' = 0)$. $0 \leq \theta_0 < 2\pi$. The travel time T to reach any point (x', z') on the ray path is

$$T = \frac{1}{k} \cosh^{-1} \left[\frac{k^2(x'^2 + z'^2)}{2VV_0} + 1 \right] \quad (2.11)$$

Of course, if $V_1 = V_2 = V_3 = V_4$, the block is homogeneous and the rays degenerate to straight lines.

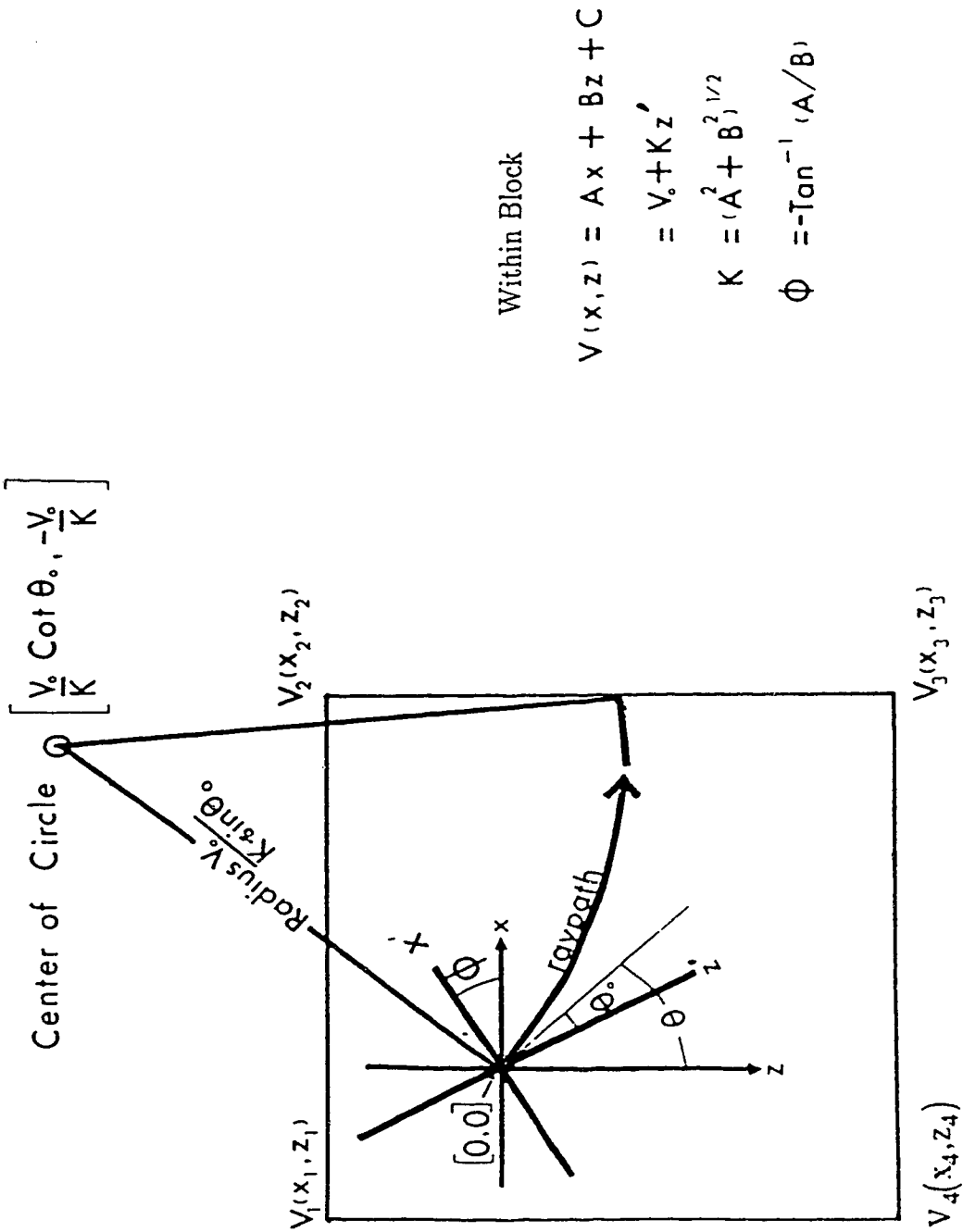


Figure 2.2 Symbols and geometry used to compute raypaths by circular approximation.

Now, the ray can be traced through the block to its exit point. Determination of the exit point is equivalent to the problem of finding the intersection between a circle (equation 2.10) and the boundaries of the current rectangular block where the ray is traveling. Since there may be up to 4 intersection points between circular raypath and the four rectangular boundaries, the criteria for determining the correct exit point are

- 1) those for which the intersection lies within rectangular boundaries
- 2) that travel time from entry point to exit point is minimal.

Then the ray crosses the boundary and enters another adjacent block. Repeating this procedure, the ray travels block by block until stopped at a receiver.

Due to the use of analytical expressions in each rectangular block, this ray tracing method considerably reduces CPU time when compared with the traditional methods. Although, there exist second order interfaces due to using local velocity field which lead to a discontinuous derivative of the ray upon crossing the block boundaries, the effect is usually small, as Section 2.4 of this chapter will demonstrate.

With a velocity field $V(x', z') = V_0 + kz'$ and initial conditions $x(0) = x_0$, $z(0) = z_0$, $\theta(0) = \theta_0$, the differential equations (2.1) take the form,

$$\begin{aligned}
 x'(t) &= \frac{\frac{V_0}{k} \tan\left(\frac{\theta_0}{2}\right)(e^{2kt} - 1)}{1 + ae^{2kt}} \\
 z'(t) &= \frac{V_0}{k} \left(\frac{(1+a)e^{kt}}{1 + ae^{2kt}} - 1 \right) \\
 \theta(t) &= 2 \tan^{-1} \left(e^{kt} \tan\left(\frac{\theta_0}{2}\right) \right) \\
 V(t) &= \frac{V_0(1+a)e^{kt}}{1 + ae^{2kt}}
 \end{aligned} \tag{2.12}$$

where $a = \tan^2\left(\frac{\theta_0}{2}\right)$.

2.3 The Effect of an Interface

The formulae derived in the previous section can be applied only when no interface exists in the medium. If a ray strikes an interface, its kinematics and dynamic properties will be changed discontinuously. The direction of the ray will be changed (reflection or transmission) according to Snell's law and a special treatment is necessary to deal with the interface. Further discussion on the effect of an interface on the ray amplitude will be presented in the next chapter.

If curvilinear interfaces are to be introduced into the model, a numerical method called parabolic spline interpolation (developed by Hron 1973) rather than cubic interpolation is used to approximate the interfaces. To show the advantage of the parabolic spline interpolation, a real model with steeply sloping interfaces is investigated by applying these two methods. Figure 2.3 shows that the parabolic spline approximates the real interface very closely. Figures 2.4 and 2.5 which are both cubic interpolations with different boundary conditions (see Forsythe et al, 1977, de Boor, 1978) show that there are some spurious oscillations at the steeply sloped zone of the interface. Furthermore, using the parabolic spline interpolation to approximate the interfaces makes it simple to compute the interface normal at the point of incidence, and the intersections between ray paths and the interfaces.

The approximation of interfaces by a piecewise continuous parabola is discussed in Appendix A.

If a ray enters a block which contains an interface, the velocity value at any corner point of the block which lies on the other side of the interface must be replaced by extrapolation among the velocities at the points nearest the point in question. If the interface is described as

EPSZ=.10, FACTOR=.1, IN THE PARABOLIC SPLINE

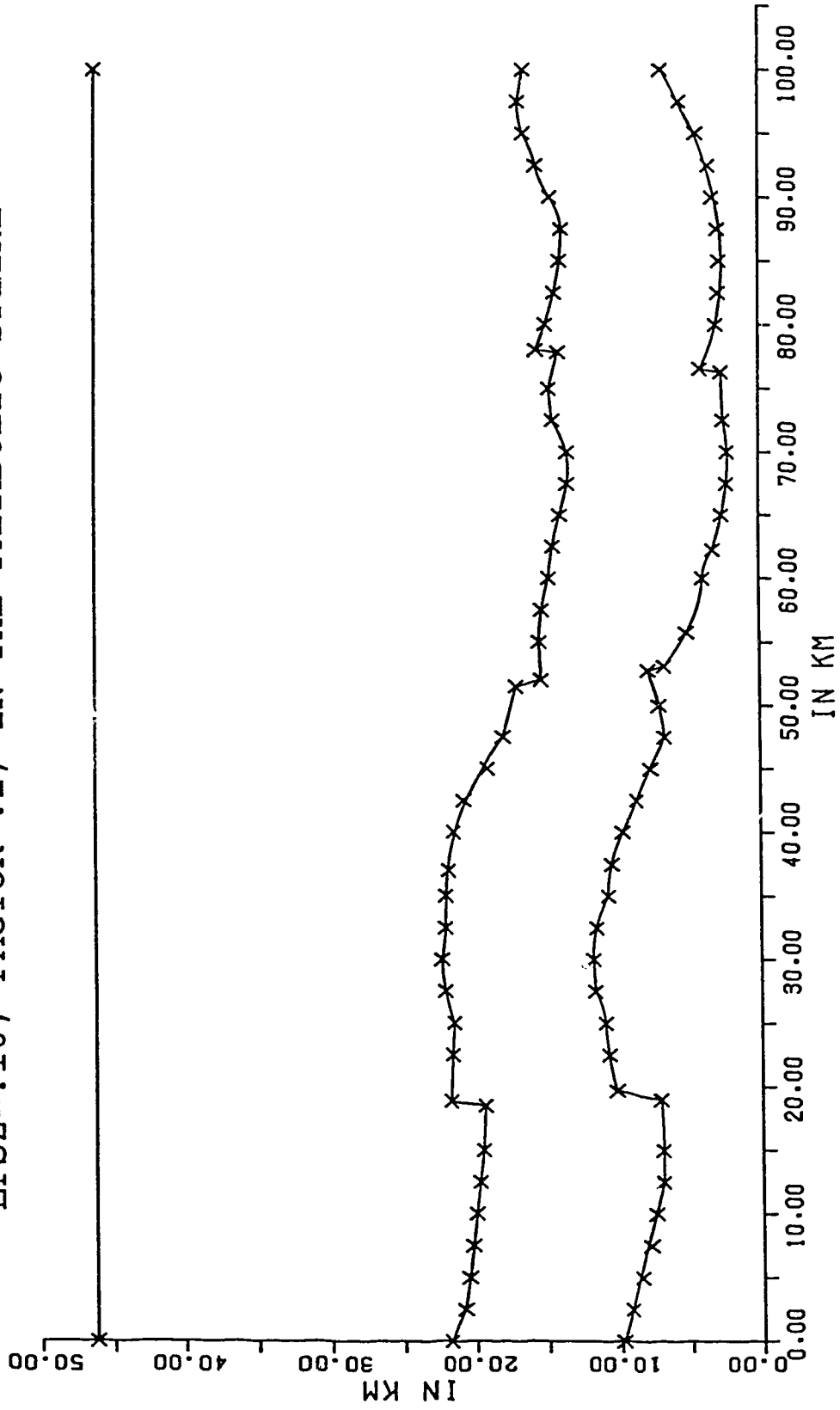


Figure 2.3 Approximation of interfaces using parabolic spline

CUBIC SPLINE INTERPOLATION IN THIS RUN

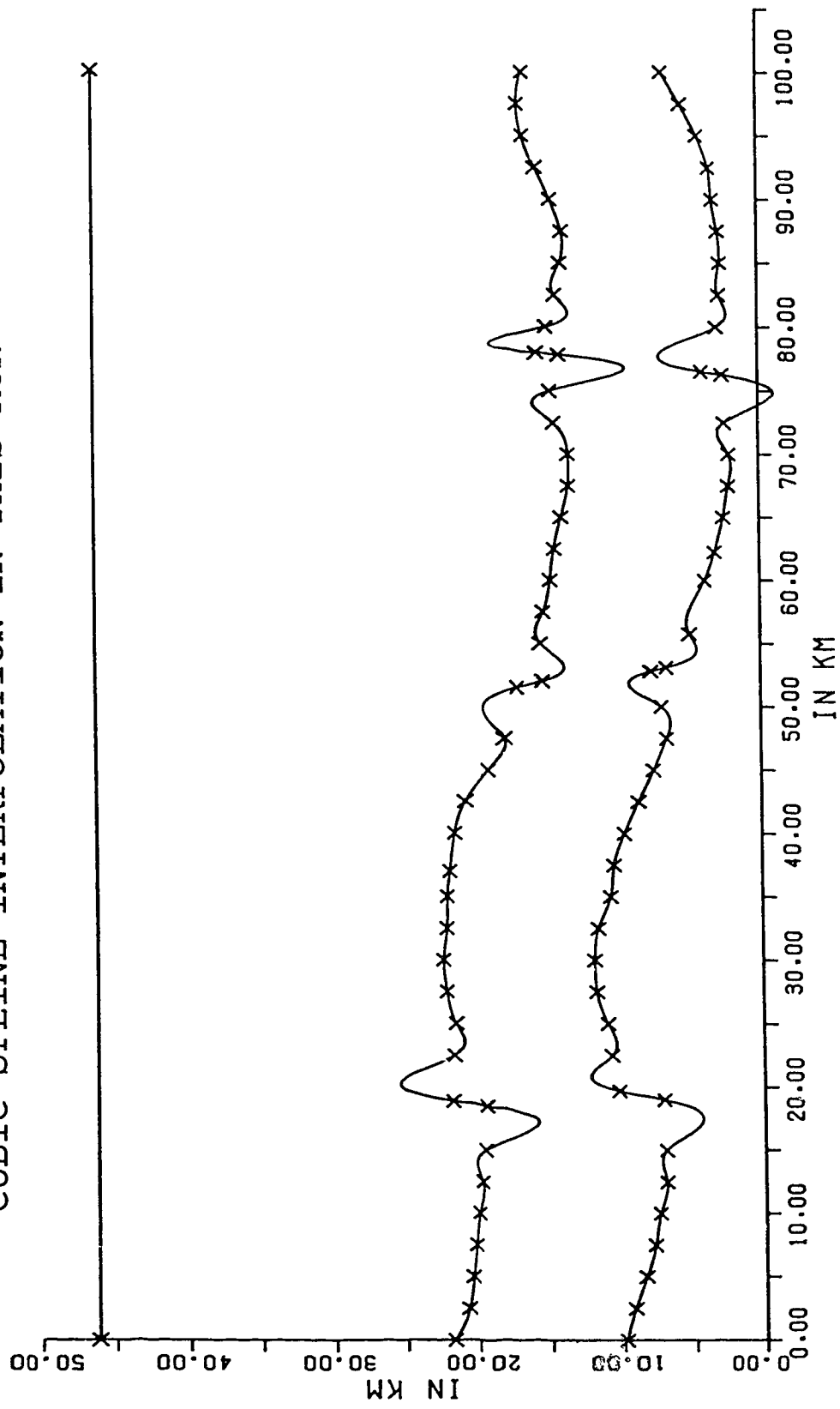


Figure 2.4 Approximation of interfaces using cubic spline (de Boor)

ANOTHER CUBIC SPLINE INTERPOLATION IN THIS RUN

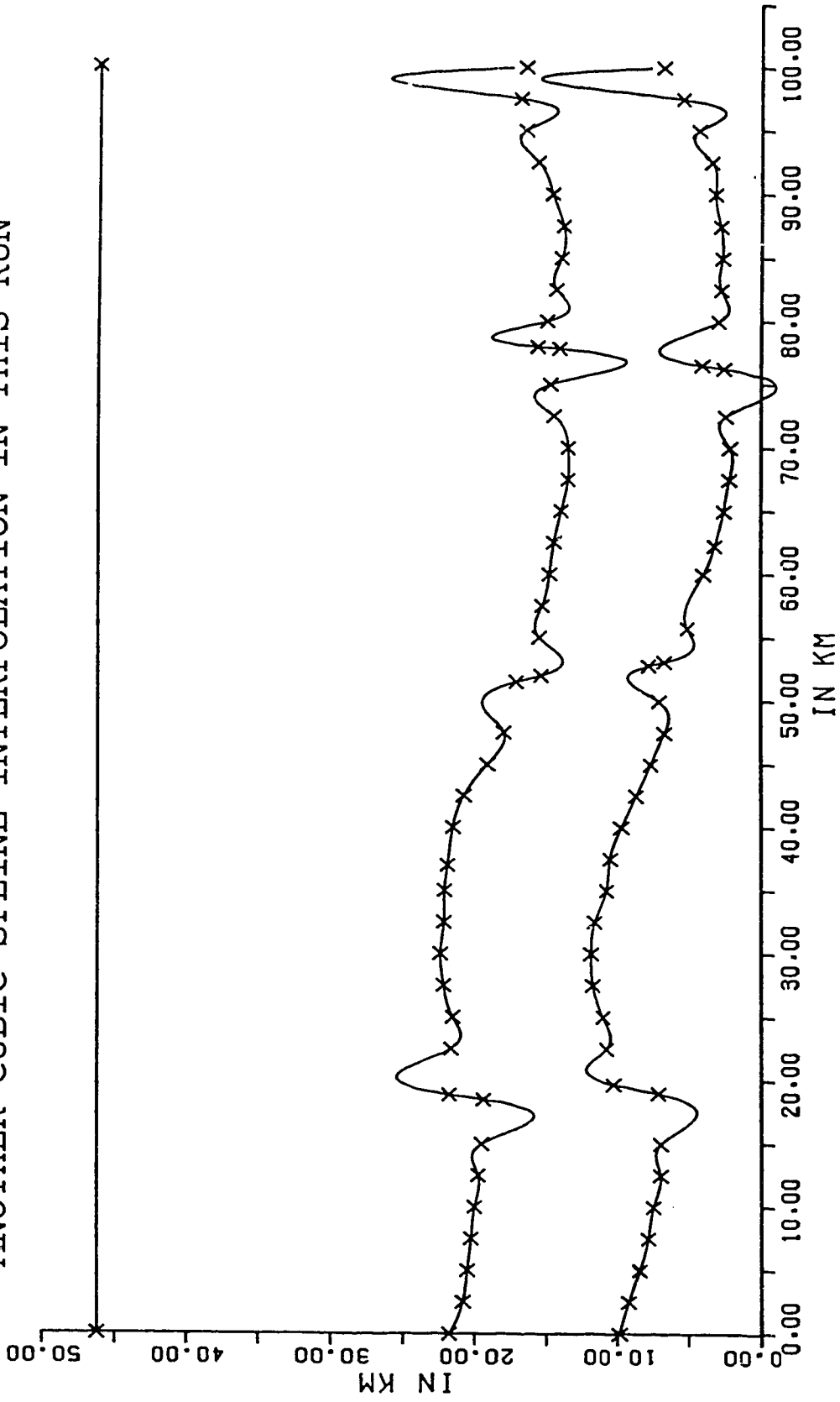


Figure 2.5 Approximation of interfaces using cubic spline (Forsythe)

$z(x) = ax^2 + bx + c$ and the ray path is given by $(x - A)^2 + (z - B)^2 = R^2$, then the points (at most 4) of intersection are the roots of the following fourth degree polynomial

$$a^2x^4 + 2abx^3 + [b^2 + 2a(c - B)]x^2 + 2[b(c - B) - A]x + [A^2 - R^2 + (c - B)^2] = 0$$

This equation can be solved numerically or sometimes analytically. After obtaining the intersection, the criteria for determining the correct exit point either at the block boundaries or at the interface is the same as the last section, i.e., by using the minimum travel time.

2.4 Conclusions: Accuracy and Stability

Here, we shall discuss the accuracy and stability of this method. A comparison between Marks' method (interpolating the velocity function in a triangle) and the new method (interpolating 2-dimensional velocity function in block) will also be conducted.

To evaluate the accuracy and stability of this method, a numerical vertical inhomogeneous model $V(z) = 6.0 + 0.1z$ is used. The model is divided into small rectangles of different sizes which range from $10\text{km} \times 5\text{km}$ to $0.25\text{km} \times 0.25\text{km}$. Figure 2.6(a) and (b) are the ray diagram for the $10 \times 5\text{km}$ and the $0.25 \times 0.25\text{km}$ blocks. Table 2.1 shows the resulting traveltimes and epicentral distance generated by this ray tracing method and the analytical solution for a harmonic source of frequency 15 Hz at the take-off angle, 52° .

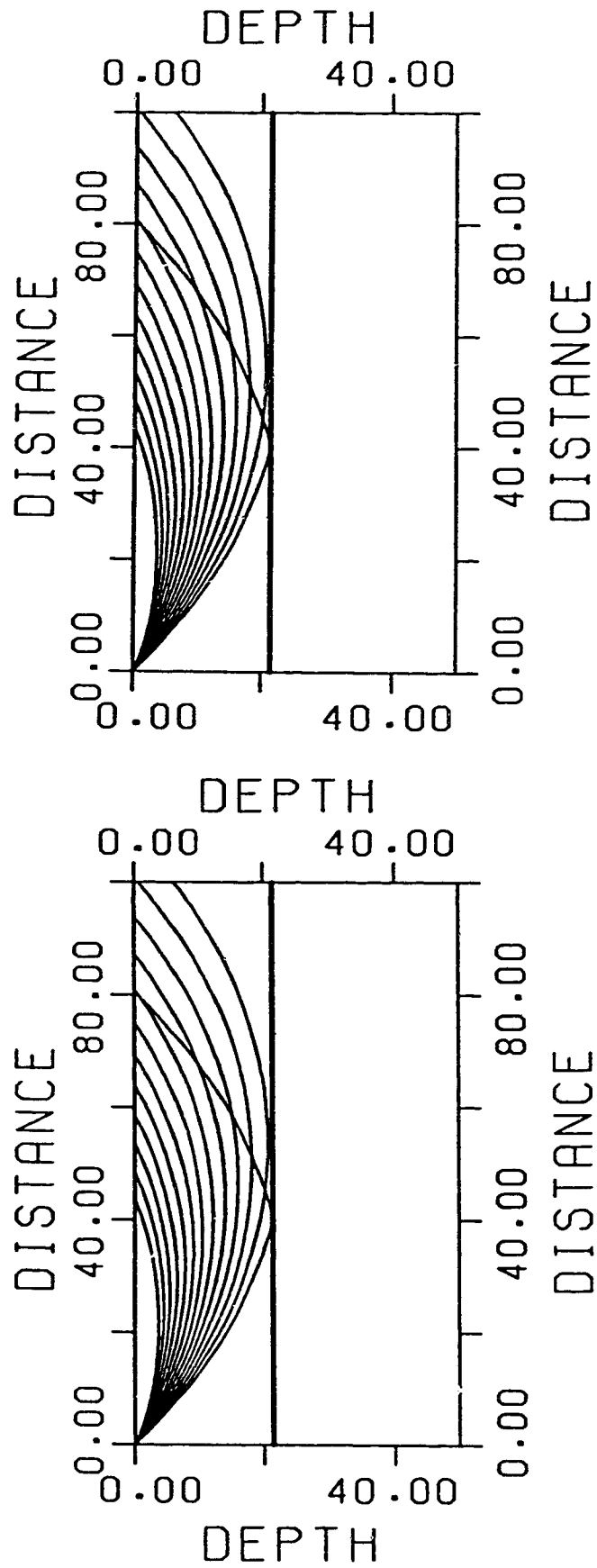


Figure 2.6 a Ray diagram with cell size 10 x 5km for model $v(z)=6+0.1z$

Figure 2.6 b Ray diagram with cell size 0.25 x 0.25km for model $v(z)=6+0.1z$

Table 2.1 Results of ray tracing and analytical solution for $V(z) = 6.0 + 0.1z$

CELL SIZE	Epicentral Distance(km)	Travel time (sec.)	CPU ¹ (sec.)
10km x 5km	93.754272	14.359759	0.025
5km x 5km	93.754272	14.359759	0.0375
1km x 1km	93.75428	14.359759	0.125
0.5km x 0.5km	93.75425	14.35976	0.3425
0.25km x 0.25km	93.754288	14.35976	1.0875
Analytical solution	93.754272	14.35976	

The results show that this ray tracing method is accurate and stable.

To further our discussion, a general model of an inhomogeneous medium used by Marks and Hron is employed. For a set of take-off angles, the traveltimes and epicentral distances are calculated by this ray tracing method and the method by solving differential equations (Cerveny, Lange, and Psencik, 1972). The results are listed in Table 2.2. Figure 2.7 is the ray diagram generated by those two methods.

Table 2.2 Results for general inhomogeneous media

Take off angle	Travel time (second)		Epicentral Distance (km)	
	Our method	Differential Eq.	Our method	Differential Eq.
1°	14.913894	14.555333	50.615040	49.36361
5°	14.950478	14.578881	55.234913	55.039056
9°	15.014661	14.646761	61.265308	61.219430
13°	15.157248	14.784711	68.380112	67.996422
17°	15.327788	14.987059	74.547684	74.739462

From the results listed in Table 2.2, one can see that these two methods match reasonably well. However, our method needs much less CPU time to calculate above rays. Furthermore, our method can handle a buried source easily. Figure 2.8 is an example

which has a buried source. It makes our method applicable to seismic tomography. The other advantage of our method is that it can be easily extended to three-dimensional media.

All the above points show that our ray tracing method is a reasonable accurate and stable method. It is reliable and efficient.

Now, for the purpose of calculating synthetic seismogram, the remaining problem is how to calculate the ray amplitude using this method. The next chapter will deal with this matter.

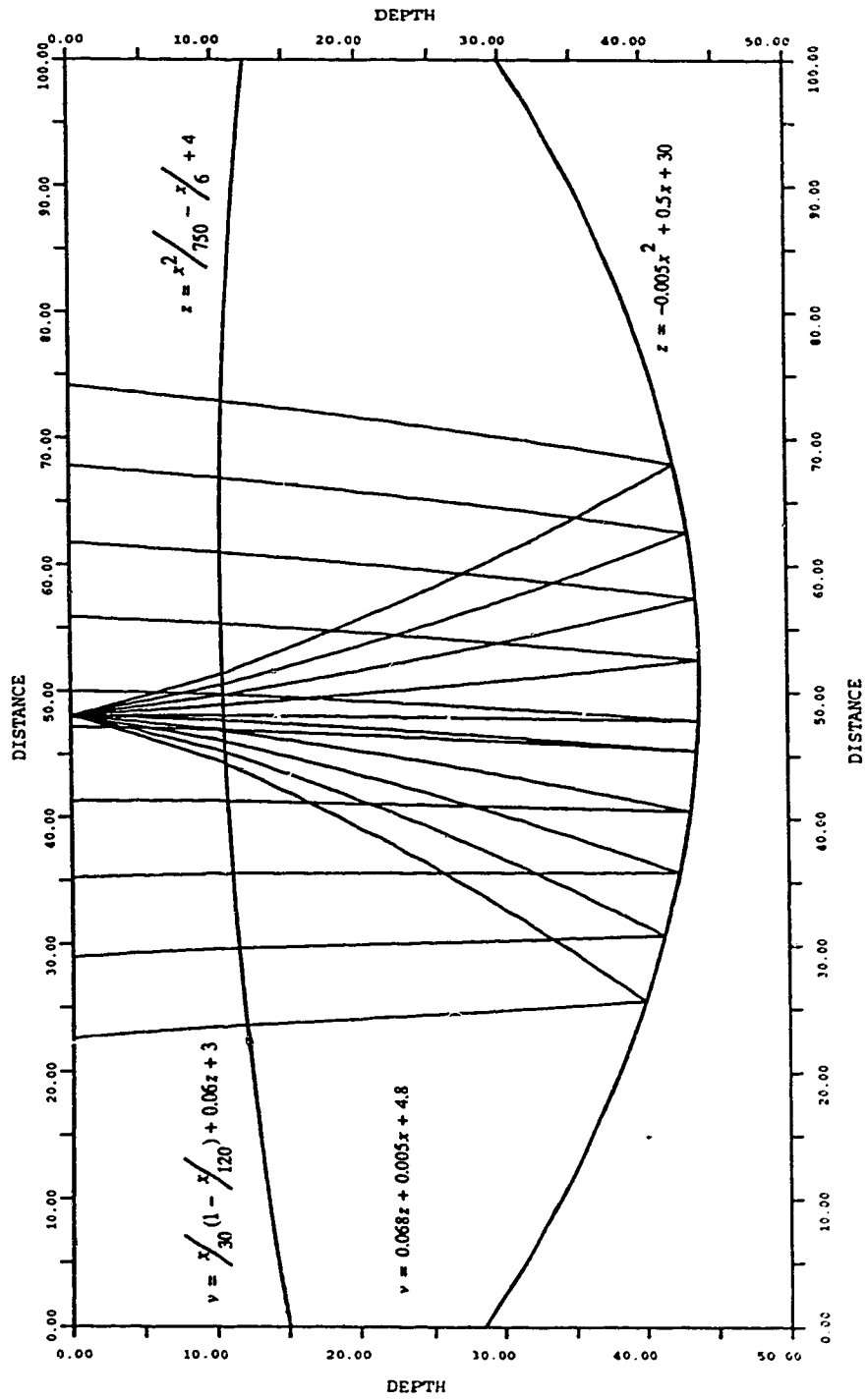


Figure 2.7 Ray in a generally inhomogeneous medium

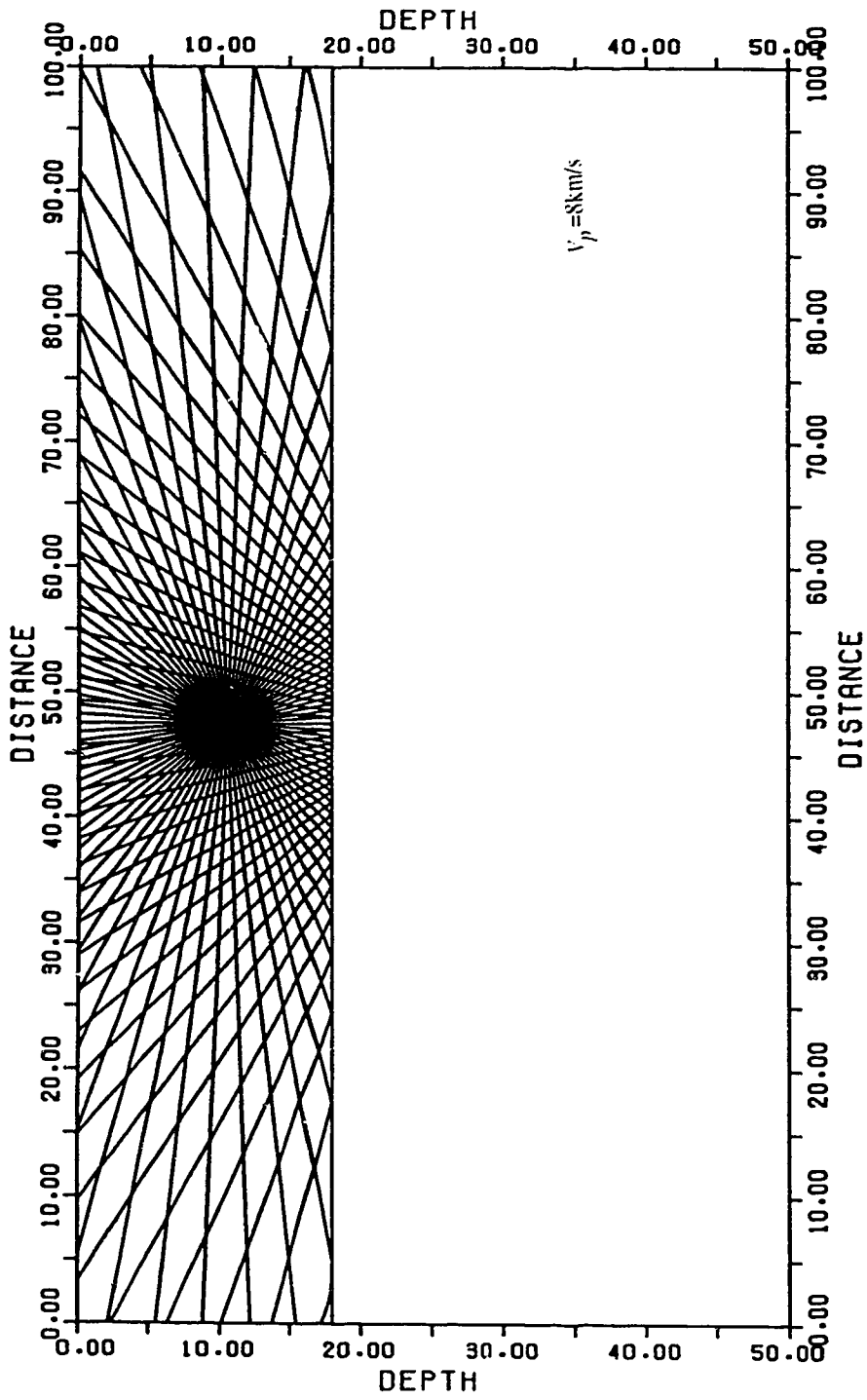


Figure 2.8 Ray diagram with a buried source at depth 10 km where the P-wave velocity of upper layer is 5 Km/s.

Chapter 3 RAY AMPLITUDE

3.1 Introduction

An important class of methods for calculating body wave synthetic seismograms is the set of ray-based schemes. These include asymptotic methods ranging in complexity and accuracy from asymptotic ray theory (Hron and Kanasewich 1971, Červený, Molotkov, Pšenčík 1977, Červený and F. Hron 1980, Wooham Kim and V. Cormier 1990) through WKBJ (Chapman, 1978) and Maslov techniques (Chapman and Drummond 1982), to highly accurate methods such as generalized ray theory (Helmberger and Harkride 1978). What these methods have in common is that they are techniques for the computation of a ray contribution to the total seismic field in the time domain. For any ray theory, the most complicated part in the computation of ray amplitudes of seismic body waves in inhomogeneous media with curved interfaces lies in the evaluation of the geometrical spreading.

In this chapter, the geometrical spreading will be given by analytical and numerical means for different media and numerical tests will be performed.

3.2 Differential equation solution for ray amplitude

Differential equations have been derived by Červený et al (1974) by which the cross sectional area of the ray tube for an inhomogeneous medium may be expressed. Even though the geometrical spreading of the ray tube may be, in some cases, evaluated quite simply, formally the geometrical spreading of the ray tube might be treated using the results of the differential geometry of surfaces. A brief summary of the above theory will be given here. For a more in-depth discussion, an interested reader is referred to the original publication.

Asymptotic ray theory is based on the concept of rays along which the seismic energy propagates from the source. Mathematically, each ray represents a characteristic line to the eikonal equation

$$|\nabla\tau| = \frac{1}{V} \quad (3.1)$$

where τ is arrival time and V is the phase velocity of the wave propagation.

Mathematically, the wavefront is defined implicitly as

$$\tau(\vec{x}) = t_0 \quad (3.2)$$

where $\vec{x} = \vec{x}(q_1, q_2, \tau) = (x_1(q_1, q_2, \tau), x_2(q_1, q_2, \tau), x_3(q_1, q_2, \tau))$ is the wavefront and (q_1, q_2, τ) are ray coordinates where q_1 represent the declination of the ray at take-off angle and q_2 the azimuthal angle. Thus, the cross sectional area of the ray tube $d\sigma$, (see Figure 3.1), is given by the standard formula from the differential geometry of a surface (Schartz, 1960), as

$$d\sigma = J dq_1 dq_2 \quad (3.3)$$

where

$$J = \left| \frac{\partial \vec{x}}{\partial q_1} \times \frac{\partial \vec{x}}{\partial q_2} \right| = \left| \vec{x}_{q_1} \times \vec{x}_{q_2} \right| \quad (3.4)$$

is the Jacobian of the transformation from Cartesian to ray coordinates.

Denoting the cross sectional area of the ray tube at s_0 by $d\sigma(s_0)$ and the area of the same ray tube at s by $d\sigma(s)$, then, according to ART, the ray amplitude of zero order is

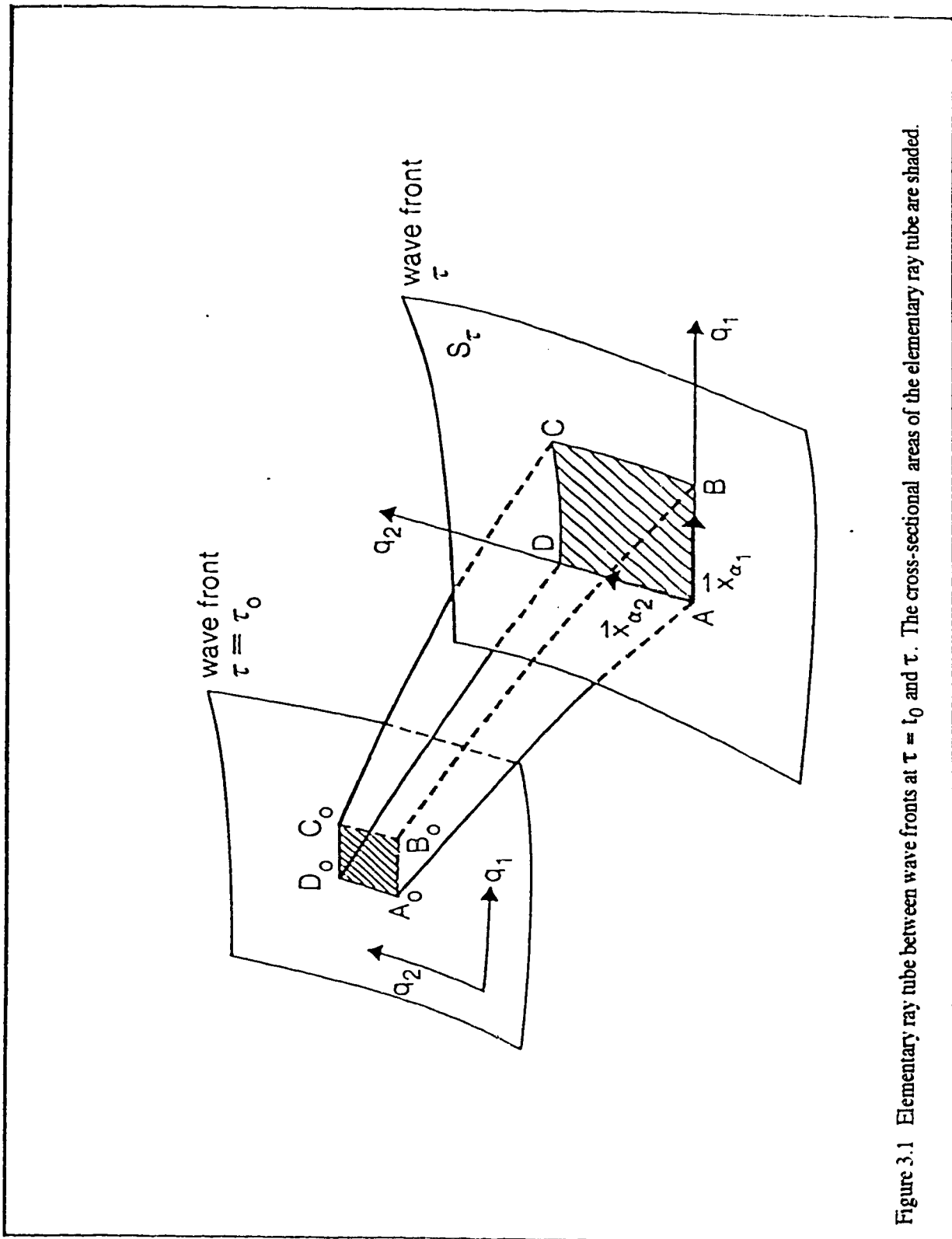


Figure 3.1 Elementary ray tube between wave fronts at $\tau = \tau_0$ and τ . The cross-sectional areas of the elementary ray tube are shaded.

$$A(s) = \left[\frac{V(s_0)\rho(s_0)d\sigma(s_0)}{V(s)\rho(s)d\sigma(s)} \right]^{1/2} A(s_0) \quad (3.5)$$

where the $\left(\frac{d\sigma(s)}{d\sigma(s_0)} \right)^{1/2} = L$ is the so called geometrical spreading function. It plays a crucial role in the computation of ray amplitude. We will derive some useful formulae for it.

From (3.3), we have

$$\begin{aligned} d\sigma(s_0) &= J(s_0)dq_1dq_2 \\ d\sigma(s) &= J(s)dq_1dq_2 \end{aligned} \quad (3.6)$$

It follows that

$$\frac{d\sigma(s_0)}{d\sigma(s)} = \frac{J(s_0)}{J(s)} \quad (3.7)$$

which can serve us as a mathematical definition of $\frac{d\sigma(s_0)}{d\sigma(s)}$, when $J(s) = |\vec{x}_{q_1} \times \vec{x}_{q_2}|$ is used.

It yields

$$\frac{d\sigma(s_0)}{d\sigma(s)} = \frac{J(s_0)}{J(s)} = \frac{|\vec{x}_{q_1} \times \vec{x}_{q_2}|_{\tau=\tau(s_0)}}{|\vec{x}_{q_1} \times \vec{x}_{q_2}|_{\tau=\tau(s)}} \quad (3.8)$$

The methods for evaluating $|\vec{x}_{q_1} \times \vec{x}_{q_2}|$ are again known from differential geometry. Using the Laplace identity $|\vec{A} \times \vec{B}|^2 = (\vec{A} \cdot \vec{A})(\vec{B} \cdot \vec{B}) - (\vec{A} \cdot \vec{B})^2$ and putting

$$\begin{aligned} E &= (\vec{x}_{q_1} \cdot \vec{x}_{q_1}) \\ F &= (\vec{x}_{q_2} \cdot \vec{x}_{q_2}) \\ G &= (\vec{x}_{q_1} \cdot \vec{x}_{q_2}) \end{aligned} \quad (3.9)$$

then

$$\left| \bar{x}_{q_1} \times \bar{x}_{q_2} \right| = (EF - G^2)^{1/2} \quad (3.10)$$

This is convenient for calculation of $\frac{d\sigma(s_0)}{d\sigma(s)}$ when the wavefront is known.

Another method to determine $\frac{d\sigma(s)}{d\sigma(s_0)}$ is to make use of the radii of curvature of the wave front. First, we write $\nabla^2\tau$ in the form

$$\nabla^2\tau = \nabla \cdot \nabla\tau = \nabla \cdot \left(\frac{\bar{t}}{V} \right) = \frac{d}{ds} \left(\frac{1}{V} \right) + \frac{1}{V} (\nabla \cdot \bar{t}) \quad (3.11)$$

where \bar{t} is a unit vector tangent to the ray. From differential geometry, we know that

$$\nabla \cdot \bar{t} = \frac{1}{r_1} + \frac{1}{r_2} \quad (3.12)$$

where r_1 and r_2 are the principal radii of the wave front (see detailed derivation in Kline and Kay, 1965, PP184 - 6). Inserting (3.11), (3.12) into

$$\left(\frac{V(s)d\sigma(s_0)}{V(s_0)d\sigma(s)} \right)^{1/2} = \exp \left\{ -\frac{1}{2} \int_{s_0}^s V \nabla^2\tau ds \right\} \quad (3.13)$$

Then, we have

$$\left(\frac{d\sigma(s_0)}{d\sigma(s)} \right)^{1/2} = \exp \left\{ -\frac{1}{2} \int_{s_0}^s \left(\frac{1}{r_1} + \frac{1}{r_2} \right) ds \right\} \quad (3.14)$$

where the integration path is along the ray. Thus, we have expressed $\frac{d\sigma(s_0)}{d\sigma(s)}$ in terms of the principal radii of curvature of the wave front.

Now, the remaining problem is how to calculate the wavefront $x_i(q_1, q_2, \tau)$, $i=1,2,3$ along with the ray tracing. The slowness vector $P_i(q_1, q_2, \tau)$ and $x_i(q_1, q_2, \tau)$,

$i=1,2,3$, can be obtained by means of partial differentiation of equation (2.1) with respect to q_α , $\alpha=1,2$. Following Marks and Hron's derivation, let us introduce

$$\begin{aligned} Y_{i\alpha}(q_1, q_2, \tau) &= \frac{\partial x_i(q_1, q_2, \tau)}{\partial q_\alpha} \\ Z_{i\alpha}(q_1, q_2, \tau) &= \frac{\partial P_i(q_1, q_2, \tau)}{\partial q_\alpha} \end{aligned} \quad (3.15)$$

We have

$$\begin{aligned} \frac{dY_{i\alpha}}{d\tau} &= 2P_i Y_{j\alpha} V \frac{\partial V}{\partial x_j} + V^2 Z_{i\alpha} \\ \frac{dZ_{i\alpha}}{d\tau} &= \frac{Y_{i\alpha}}{V^2} \left[\frac{\partial V}{\partial x_i} \frac{\partial V}{\partial x_j} - V \frac{\partial^2 V}{\partial x_i \partial x_j} \right] \end{aligned} \quad (3.16)$$

This system of equations (3.16) must be solved simultaneously with the ray tracing equation (2.1), to obtain both kinematic and dynamic properties of waves in inhomogeneous media.

3.3 Computation of geometrical spreading by Dynamic Ray Tracing

As described in the previous section, the geometrical spreading of a ray tube is closely related to the curvature of the wavefronts $\bar{x}(q_1, q_2, \tau)$ with τ fixed. Cerveny and Hron (1980) studied the problem of computation of ray amplitude in generally inhomogeneous medium with curvilinear interfaces. They introduced the process of 'Dynamic Ray Tracing (DRT)', which employs second derivatives of the seismic time field with respect to the ray coordinates. The matrix of ray curvatures along the ray can be obtained by solving a system of non-linear differential equations. Some equations will be presented here and an interested reader can find the rigorous derivation by Cerveny and

Hron in their already classic paper (Cerveny and Hron 1980). Some other methods such as vicinity ray tracing by Wooham Kim and F. Cormier(1990) and Hubral(1979) had some similar results as DRT.

For an inhomogeneous 2-dimensional medium, the dynamic ray tracing system reduces to a single first order differential equation of the Riccati type. The phase matching method is used to determine the discontinuities of the individual properties in DRT when the wave impinges a curved boundary separating two generally inhomogeneous media.

Following the derivation of Cerveny and Hron (1980), for our type of media, which has constant velocity gradient in each block, the dynamic ray tracing system is

$$\begin{aligned}\frac{dM_{11}}{ds} + VM_{11}^2 &= 0 \\ \frac{dM_{22}}{ds} + VM_{22}^2 &= 0\end{aligned}\tag{3.17}$$

where $M_{ij} = \frac{\partial^2 \tau}{\partial q_i \partial q_j}$, $i, j = 1, 2$.

Equation (3.12) corresponds to equation (88) of the above reference(Cerveny and Hron 1980). The variable M_{11} represents the product of the wavefront's radius of curvature (in the plane of propagation) divided by the velocity of propagation at that time τ . The variable M_{22} is similar to M_{11} but for the radius of curvature perpendicular to the plane of propagation.

It follows that, the spreading function J for ray amplitude is given by

$$J(\tau) = J(\tau_0) \exp \left\{ \int_{\tau_0}^{\tau} V^2 (M_{11} + M_{22}) d\xi \right\}\tag{3.18}$$

If we consider first ray segment radiated from the source, then $\tau_0 = \frac{1}{V_0}$ corresponds to the ray travel time for a homogeneous unit sphere surrounding to the source. V_0 is the velocity at the source and $J(\tau_0) = \sin \theta_0$, θ_0 is the ray take-off angle as measured from the vertical at

the source. Otherwise, τ_0 is the time at the beginning of the current ray segment. If the medium has constant velocity gradient, we can obtain the analytical geometrical spreading by using DRT.

Incorporation DRT into our ray tracing method, we can calculate the geometrical spreading of a ray from source to receiver block by block (Personal communication with Dr. F. Hron), each of which has the same constant velocity gradient. We use the numerical model $V(z)=6.0+0.1z$ (see Figure 2.6a) to calculate the geometrical spreading using DRT. The results are listed in Table 3.1

Table 3.1 Geometrical spreading by DRT

Take-off Angle	DRT	Analytical solution
52°	118.976	118.976
54°	107.767	107.767
56°	97.6325	97.6325
58°	88.4199	88.4199
60°	80.000	80.000

From Table 3.1, one finds the spreading calculated by DRT is identical with the analytical solution for vertical inhomogeneous media with a constant velocity gradient.

If the ray strikes a curved interface, special treatment is needed. The phase matching method can obtain the same formula as those of Gel'chinskiy (1961). The next section will deal with this problem.

3.4 The behavior of an interface

If the ray is incident on an interface which separates two different media, equations (2.1), (3.16) and (3.17) must be supplemented by the appropriate boundary conditions at the point of incidence. This is due to the fact that some variables such as the slowness

vector and the curvature of the wavefront will change discontinuously due to the existence of the interface. The change depends on both the velocity contrast across the interface and the curvature of the interface.

The change of slowness vector can be obtained easily from Snell's law. The exact derivation of the change of curvature of the wavefront is again carried out with the help of the differential geometry of surfaces. Since the algebra involved is rather tedious, only the final formulae as derived by Gel'chinsky (1961) are presented below.

Gel'chinsky showed that when the ray strikes an interface of a two dimensional medium with constant velocity gradient, the unknown principal radii of curvature of the wavefront leaving the interface after reflection or transmission can be written as

$$\begin{aligned} r_1^v &= r_{\parallel}^v = \frac{r_{\parallel}^0}{\Delta_{\parallel}} \\ r_2^v &= r_{\perp}^v = \frac{r_{\perp}^0}{\Delta_{\perp}} \end{aligned} \quad (3.19)$$

where

$r_{\parallel}^0, r_{\perp}^0$ are the principal radii of curvature of the incident wavefront at the point of incidence.

$$\begin{aligned} \Delta_{\parallel} &= \frac{V_v \cos^2 \theta_0}{V_0 \cos^2 \theta_v} + \frac{r_{\parallel}^0}{R_{\parallel} \cos^2 \theta_v} \left[\frac{V_v}{V_0} \cos \theta_0 \pm \cos \theta_v \right] \\ \Delta_{\perp} &= \frac{V_v}{V_0} \end{aligned}$$

R_{\parallel} is principal radius of the curvature of the curved interface at the point of incidence.

The new ray curvature, serves as the initial value for the dynamic ray tracing system (3.17) or differential equation (3.16). In this way, the final kinematic and dynamic properties of the ray can be traced again from the source to the receiver.

If there exist several interfaces in the medium along a ray from a point source M_0 to receiver M , the ray can be broken into k ray segments passing through $(k-1)$ points of incidence $o_k, j=1, \dots, k-1$. This is schematically shown in Figure 3.2 where o_k denotes the end of the ray at M , and o_0 corresponds to the point on the ray with the unit radius of curvature of the spherical wavefront. According to Asymptotic Ray Theory (Cerveny and Ravindra 1971, P75), the ray amplitude of the wave arriving at the receiver $M=o_k$ equals

$$A(M) = \frac{\tilde{g}(q_1, q_2)}{L} \left[\frac{V_0 \rho_0}{V(M) \rho(M)} \right]^{1/2} \prod_{j=1}^k \left[\frac{\tilde{V}(o_j) \tilde{\rho}(o_j)}{V(o_j) \rho(o_j)} \right]^{1/2} R_j \quad (3.20)$$

where

- \tilde{g} ... radiation characteristic of the source (taken as unity for this study)
- o_j ... point of incidence of the ray upon the j -th interface that it encounters.
- $V_0 \rho_0$... wave velocity and density at source
- $\theta(o_j)$... angle of incidence upon the j -th interface
- $\tilde{\theta}(o_j)$... angle after reflection or transmission upon the j -th interface

and the relative geometrical spreading is

$$L = \left(\frac{d\sigma(M)}{d\sigma(M_0)} \right)^{1/2} \prod_{j=1}^k \left(\frac{d\sigma(o_j)}{d\tilde{\sigma}(o_j)} \right)^{1/2} \quad (3.21)$$

where $\frac{d\sigma(o_j)}{d\tilde{\sigma}(o_j)} = \frac{\cos\theta(o_j)}{\cos\tilde{\theta}(o_j)}$ and $\frac{d\sigma(M)}{d\sigma(M_0)}$ is determined by (3.7), (3.14) or (3.18).

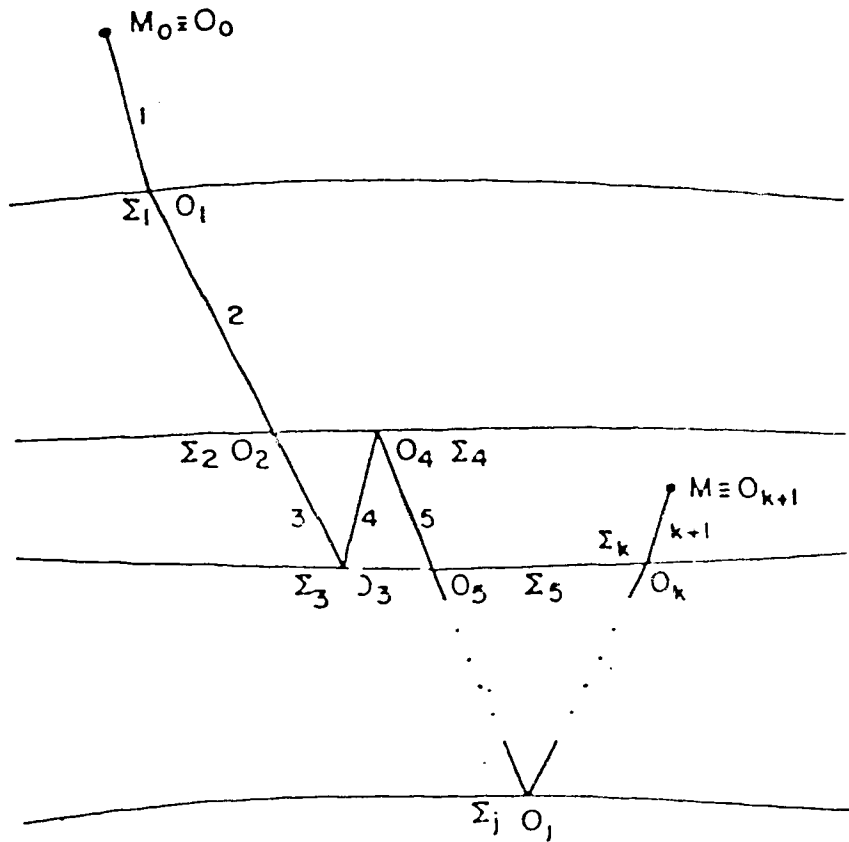


Figure 3.2 Explanation of various symbols for a ray in a medium with an arbitrary number of interfaces which may not be plane. The ray paths may be curved.

Employing this procedure, the analytical geometrical spreading for our circular approximation can be obtained. However, we'll present a numerical method to calculate the amplitude based on the circular approximation.

3.5 Ray amplitude by circular approximation

All quantities in equation (3.20) are easily computed except the geometrical spreading L because it includes $d\sigma(M)$. We shall develop an algorithm to compute $d\sigma(M)$ for laterally inhomogeneous media with curved interfaces by means of the circular approximation described in Chapter 2.

From the geometry of Figure 3.3

$$\begin{aligned} d\sigma(M) &= \cos(\theta_M) \frac{\partial y}{\partial \phi_0} dr d\phi_0 \\ &= \frac{\partial r}{\partial \theta_0} \cos(\theta_M) \frac{\partial y}{\partial \phi_0} d\theta_0 d\phi_0 \end{aligned} \quad (3.22)$$

where r is the magnitude of the vector pointing from source M_0 to receiver M . Within the unit sphere surrounding the source we assume it to be homogeneous. Then we have

$$d\sigma(M_0) = \sin \theta_0 d\theta_0 d\phi_0 \quad (3.23)$$

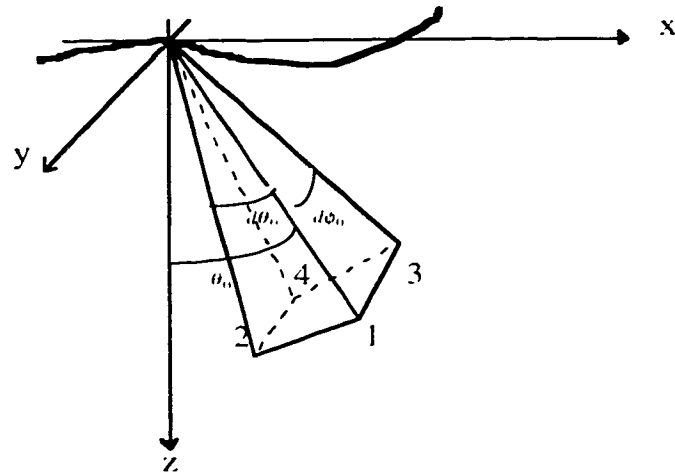
and

$$\frac{d\sigma(M)}{d\sigma(M_0)} = \frac{\partial r}{\partial \theta_0} \frac{\cos(\theta_M)}{\sin \theta_0} \frac{\partial y}{\partial \phi_0} \quad (3.24)$$

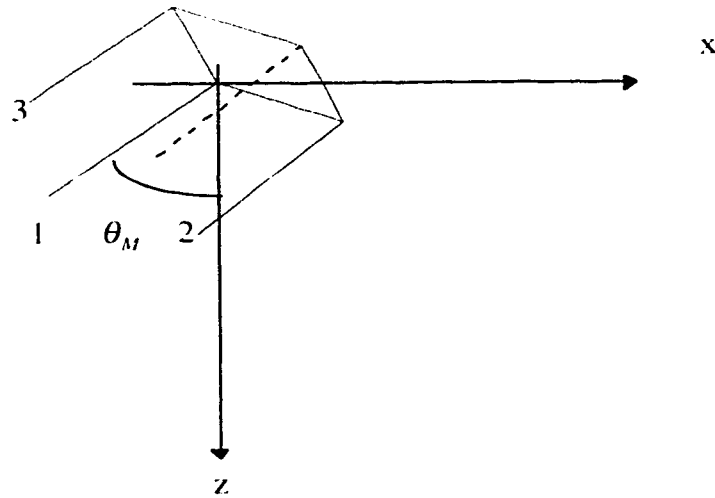
where $\frac{\partial r}{\partial \theta_0}$ may be determined by numerical or analytical means. Numerically, the

procedure is:

- (1) Shoot three rays on either side of the ray arriving at the receiver, this may be done by subtracting or adding small amounts $\Delta\theta_0$ from the take-off angle. The change of θ_0 should yield a change in epicentral distance.
- (2) Fit a cubic spline through the seven (θ_0, r) data.
- (3) Evaluate the derivative $\frac{\partial r}{\partial \theta_0}$ and the second derivative $\frac{\partial^2 r}{\partial \theta_0^2}$.



Source (M_0)



RECEIVER (M)

Fig. 3.3 Geometry of the ray tube at source and receiver. The heavy line represents the earth's surface. The angle θ_0 is confined to x-z plane, while ϕ_0 is confined to the y-z plane

Analytically,

$$\frac{\partial r}{\partial \theta_0} = \frac{V_0}{\sin \theta_0} \sum_{i=0}^N \frac{1}{k_i} \frac{(\cos \theta_i - \cos \theta_{i+1})}{\cos \theta_{i+1} \sin \theta_i} \quad (3.25)$$

and

$$\frac{\partial^2 r}{\partial \theta_0^2} = -\frac{V_0}{\sin \theta_0} \sum_{i=0}^N \frac{1}{k_i} \frac{(\cos \theta_i - \cos \theta_{i+1})(\cos \theta_i + \cos \theta_{i+1} - 2 \cos \theta_i \cos^2 \theta_{i+1})}{\cos^3 \theta_{i+1} \sin^2 \theta_i} \quad (3.26)$$

where N is the total number of blocks which the ray passes from source to receiver. According to Cerveny et al (1974), $g = \frac{\partial y}{\partial \theta_0}$ is defined by the following differential equation for a two dimensional medium,

$$\frac{dg}{dt} = \frac{\sin \theta_0}{V_0} V^2(t) \quad (3.27)$$

where t is the travel time. Integrating (3.27) and summing over all N blocks that the ray passes through, we have

$$g = \frac{\sin \theta_0}{V_0} \sum_{i=1}^N V_{0i}^2 (1 + a_i)^2 \int_{t_{i-1}}^{t_i} \frac{e^{2k_i(t-t_{i-1})}}{(1 + a_i e^{2k_i(t-t_{i-1})})^2} dt \quad (3.28)$$

where

V_{0i} ... velocity at entry point of i-th block

θ_{0i} ... angle of incidence upon entry of i-th block

$$a_i = \tan^2\left(\frac{\theta_{0i}}{2}\right)$$

k_i ... constant velocity gradient in i-th block

t_{i-1}, t_i ... ray travel time of the i-th block from entry to exit

Note that $t_0 = 0$, $t_N =$ total ray travel time from source to receiver. Upon performing the integration (3.26) and inserting the result into equation (3.24), we have

$$\frac{d\sigma(M)}{d\sigma(M_0)} = \frac{\partial r}{\partial \theta_0} \frac{\cos(\theta_M)}{V_0} \sum_{i=1}^N \frac{V_{0i}^2 (1 + a_i)}{2k_i} \left(\frac{e^{2k_i(t_i - t_{i-1})} - 1}{1 + a_i e^{2k_i(t_i - t_{i-1})}} \right) \quad (3.29)$$

If the gradient $k_i = 0$ in any of the blocks, the term to be added must be $V_{0i}^2(t_i - t_{i-1})$. The computation of ray amplitude in two dimensionally inhomogeneous media with curvilinear interfaces is now given by equations (3.20) and (3.21) and (3.27).

To assess the accuracy of the circular approximation, we calculated the geometrical spreading by using both circular approximation and the analytical method for the velocity model $v(z)=6+0.1z$. In Figure 3.4, we can see that the circular approximation is accurate enough to calculate the ray amplitude. Further comparisons will be made in the next section.

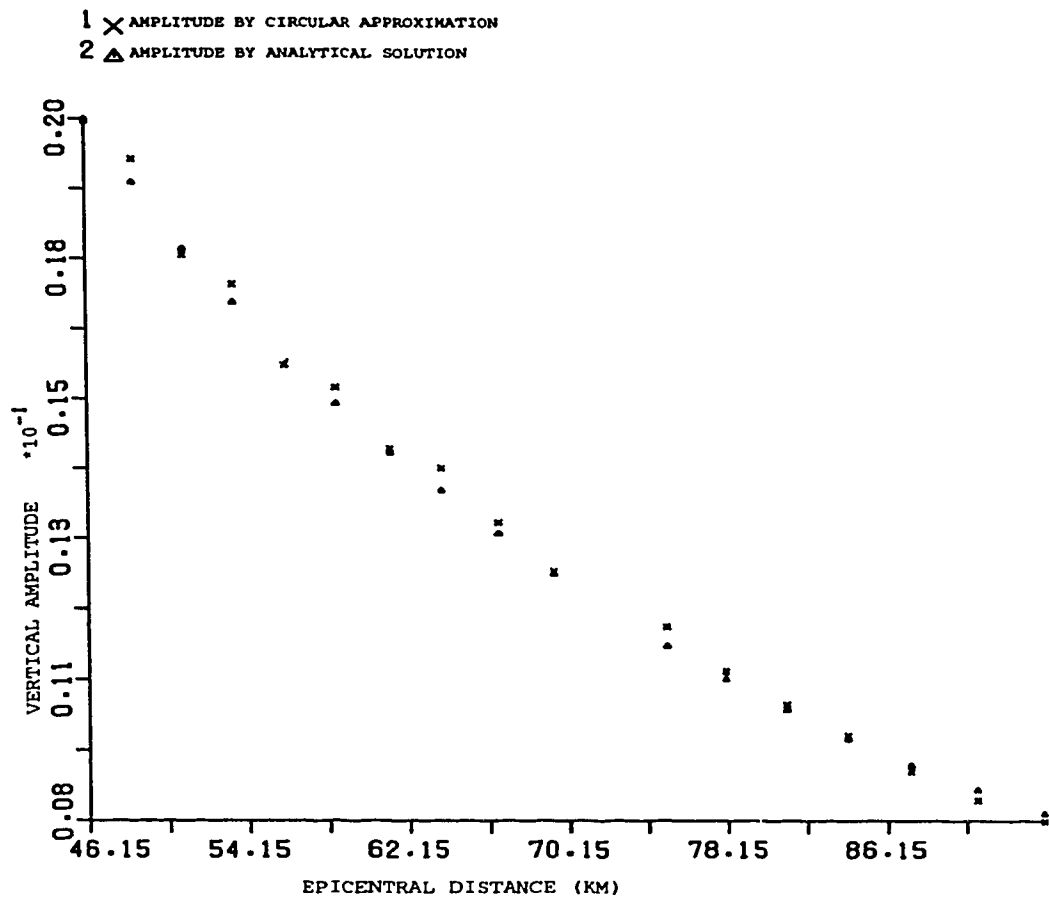


Figure 3.4 Numerical and analytical geometrical spreading for model $v(z)=6. +0.1z$.

3.6 Numerical tests

FORTTRAN programs have been developed to calculate the kinematic and dynamic characteristics of waves in two-dimensional inhomogeneous media using the circular approximation and DRT. In this section, a comparison between these methods is conducted. The shear wave velocity and volume density for all the models that we used are given by

$$V_s(x,z) = \frac{V_p(x,z)}{\sqrt{3}}, \quad \rho(x,z) = \sqrt{3}V_p^{1/4}(x,z)$$

from Gardner et al (1974).

We use different methods to calculate the ray amplitude of a converted wave in a three-layer model of a converted wave. Figure 3.5 is the description of the model showing converted wave SIP2P2P2S2S2S2P2P2S2P2S1 ray paths using the same model. Table 3.2 shows the amplitudes of each ray as calculated by the different methods.

Table 3.2 The amplitude for wave SIP2P2P2S2S2S2P2P2S2P2S1

Epicentral Distance (km)	Vertical Amplitude		Horizontal Amplitude	
	Circular method	Hron's method	Circular method	Hron's method
2.5	$1.09947 * 10^{-16}$	$1.129 * 10^{-16}$	$2.10577 * 10^{-15}$	$2.161 * 10^{-15}$
5.0	$7.82487 * 10^{-15}$	$8.034 * 10^{-15}$	$7.58424 * 10^{-14}$	$7.785 * 10^{-14}$
7.5	$5.10505 * 10^{-14}$	$5.244 * 10^{-14}$	$3.36458 * 10^{-13}$	$3.456 * 10^{-13}$
10.0	$1.02549 * 10^{-13}$	$1.055 * 10^{-13}$	$5.20777 * 10^{-13}$	$5.356 * 10^{-13}$

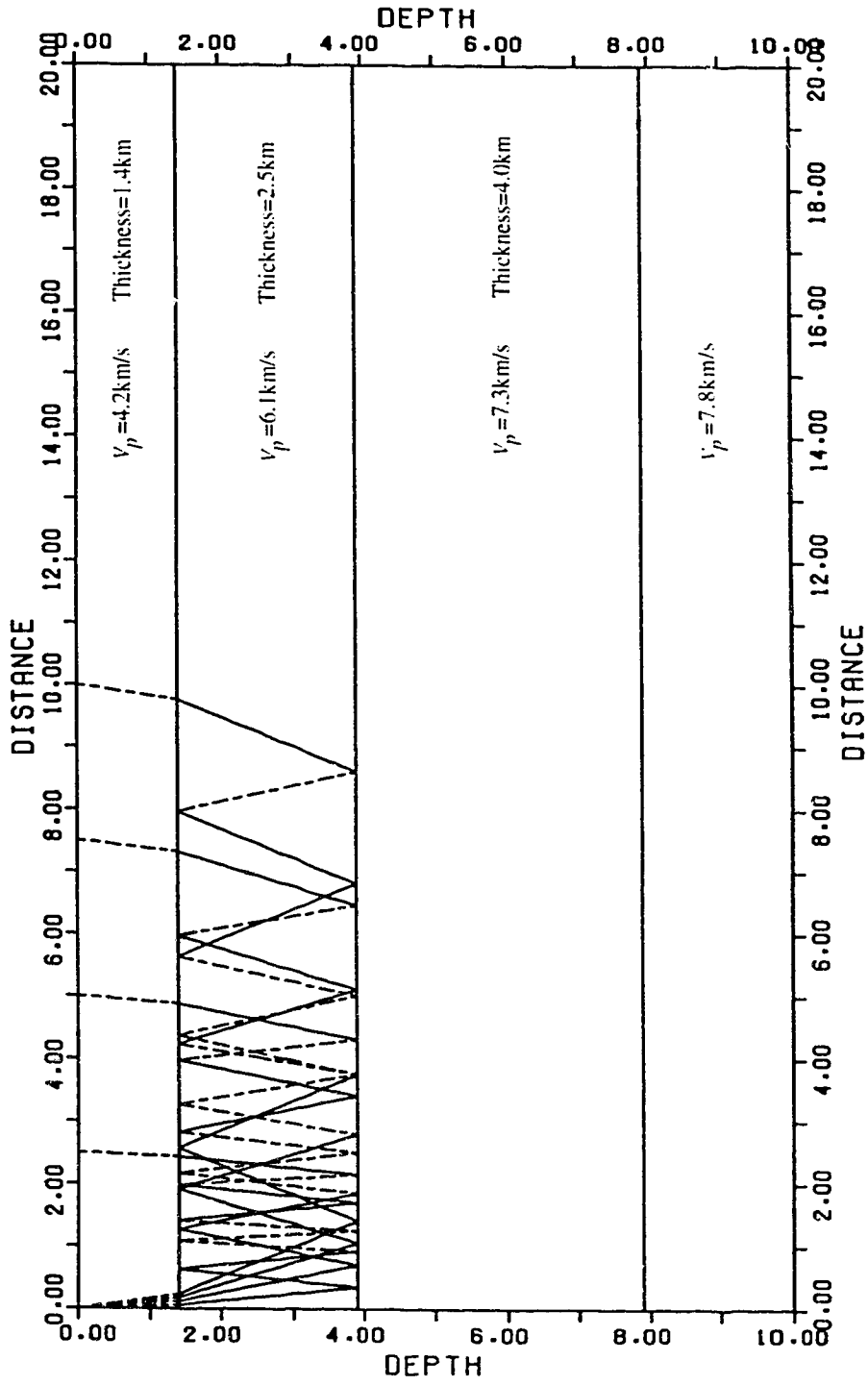


Figure 3.5 Ray diagram of wave SIP2P2S2S2P2P2S2P2S1 in a three-layered model

The ray amplitudes for generally inhomogeneous media are found in chapter 5. The results shows our method is reliable in calculating the ray amplitude even in generally inhomogeneous media. However, it is not applicable to calculate the ray amplitude in the vicinity of a caustic where an alternative high frequency method must be used.

Chapter 4 RAY AMPLITUDE IN THE VICINITY OF A CAUSTIC

4.1 Introduction

In Chapter 1, we noted that ray theory is not applicable near a caustic due to it predicting an infinite amplitude for the particle displacement. To find the correct dynamic properties of the wave field in the vicinity of a caustic, more exact methods must be used.

The basic theoretical problems associated with caustics have been investigated by Brekhovskikh(1960,1990), Ludwig(1966), Sato (1969), and others. In this Chapter, following Choi and Hron (1981), the formal integral propagating in a vertically inhomogeneous medium solution for an arbitrary ray is presented using a modified version of the third-order saddle approximation yielding a new expression for the amplitude in the vicinity of a caustic. This result is shown to be more accurate than a traditional Airy approximation. Both the Airy approximation and the modified Airy approximation will be introduced in this chapter and incorporated into our ray tracing program.

4.2 Airy Approximation

For a perfectly elastic, isotropic vertically inhomogeneous medium with interfaces (Figure 4.1), the WKB solution for a P wave in frequency domain (Appendix B) may be expressed formally as

$$u(M,\omega) = (-1)^\varepsilon S(\omega) \left(\frac{\omega}{2\pi r} \right)^{\frac{1}{2}} e^{i(n\frac{\pi}{2} - \frac{\pi}{4})} \int_{-\infty}^{\infty} f(p) e^{-i\omega\tau(p,r)} dp \quad (4.1)$$

where

ε is the number of turning SV ray segments and is zero for P and SH waves.

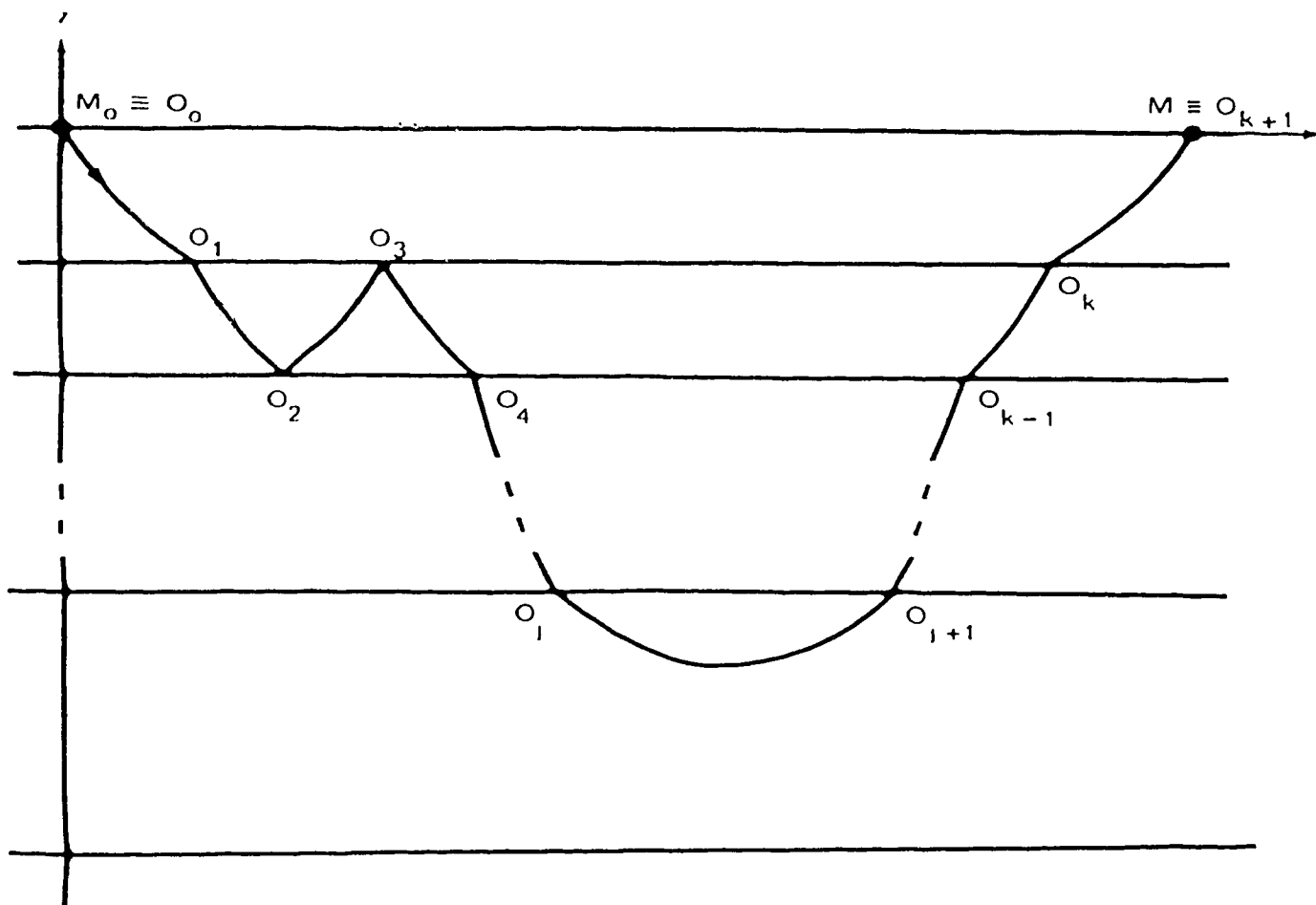


Figure 4.1 Ray character of a vertically inhomogeneous medium

$$\Gamma(p) = \frac{p^{1/2} G(M_0)}{q_p(M_0) G(M)} \prod_{j=1}^k \frac{G(O_j^-)}{G(O_j^+)} R(O_j) \quad (4.2)$$

which involves the product of reflection, transmission and surface conversion coefficients R along the ray. Also,

$$q_p = \left(\frac{1}{v_p^2} - p^2 \right)^{1/2}$$

$$G = \left(\frac{\rho}{q_p} \right)^{1/2} \cos \theta$$

and the phase function is

$$\tau(p, r) = pr + \psi(p) \quad (4.3)$$

$$\psi(p) = \sum_{j=1}^{k+1} \psi_j(p)$$

with

$$\psi_j(p) = \left| \int_{z_{j-1}}^{z_j} q(p, \xi) d\xi \right|$$

if the ray has no turning point between $o_{j-1} = (r_{j-1}, z_{j-1})$ and $o_j = (r_j, z_j)$, and

$$\psi_j(p) = 2 \left| \int_{z_j^*}^{z_j} q(p, \xi) d\xi \right|$$

if the ray has a turning point at (r^*, z^*) between o_{j-1} and o_j .

For high frequencies, the second-order saddle point method may be applied to (4.1) to give

$$u(M, \omega) = \frac{(-1)^{\epsilon} S(\omega) f(p_r)}{\left| r \frac{\partial^2 \tau}{\partial p^2} \right|_{p_r}^{1/2}} e^{i \left[n \frac{\pi}{2} - \frac{\pi}{4} \left[\text{sgn} \left(\frac{\partial^2 \tau}{\partial p^2} \right)_{p_r} + 1 \right] \right] - i \omega \tau(p_r, r)} \quad (4.4)$$

where p_r is defined by the saddle point condition

$$\frac{\partial \tau}{\partial p}(p_r) = 0$$

From the definition of the phase function (4.3), we see that p_r must in fact be the geometrical ray parameter of the ray reaching the receiver. Therefore, $\tau_r \equiv \tau(p_r, r)$ is the geometrical arrival time. Therefore, this (4.4) is called the geometrical ray approximation and is identical with the zero order approximation of asymptotic ray theory.

However, the above approximation (4.4) tends to infinity as $\frac{\partial^2 \tau}{\partial p^2}(p_r, r) \rightarrow 0$ near a caustic, which is physically meaningless. For regions near a caustic, we can expand the phase function in a power series of $\xi = p - p_c$ where p_c is the geometrical ray parameter of the ray forming a caustic at epicentral distance r_c . Since $\frac{\partial^2 \tau}{\partial p^2}(p_c, r_c) = 0$, the Taylor expansion yields

$$\tau(p, r) = \tau_c + \tau'_c \xi + \frac{1}{6} \tau''_c \xi^3 + \dots$$

where

$$\tau_c = \tau(p_c, r)$$

$$\tau'_c = \frac{\partial \tau}{\partial p}(p_c, r) = r - r_c$$

$$\tau''_c = \frac{\partial^3 \tau}{\partial p^3}(p_c, r) = -\frac{\partial^2 r_c}{\partial p^2}$$

Using up to the cubic term of this expansion, the displacement amplitude (4.1) may be approximated by

$$u(M, \omega) = (-1)^{\epsilon} S(\omega) \left(\frac{\omega}{2\pi\tau} \right)^{1/2} e^{-i\omega\tau_c + i\left(n\frac{\pi}{2} - \frac{\pi}{4}\right)} I \quad (4.5)$$

where

$$I = \int_{-\infty}^{\infty} f(p) e^{-i\omega\left(\tau_c \xi + \frac{1}{6} \tau_c'' \xi^3\right)} d\xi$$

Bringing the function $f(p)$ outside the integral sign at $p = p_c$ (since $f(p)$ is a slowly varying function) and introducing a new variable of integration

$$s = \text{sgn}(\tau_c''') \left| \frac{\omega \tau_c'''}{2} \right|^{1/3} \xi \quad (4.6)$$

we obtain

$$I = \left| \frac{2}{\omega \tau_c'''} \right|^{1/3} f(p_c) \int_{-\infty}^{\infty} Y(y, s) ds \quad (4.7)$$

where

$$Y(y, s) = e^{-i\left(\frac{s^3}{3} + ys\right)}$$

$$y = \text{sgn}(\tau_c' \tau_c''') \left| \omega \tau_c' \right| \left| \frac{2}{\omega \tau_c'''} \right|^{1/3}$$

The last Integral is the Airy function Ai (Abramowitz and Stegun 1965) and

$$I = 2\pi \left| \frac{2}{\omega \tau_c'''} \right|^{1/3} f(p_c) \text{Ai}(y) \quad (4.8)$$

Using this together with (4.2) in (4.5), we obtain the displacement in the vicinity of a caustic

$$u(M, \omega) = \frac{\chi(M, \omega, p_c)}{L(M)} e^{-i\omega\tau_c + i(n\frac{\pi}{2} - \frac{\pi}{4})} \quad (4.9)$$

where

$$\chi(M, \omega, p_c) = (-1)^E S(\omega) \left| \frac{(V\rho)_{M_0}}{(V\rho)_M} \right|^{1/2} \prod_{j=1}^k \left| \frac{(V\rho)_{o_j^-}}{(V\rho)_{o_j^+}} \right|^{1/2} R(o_j)$$

and

$$L(M) = \frac{\left| \frac{\partial^2 r_c}{\partial p^2} \right|^{1/3}}{2^{5/6} \omega^{1/6} \text{Ai}(y)} \left\{ \left[\frac{r \cos \theta_M \cos \theta_0}{\pi V_0 \sin \theta_0} \right]^{1/2} \prod_{j=1}^k \left[\frac{\cos \theta(o_j^+)}{\cos \theta(o_j^-)} \right]^{1/2} \right\}_{p_c}$$

A graph of the Airy function $\text{Ai}(y)$ is shown in Figure 4.2. It decreases monotonically with increasing $|y|$ if $y > 0$, and decreases in an oscillatory manner for $y < 0$. The physical meaning of this is that $y > 0$ and $y < 0$ correspond respectively to the shadow and illuminated zones of the caustic. At each point near the caustic on the illuminated side, two rays arrive almost simultaneously and the oscillation is due to the interference between these rays. On the shadow zone, no ray present and the diffracted energy decays exponentially with distance away from the caustic.

The above method has been used by Brekhovskikh (1960,1990), Sachs and Silbiger (1970), Cerveny and Zahradnik (1972), Hron and Chapman (1973), among others.

4.3 Modified Airy Approximation

The Airy approximation presupposes that $f(p)$ (equation 4.2) is slowly varying near a caustic. For rays in the illuminated zone of the caustic ($y < 0$), Choi and Hron (1981) proposed a different approach which avoids this limitation. We will briefly introduce their method and incorporate it into our ray tracing program.

Making the change of variable (4.6) but keeping $f(s)$ inside the integral, we have

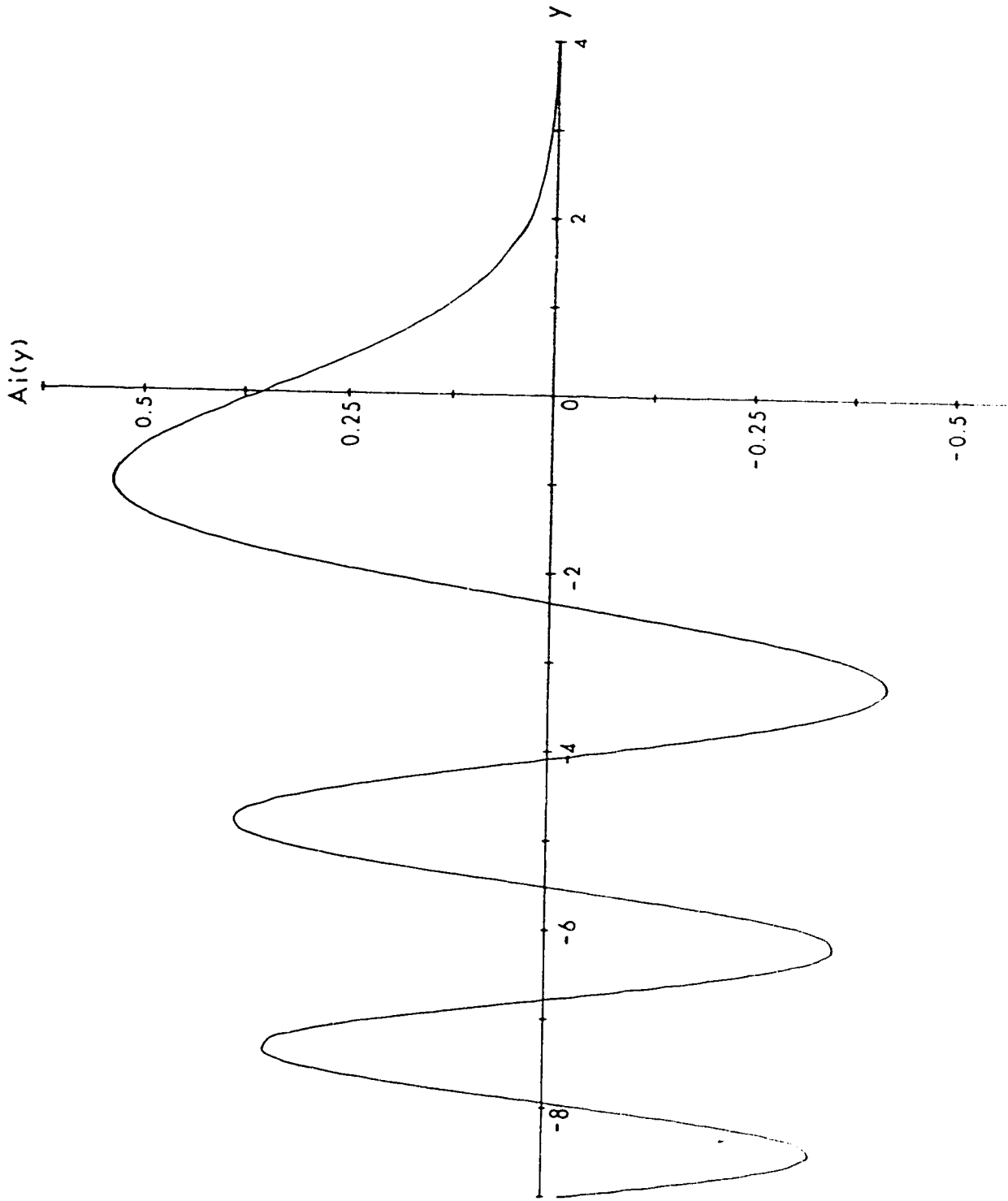


Figure 4.2 A graph of Airy function

$$I = \left| \frac{2}{\omega \tau_c'''} \right|^{\frac{1}{2}} \int_{-\infty}^{\infty} f(s) Y(y, s) ds \quad (4.10)$$

The saddle points of this integral are

$$s_m = \mp \sqrt{-y} : \quad m=1, 2 \quad (4.11)$$

which correspond to

$$p_m = p_c \mp \operatorname{sgn}(\tau_c''') \left| \frac{2\tau_c'}{\tau_c'''} \right|^{\frac{1}{2}} \quad (4.12)$$

Thus, it follows that

$$r = r_c + \frac{1}{2} \frac{\partial^2 r_c}{\partial p^2} (p_m - p_c)^2 \quad m=1, 2 \quad (4.13)$$

Comparing this with the Taylor expansion, we see that p_1 and p_2 are in fact the ray parameters of the two geometrical rays arriving at the same epicentral distance r . Specifically, p_1 and p_2 correspond respectively to the arrival on the direct and reverse geometrical ray branches which meet at the caustic.

Next, we deform the path of integration in (4.10) from the real s -axis to an alternate contour in the complex s -plane. The saddle points, branch cuts and poles in the complex s -plane are shown in Figure 4.3.

Using the contours of the integration as shown in Figure 4.2, we obtain from (4.10)

$$I = \left| \frac{2}{\omega \tau_c'''} \right|^{\frac{1}{2}} \left\{ f(p_1) \int_{\Gamma_1} Y(y, s) ds + f(p_2) \int_{\Gamma_2} Y(y, s) ds \right\} \quad (4.14)$$

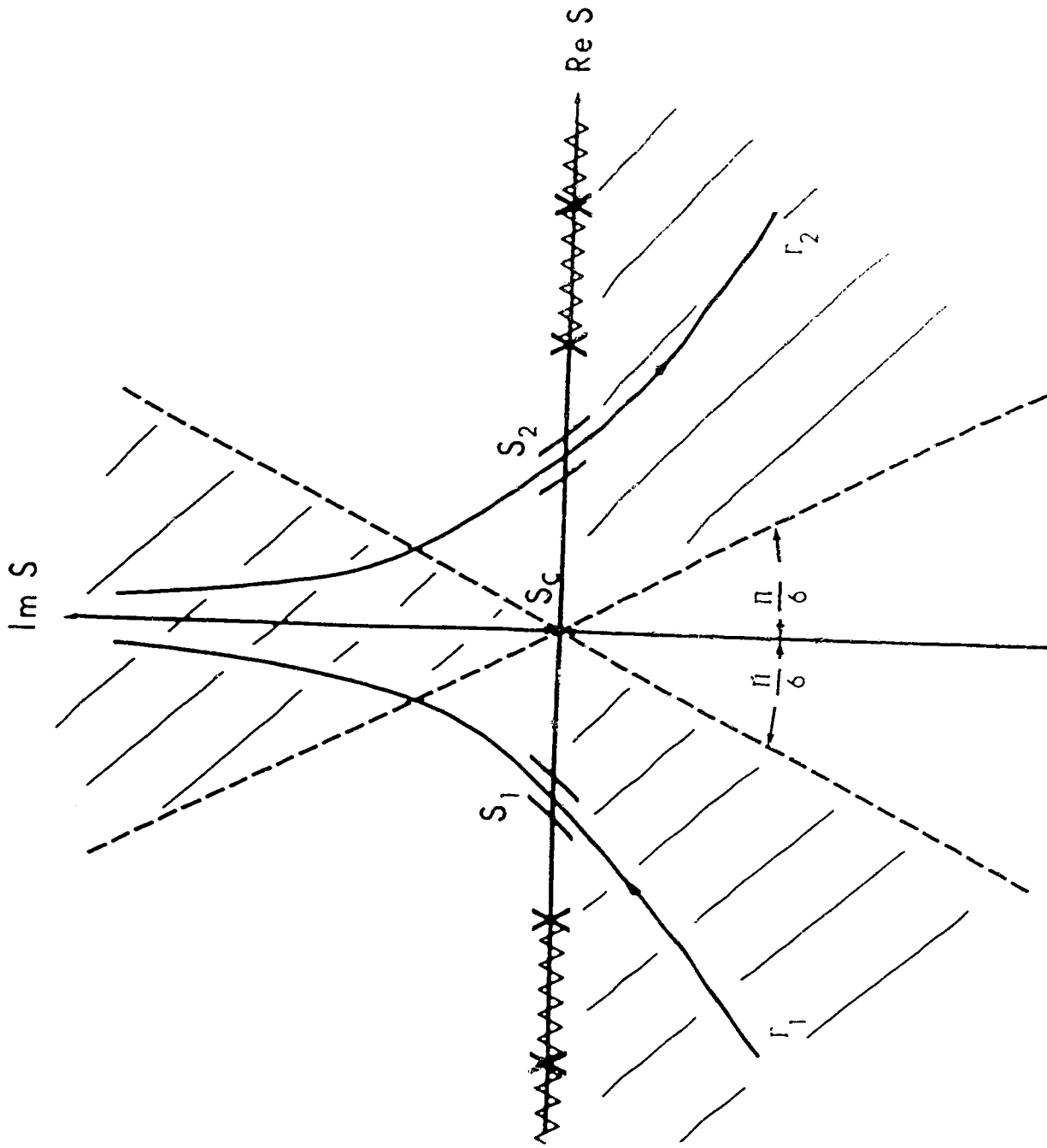


Figure 4.3 Poles, branch cuts, saddle points and contours on the s-plane for the integral 4.14

If the endpoints of the new contours are kept within the shadow zones in Figure 4.3, the integrals can be expressed as linear combinations of the Airy functions Ai and Bi. Then

$$I = \pi \left| \frac{2}{\omega \tau_c'''} \right|^{\frac{1}{3}} \left\{ f(p_1) [Ai(y) + iBi(y)] + f(p_2) [Ai(y) - iBi(y)] \right\} \quad (4.15)$$

This, together with (4.2) and (4.5), yields the displacement amplitude

$$u(M, \omega) = \sum_{m=1}^2 u_m(M, \omega) \quad (4.16)$$

where

$$u_m(M, \omega) = \frac{\chi(M, \omega, p_m)}{L_m(M)} e^{-i\omega \tau_c + i(n\frac{\pi}{2} - \frac{\pi}{4})}$$

and

$$L_m(M) = \frac{2^{\frac{1}{6}} \left| \frac{\partial^2 r_c}{\partial p^2} \right|^{\frac{1}{3}}}{\omega^{\frac{1}{6}} [Ai(y) \pm iBi(y)]} \left\{ \left[\frac{r \cos \theta_M \cos \theta_0}{\pi V(M_0) \sin \theta_0} \right]^{\frac{1}{2}} \prod_{j=1}^k \left[\frac{\cos \theta_j^+}{\cos \theta_j^-} \right]^{\frac{1}{2}} \right\}_{p_m}$$

where $\chi(M, \omega, p_m)$ denoted in (4.9) involves the product of reflection, transmission and conversion coefficients. This result is called as modified Airy approximation by Choi and Hron(1981).

If the function $f(p)$ is really slowly varying near caustic, then $f(p_1) = f(p_2) = f(p_c)$ and (4.16) reduces to the Airy approximation (4.9) as is expected.

All quantities in equation (4.4),(4.9) and (4.16) are easy to evaluate by the circular approximation method of ray tracing, which renders the expressions very useful in computing amplitude-distance curves or synthetic seismograms. The accuracy is closely related to $\frac{\partial r_c}{\partial \theta}$ and $\frac{\partial^2 r_c}{\partial \theta^2}$ which is discussed in section 3.5. Further discussion will be undertaken in the next Chapter. As pointed out by Choi and Hron (1981) or Choy and

Richards (1975), a $\pi/2$ phase shift is attributed to the seismic pulse each time the ray passes through an internal caustic. The circular approximation ray tracing as developed in Chapter 2 is well suited to determining the location and number of these caustics by simultaneously tracing two rays, separated by a small amount in take-off angle, and calculating the number and location of their intersections. Figures 4.4 and 4.5 are two numerical results which calculated the location of caustics using our circular approximation described above and analytical method which analytically calculated the ray curvature along the ray (personal communication with Dr. Hron). The caustic locations calculated by our circular approximation and the analytical method are exactly the same for this type medium.

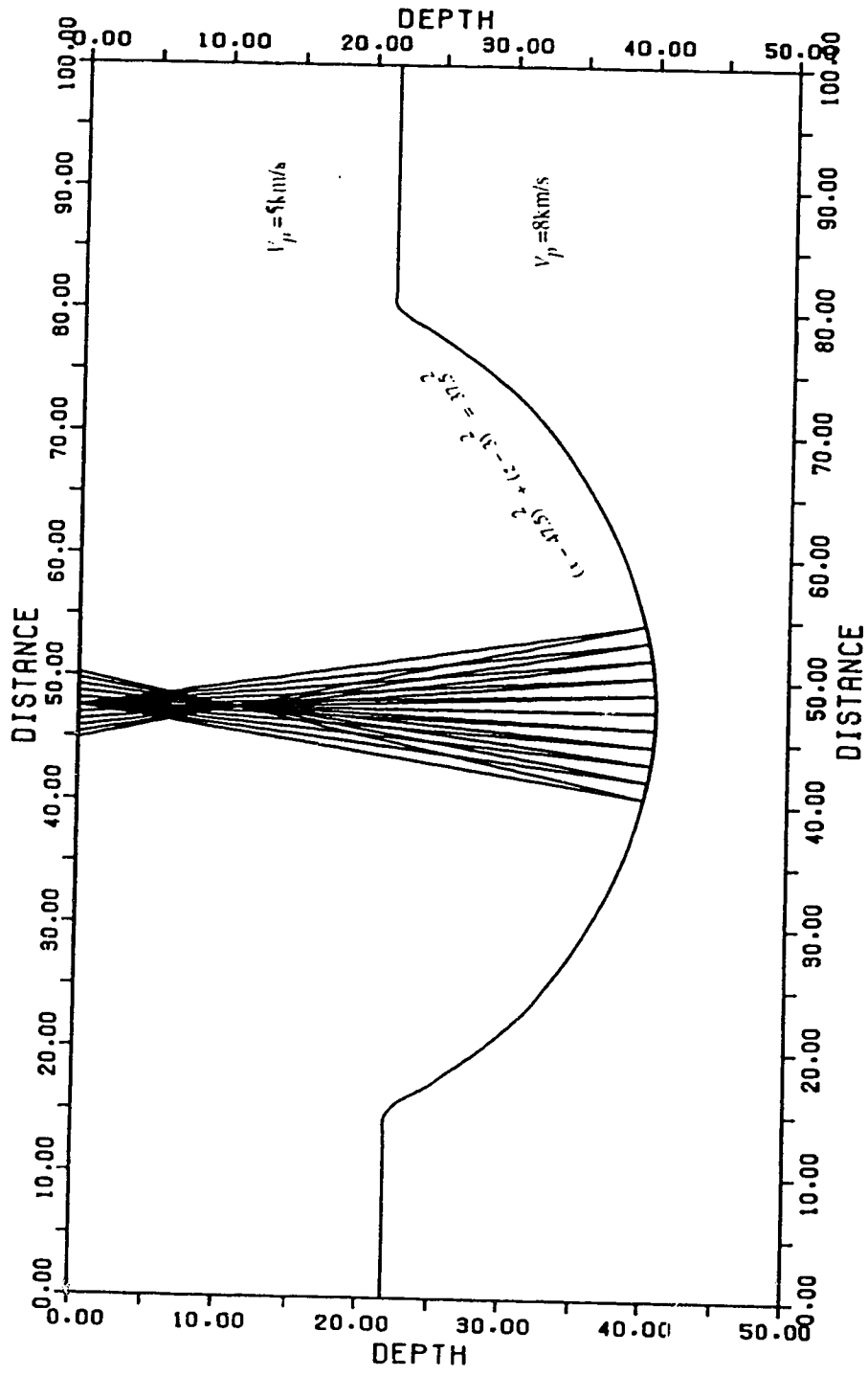


Figure 4.4 The focusing point of the wave PIP1 generated by a curved interface

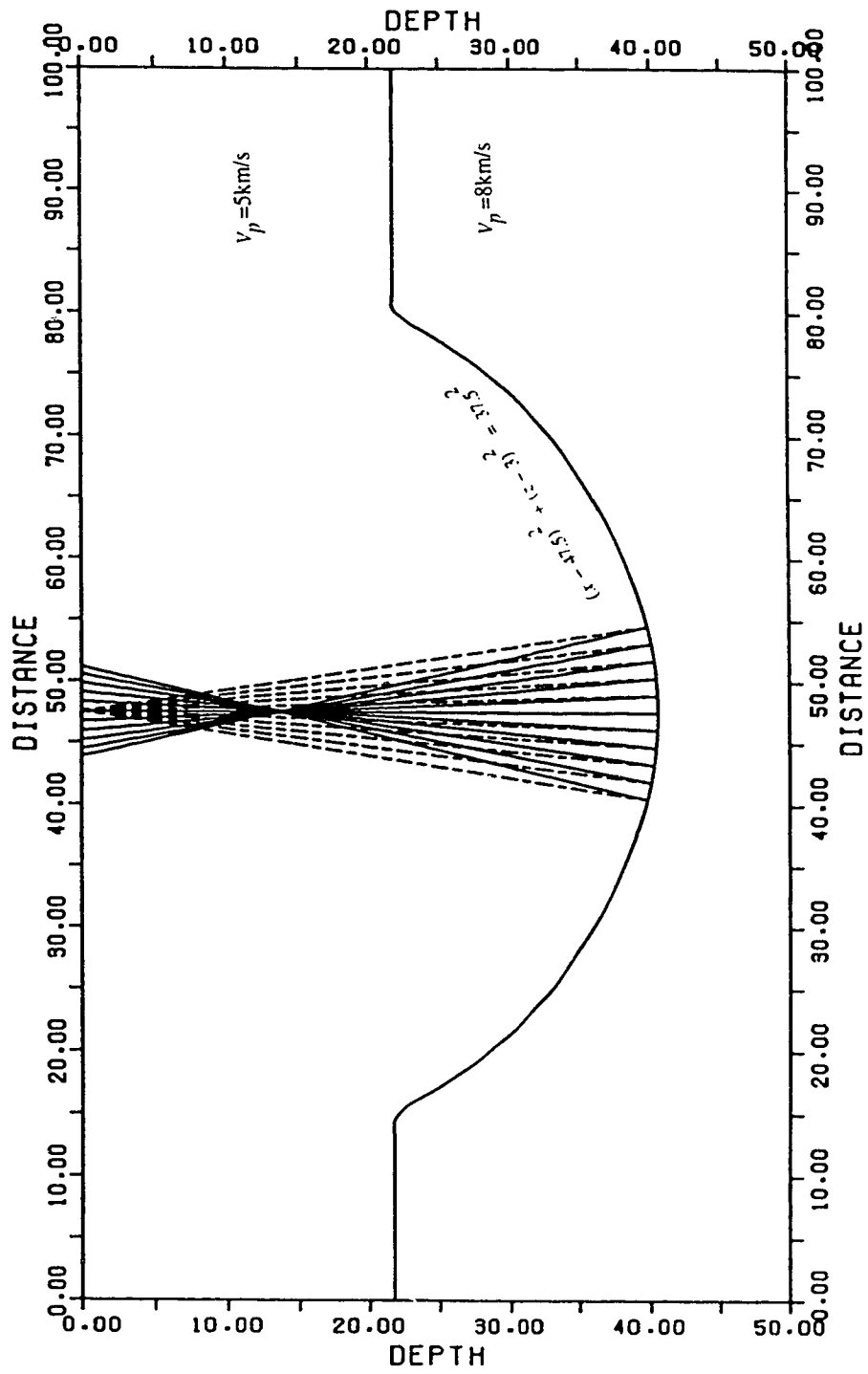


Figure 4.5 The focusing point of the wave PIS1 generated by a curved interface

Chapter 5 NUMERICAL RESULTS

5.1 Introduction

The results of tracing seismic ray and computing the geometrical spreading of wave fronts in two dimensional inhomogeneous media will be presented in this chapter.

5.2 Cerveny's Model

A vertically inhomogeneous model, which was used by Cerveny and Zahradnik (1972), was employed to study the wave field near a caustic. It consists of an upper layer with a linear velocity gradient overlying a homogeneous halfspace (Figure 5.1). The ray diagram and travel time curves are shown in Figure 5.2. A surface caustic at epicentral distance 120 Km can be calculated by both analytical techniques (Brekhoskikh 1960 and Choi and Hiron 1981), and our method. To compute the ray amplitude near this caustic (by equations 4.9 and 4.16), $\frac{\partial^2 r_c}{\partial \theta^2}$ or $\frac{\partial^2 r_c}{\partial p^2}$ must be first calculated. We use both analytical methods and the circular approximation to calculate the values listed in Table 5.1.

Table 5.1 The second derivative at caustic calculated by different methods

Method	$\frac{\partial^2 r_c}{\partial \theta^2}$	$\frac{\partial^2 r_c}{\partial p^2}$
Circular Approximation	762.633	121591.267
Formula (3.25)	759.779	121122.986
Analytical solution	761.509	121399.624

Figure 5.3 contains the vertical amplitude in the vicinity of the caustic calculated by the ray method, the Airy approximation and by the modified Airy approximation. It

indicates that the ray branches no longer have comparable amplitude near the caustics when calculated by the ray method. So, near the caustic, the ray method is inapplicable and Airy and modified Airy approximations provide more accurate amplitudes. But, our ray tracing program can reasonably calculate the $\partial^2 r / \partial p^2$ (Table 5.1). Figure 5.4 contains the ray amplitudes using the numerical $\partial^2 r / \partial p^2$.

The results show that our ray tracing methods provide reliable calculations of amplitudes whether or not caustics are present.

Using two point ray tracing and some ray generation schemes (Hron, 1972, 1973, Clarke), we can easily obtain the synthetic seismogram for a given receiver.

VELOCITY MODEL

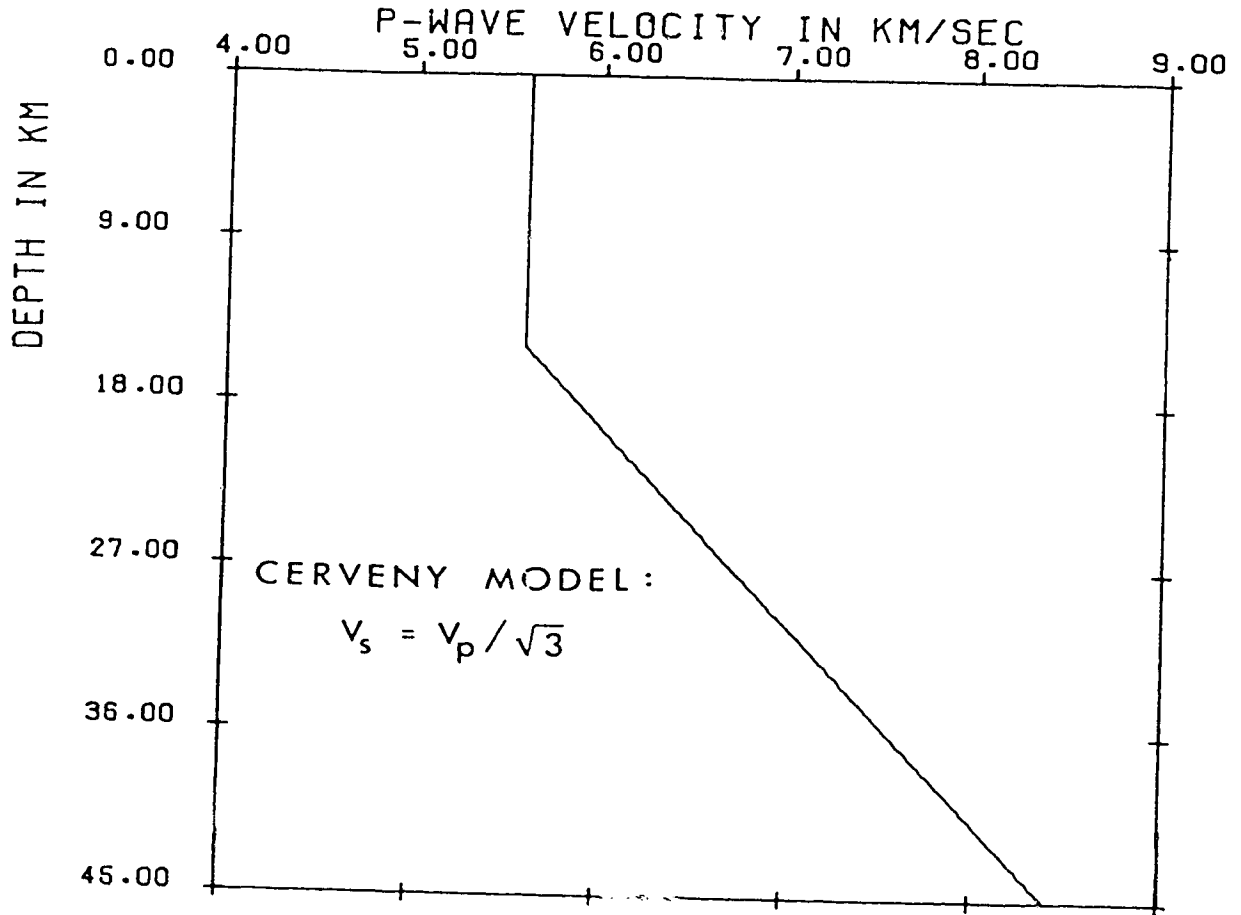


Figure 5.1 Cerveny's model to investigate a caustic at surface

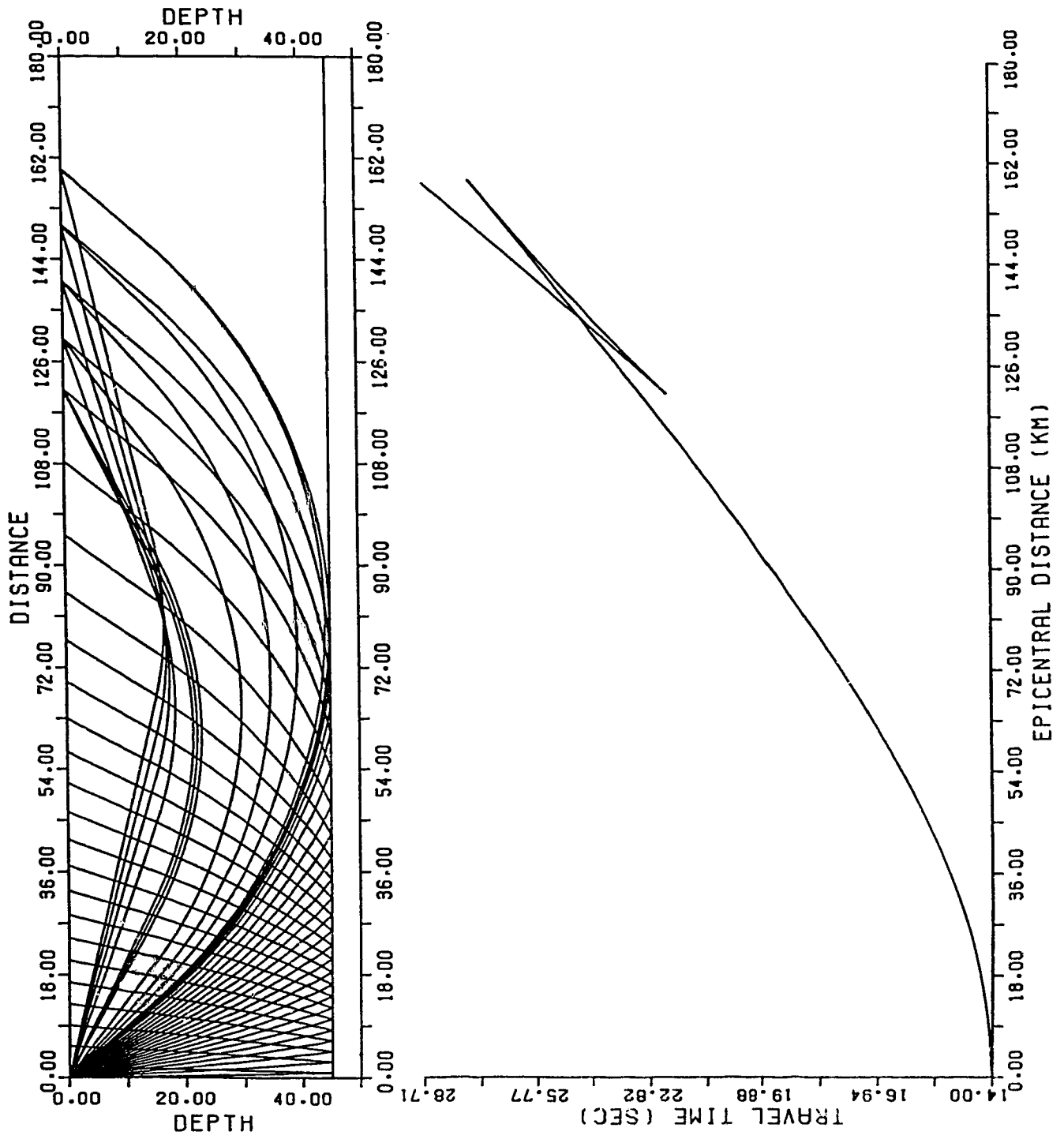


Figure 5.2 Ray diagram and travel time-distance curve for the Cerveny's model

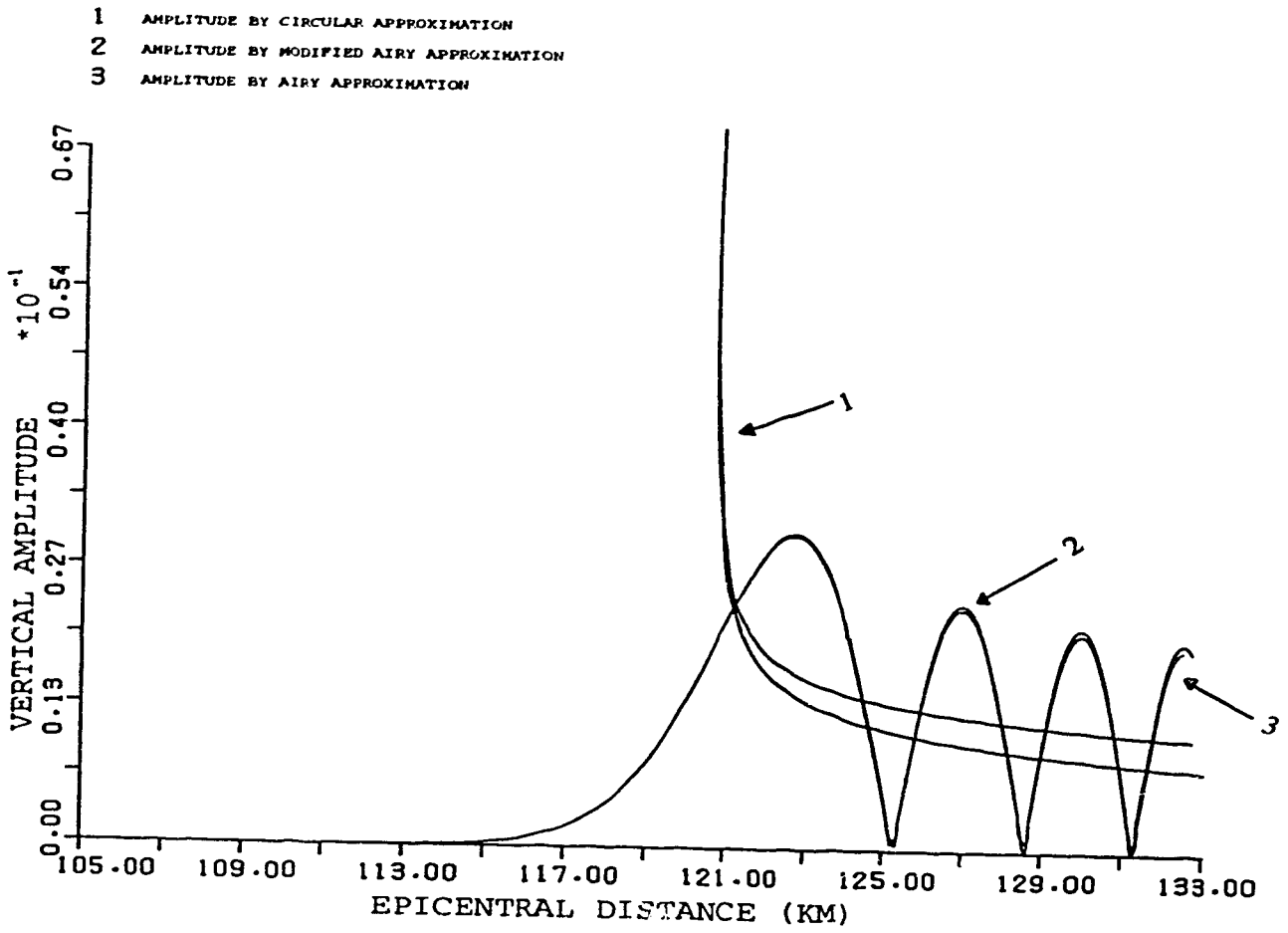


Figure 5.3 Amplitude-distance curves of refracted P waves calculated by ray method and modified Airy approximation. $\frac{\partial^2 r}{\partial \phi^2}$ is analytical.

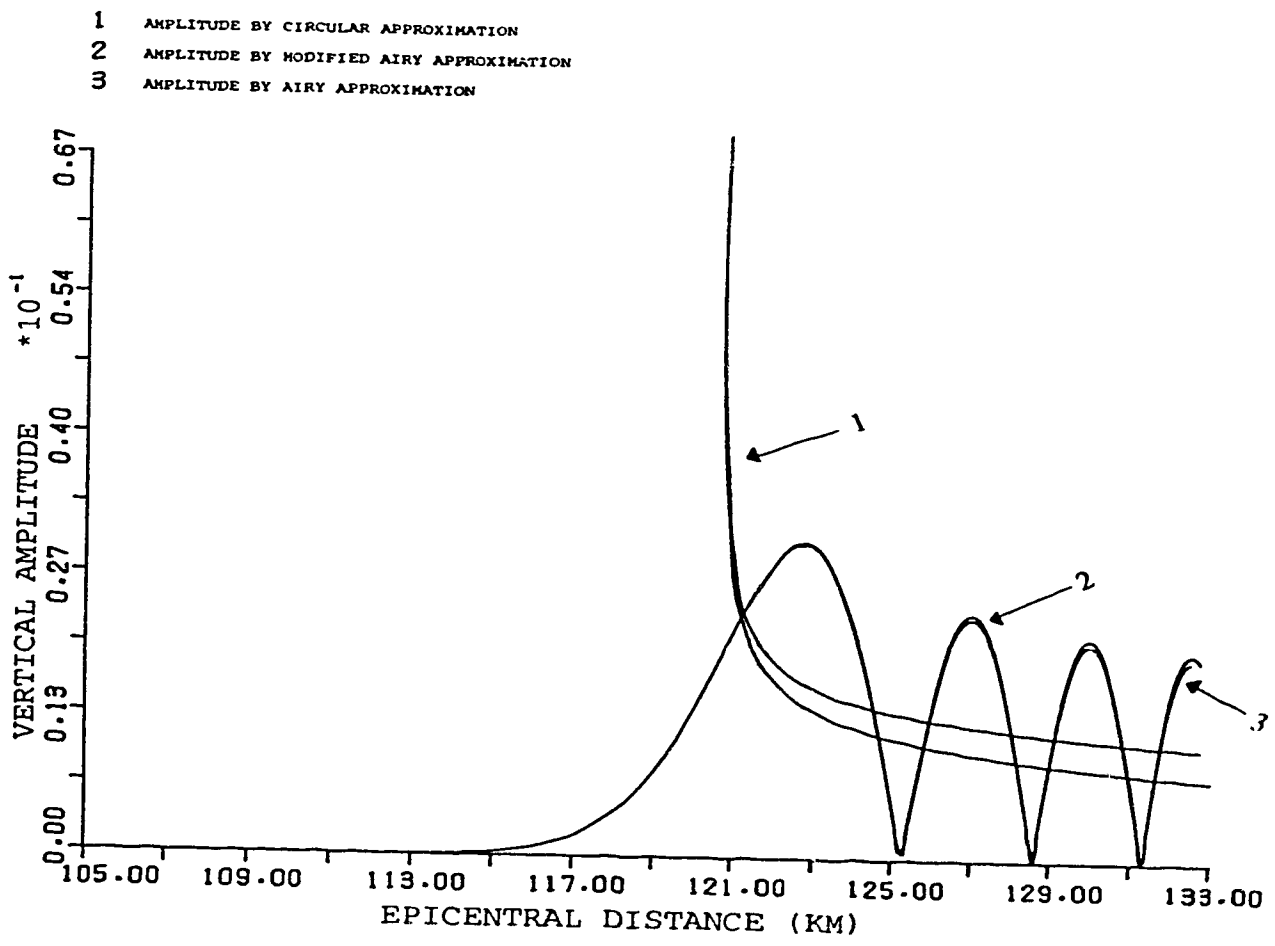


Figure 5.4 Amplitude-distance curves of refracted P waves calculated by ray method and modified Airy approximation. $\frac{\partial^2 r}{\partial \phi^2}$ is obtained by numerical method from our ray tracing program

5.3 A generally inhomogeneous medium

Two models (one has homogeneous layers as shown in Figure 5.5, and the other has generally inhomogeneous layers, as shown in Figure 5.6 but both have the same curved interface) are designed to show that either an inhomogeneity or a curved interface can form a focusing point. Figure 5.5 shows that there is no focusing point in the layer for the chosen rays while Figure 5.7 shows clearly that there is a focusing point formed by those rays due to the inhomogeneity of the medium.

The following will find the ray amplitudes, or its vertical component of P-waves for harmonic source of frequency $f=15$ Hz for this type of medium. Figure 5.8 is the travel time - epicentral distance curve for the rays of the velocity model shown in Figure 5.7. Figure 5.9 contains the ray amplitude-distance curves for different ray branches calculated by the ray method, which again no longer have physically justified amplitudes near the caustic. Figure 5.10 contains the amplitude curves calculated by our modified Airy approximation, which has reasonable accurate results in the vicinity of caustics. This shows our method can handle generally inhomogeneous media successfully.

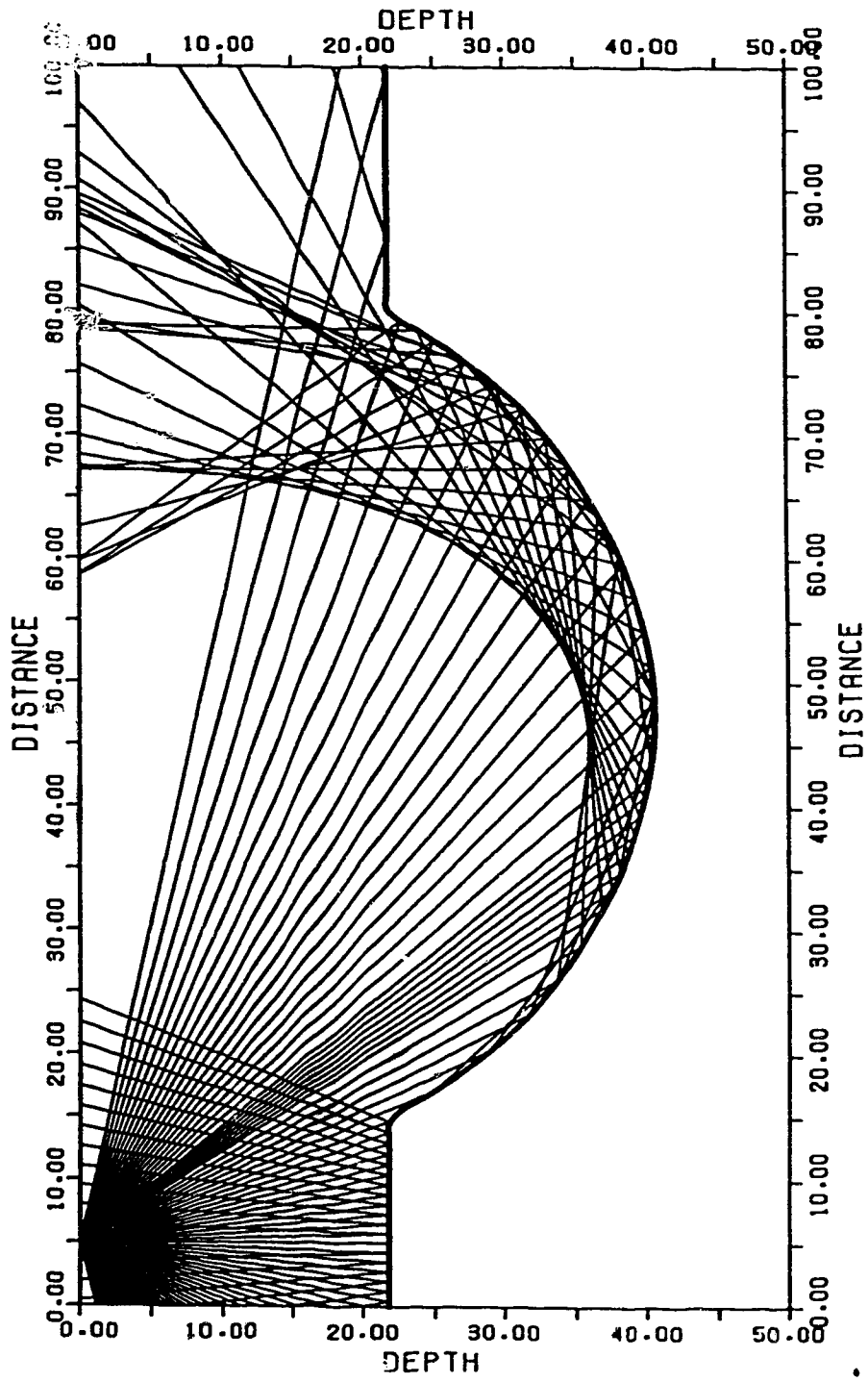


Figure 5.5 Ray diagram for an medium with curved interface and homogeneous layers (The same model for Fig. 4.4)

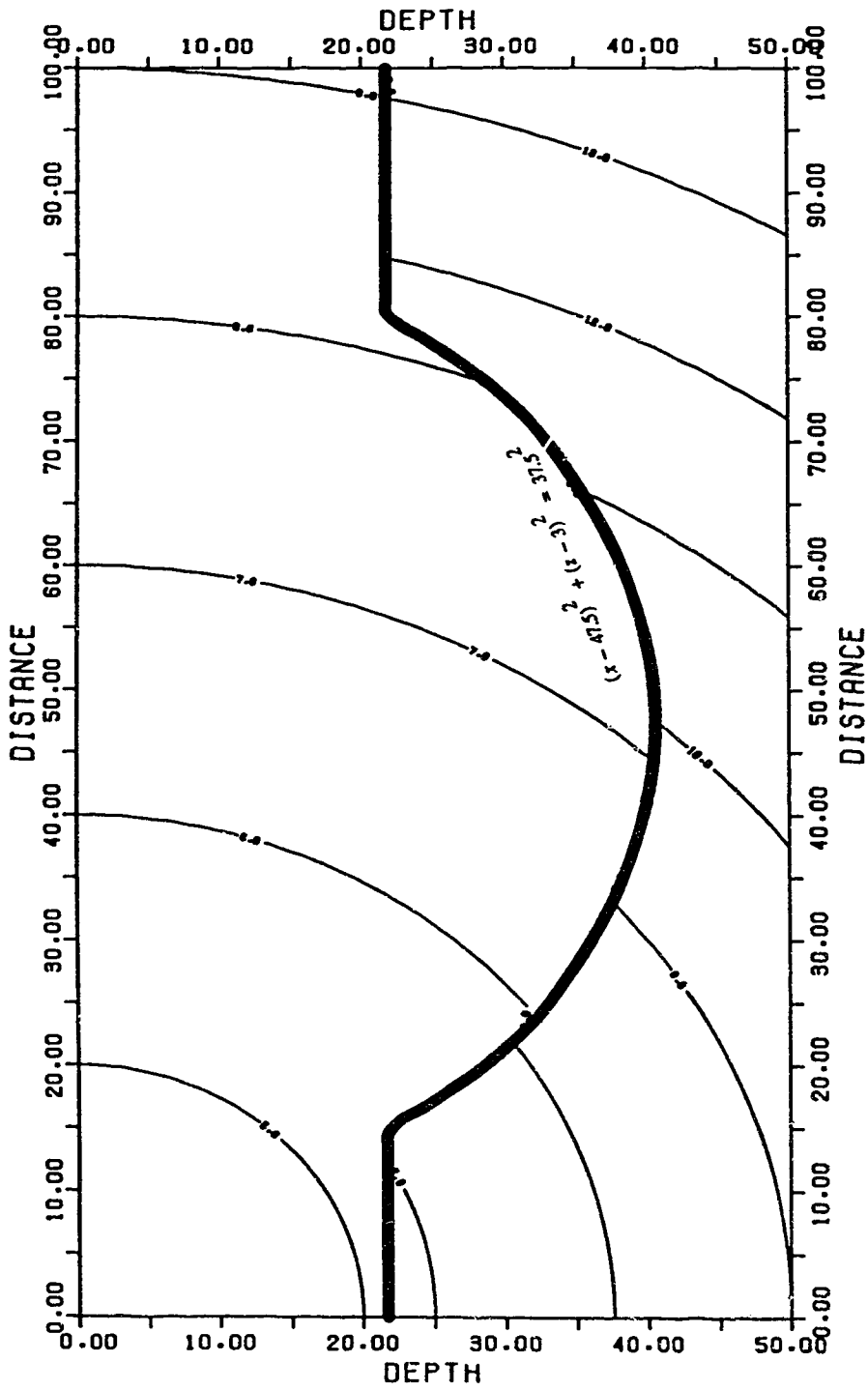


Figure 5.6 A laterally inhomogeneous model

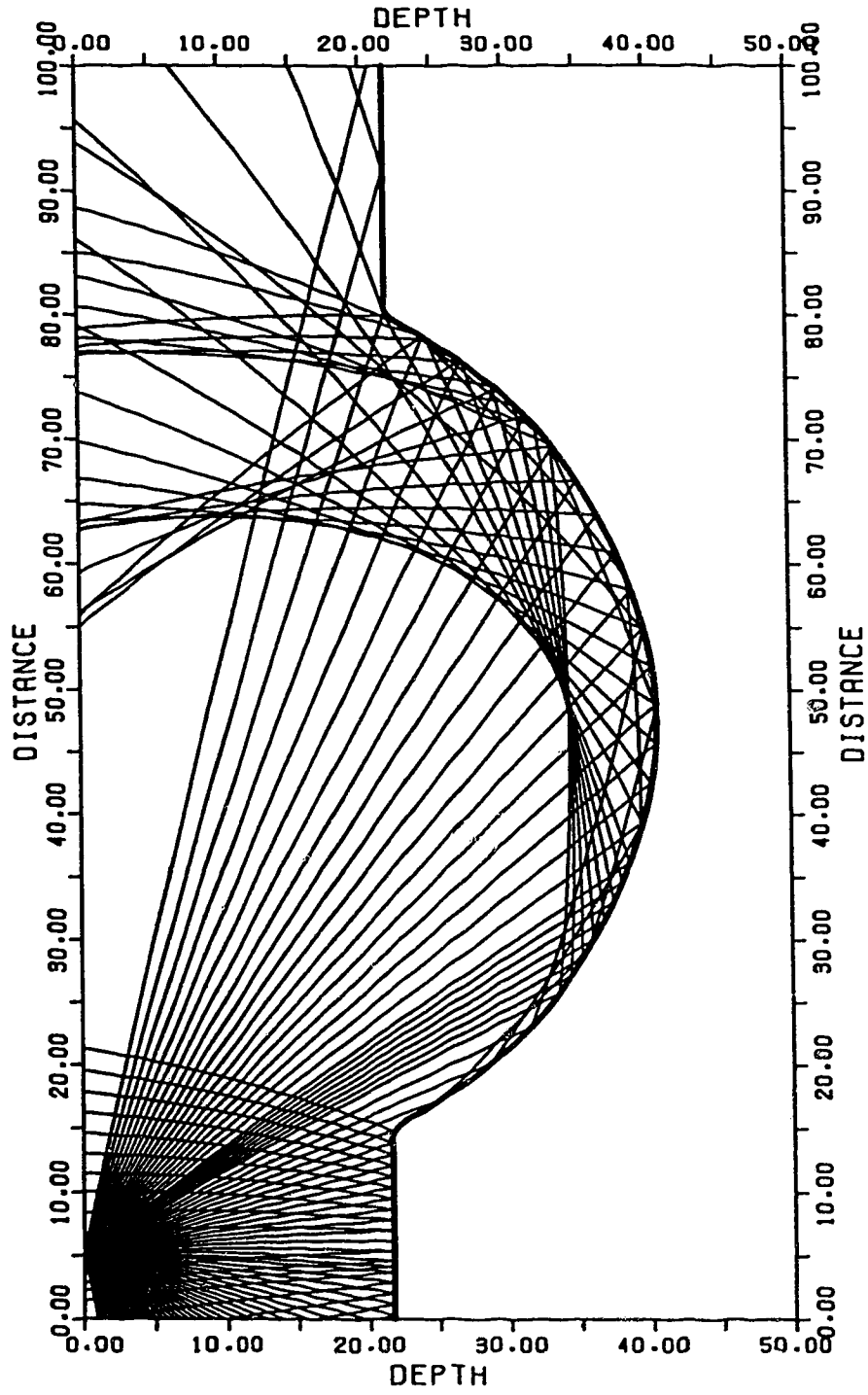


Figure 5.7 Ray diagram for this laterally inhomogeneous medium

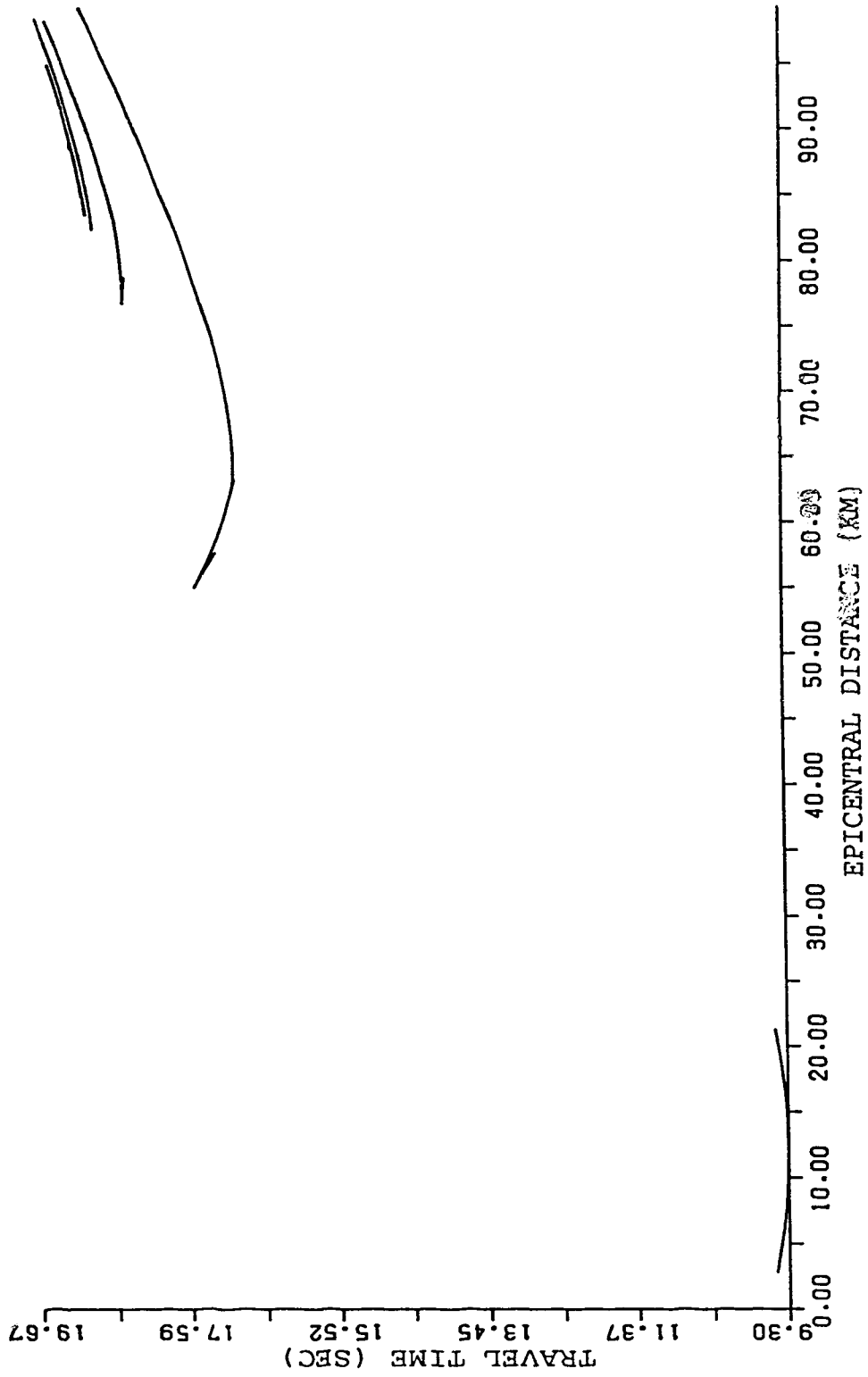


Figure 5.8 Travel time-distance curve

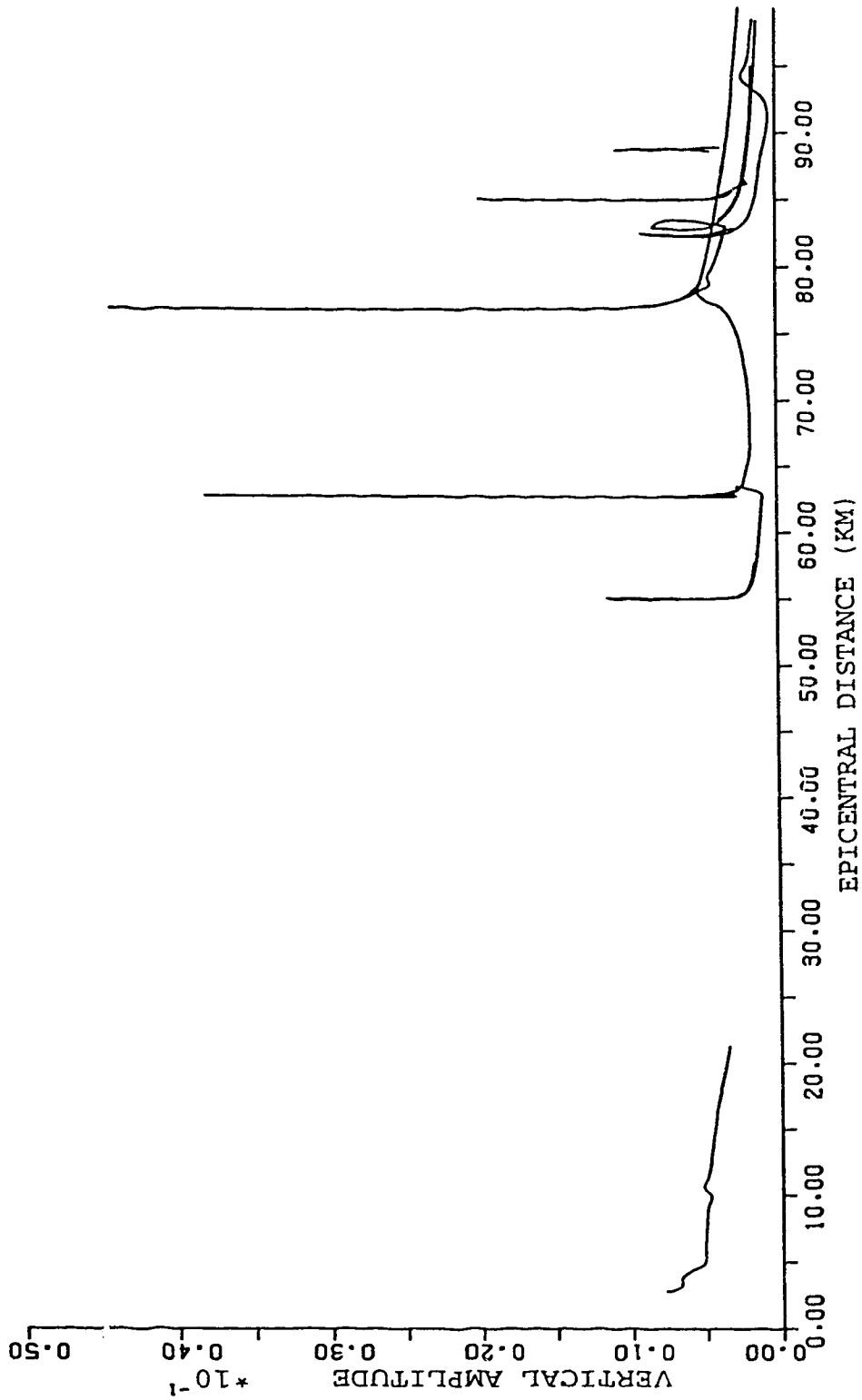


Figure 5.9 Vertical amplitude calculated by ray method

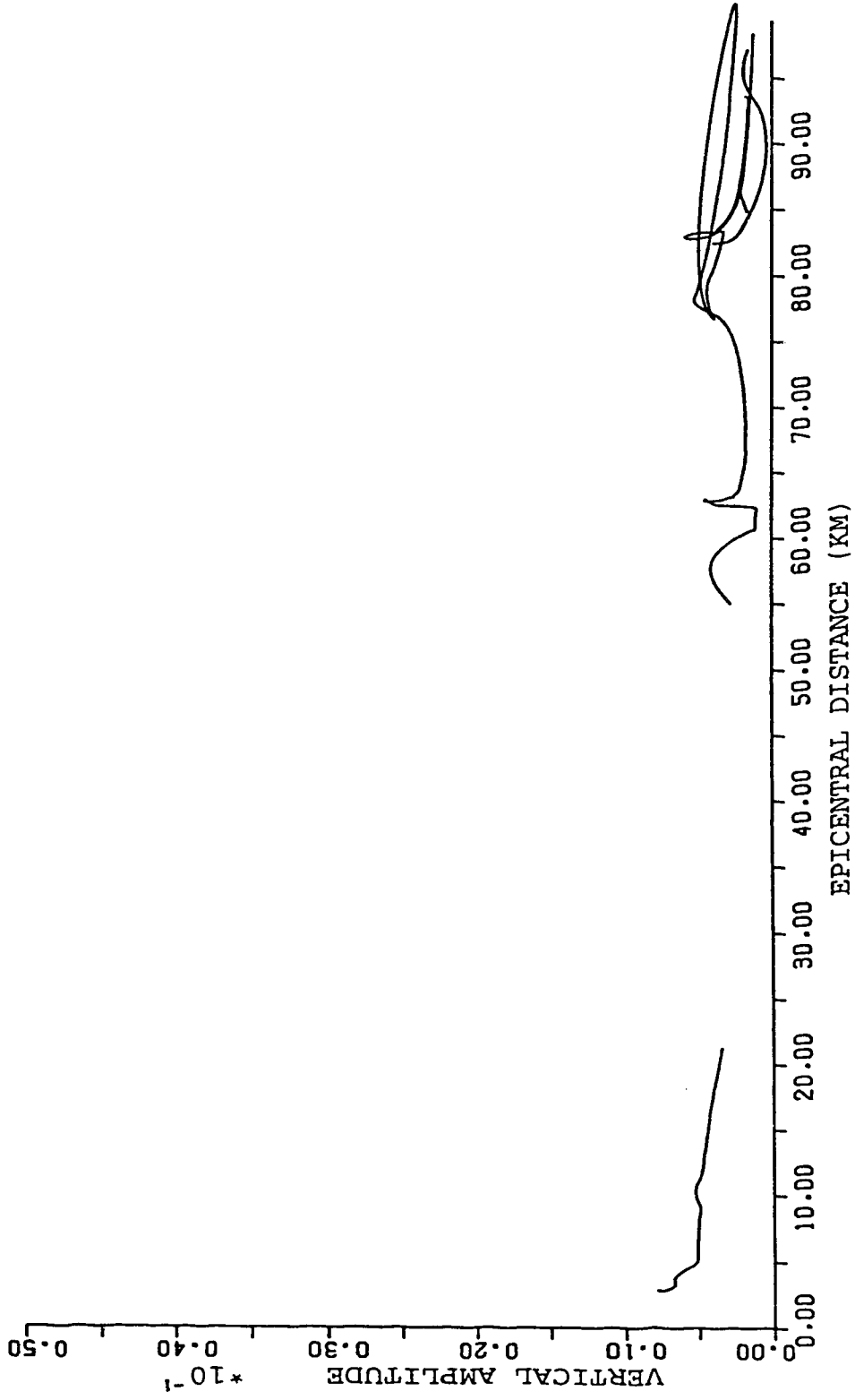


Figure 5.10 Vertical amplitude calculated by modified Airy approximation

5.4 Bohemian Massif

The Bohemian Massif (see the P wave velocity model in Figure 5.11, which is generated by interpolation from the known velocity values) was used extensively by Psencik (1972) to study the travel time of primary P waves. This model for the earth's crust allows a full demonstration of the general modelling process for seismic waves in laterally inhomogeneous media. Figure 5.12 shows the ray diagram of reflected and refracted P rays from a source located at (155.2 km, 0 km) . To see the accuracy of our method, a comparison between the differential equation method(Marks and Hon 1980) and our method is listed in Table 5.2 for a ray taking off at the angle of 40° measured from the vertical.

Table 5.2 The comparison of P rays computed by different methods

Ray method	Take-off angle (degree)	Arrival time (sec)	Angle with vertical (degree)	Emergent distance (km)
Differential Eq.	40.	18.301	40.339	247.454
Circular approx.	40.	18.371	41.630	247.835

To further investigate the accuracy and stability of our method for this type of media, we used different cell sizes to divide the medium and calculate two rays' travel time, emergence distance and emergence vertical angle, both of which are necessary to calculate the ray amplitude. One is a reflected ray with a take-off angle of 40°, and the other is a refracted ray with a take-off angle of 60°. The results are listed in Table 5.3 and the ray diagram are in Figure 5.13. It appears that although there are some differences between the results, they are acceptable. The error is mainly introduced by the velocity interpolation when using different cell sizes.

Table 5.3 Rays in a medium divided by different cell sizes

Cell size	0.5 × 0.25km		2 × 1km		4 × 1km	
	40°	60°	40°	60°	40°	60°
Offset (Km)	246.382	273.312	247.835	274.676	249.186	275.127
Arrival time (sec)	18.217	20.702	18.371	20.866	18.530	20.992
Emergency Angle	42.94°	58.317°	41.63°	55.783°	41.863°	59.463°

We'll use mesh size 2 × 1km to calculate the ray diagram and amplitude. Figure 5.14 is the travel time - distance curve. Figure 5.15 is the amplitude curve calculated by the ray method and Figure 5.16 shows the the reasonable ray amplitude in the vicinity of caustics calculated by the modified Airy function. Further investigation was made at take-off angles ranging from 73.70° to 74.37° (where a surface caustic is located at (297.8 km, 0)), and from 74.60° to 81°. Figures 5.17 and 5.18 are two ray branches near the caustic and Figure 5.19 is the travel time - distance curve of these two ray branches. Figure 5.20 shows the amplitude - distance curves calculated by the ray method and and the modified Airy approximation. It shows again that the modified Airy approximation can get more reasonable results near caustics. Figures 5.21 to 5.23 contain ray diagram and the travel time, amplitude curves for refracted rays without caustics.

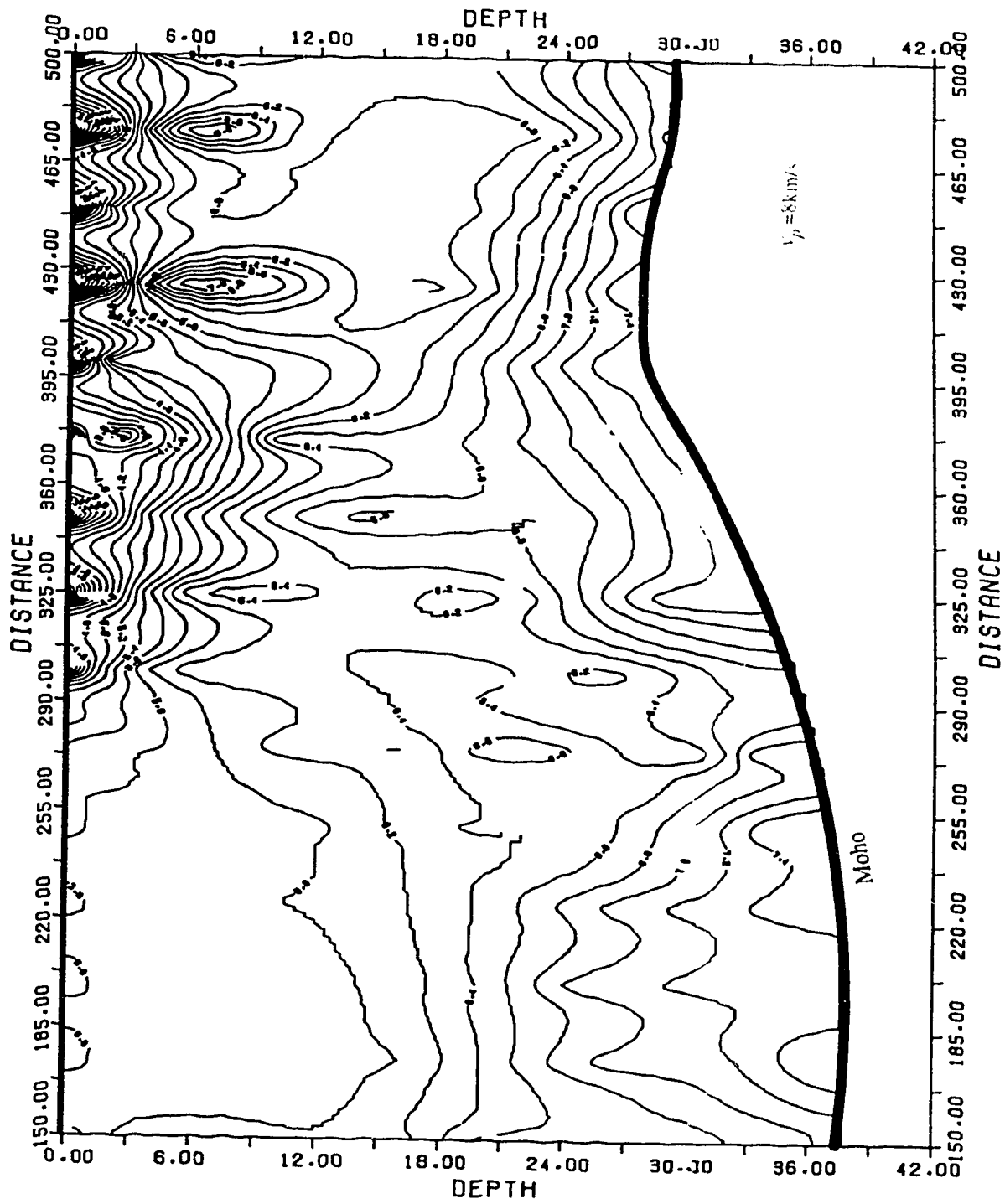


Figure 5.11 P-wave isovelocity contour of Bohemian Massif

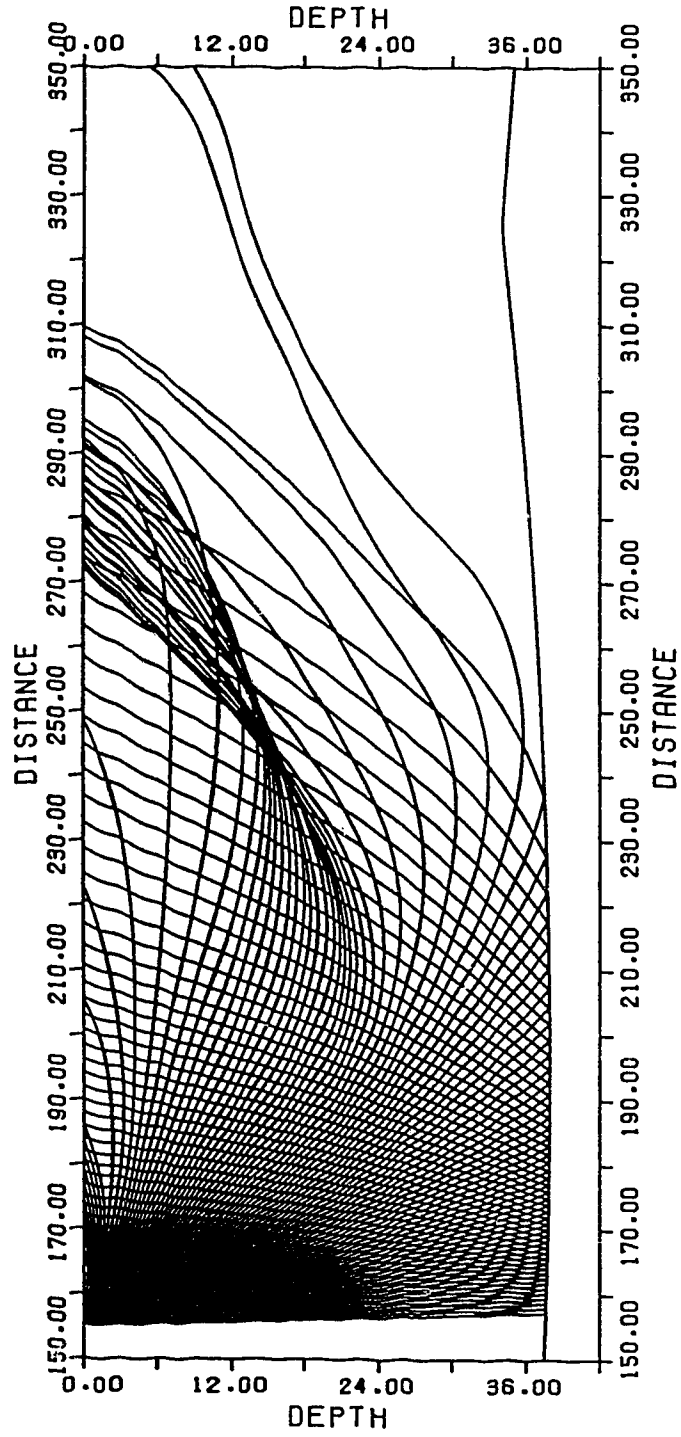
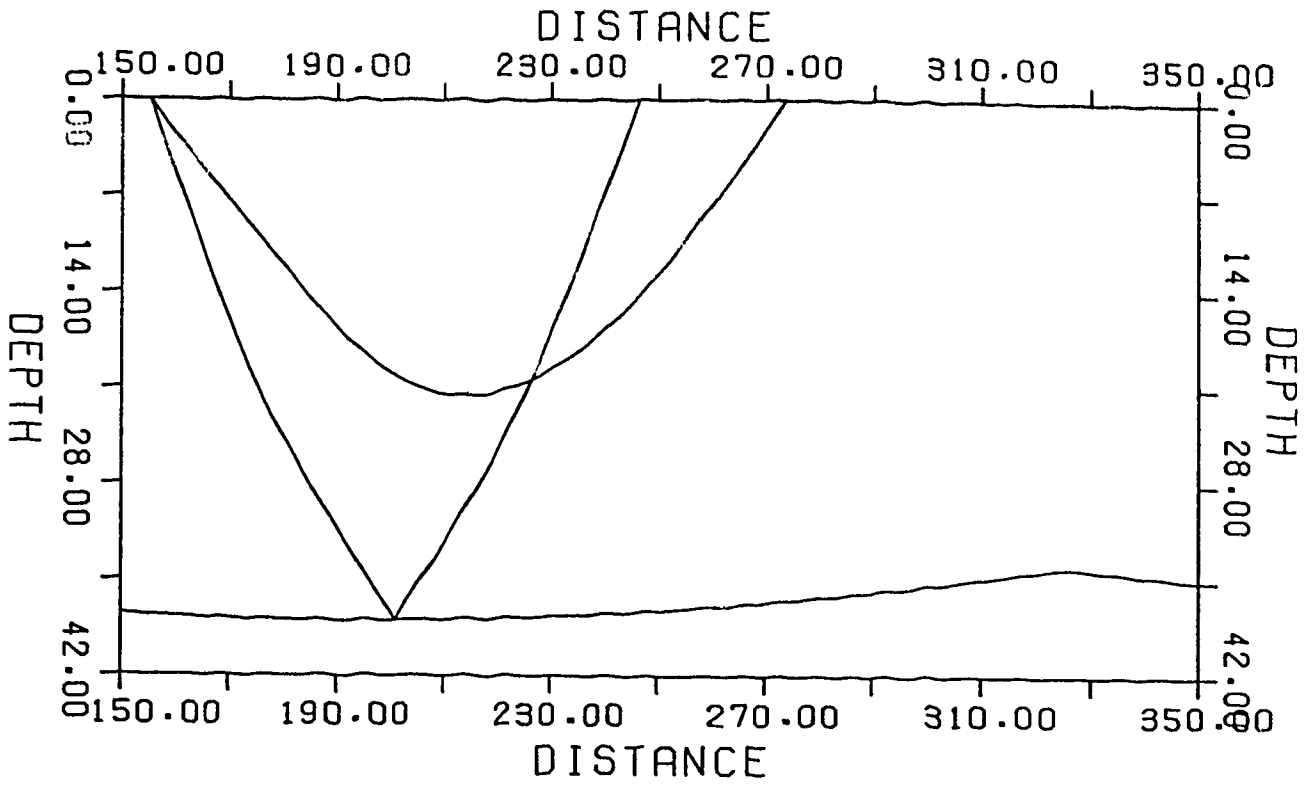
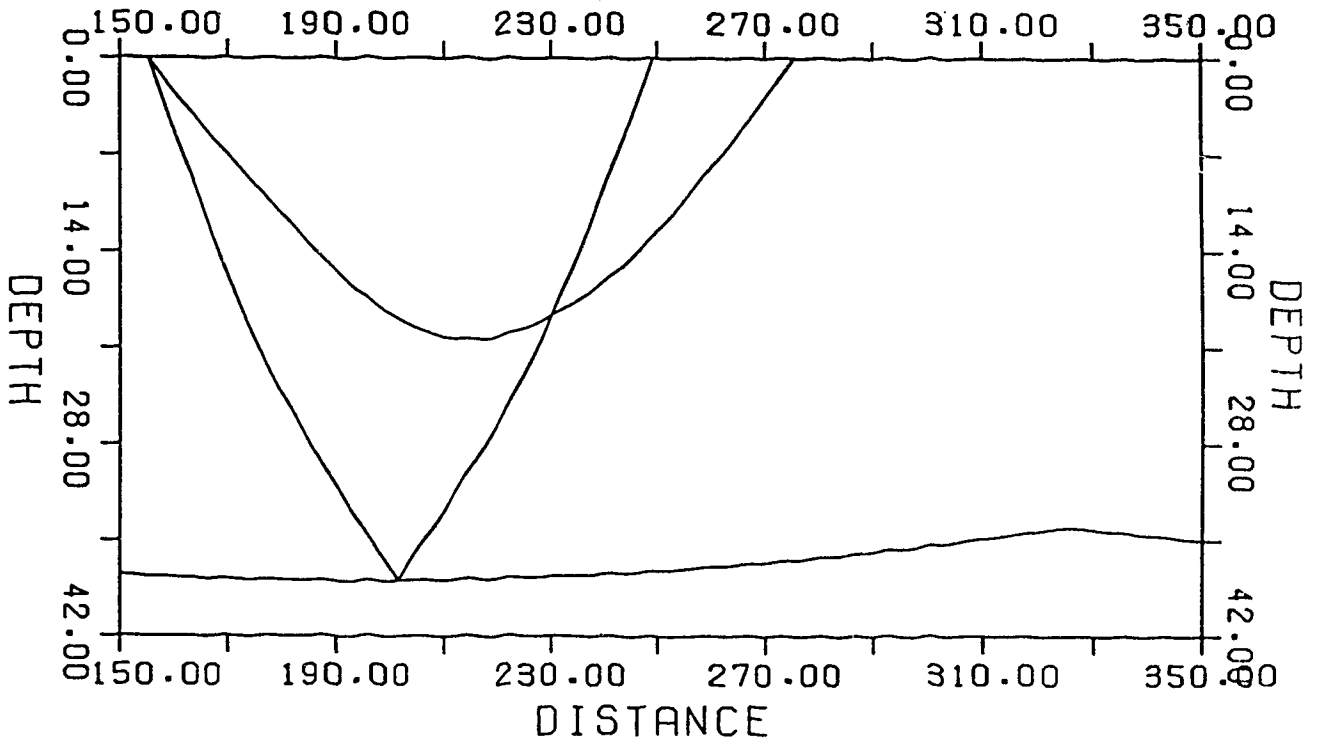


Figure 5.12 Ray diagram of reflected and refracted P wave with source at 155.2 km



a



b

Figure 5.13 a) Ray diagram with cell size $0.5 \times 0.25 \text{ Km}$ b) Ray diagram with size $4 \times 1 \text{ Km}$

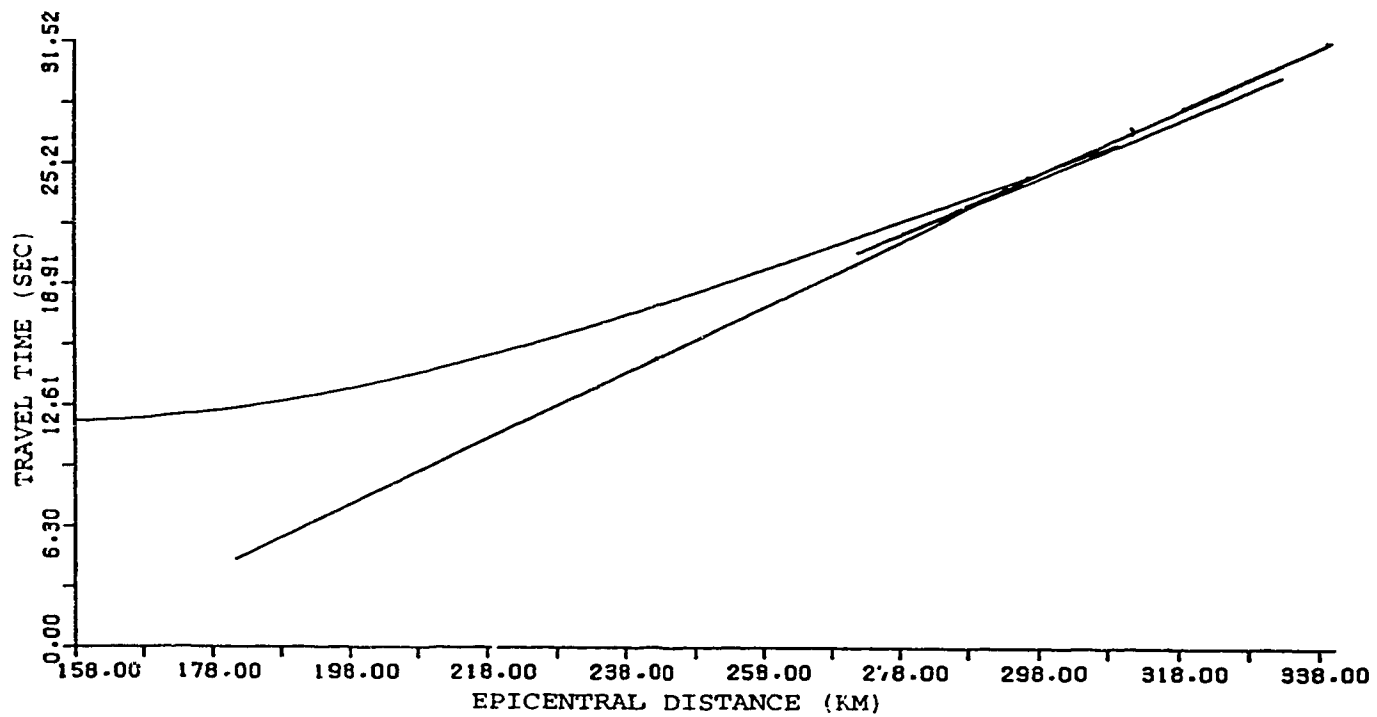


Figure 5.14 Travel time - distance curve

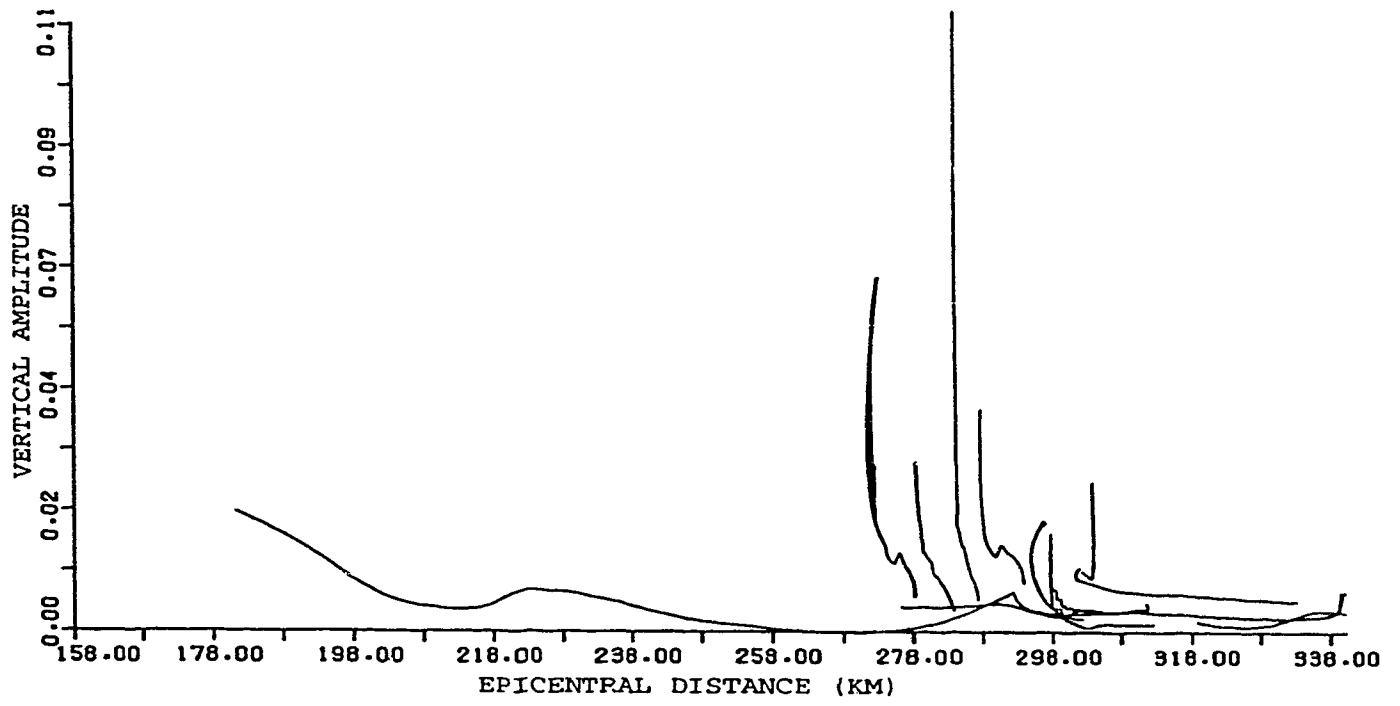


Figure 5.15 Ray amplitudes calculated by ray method

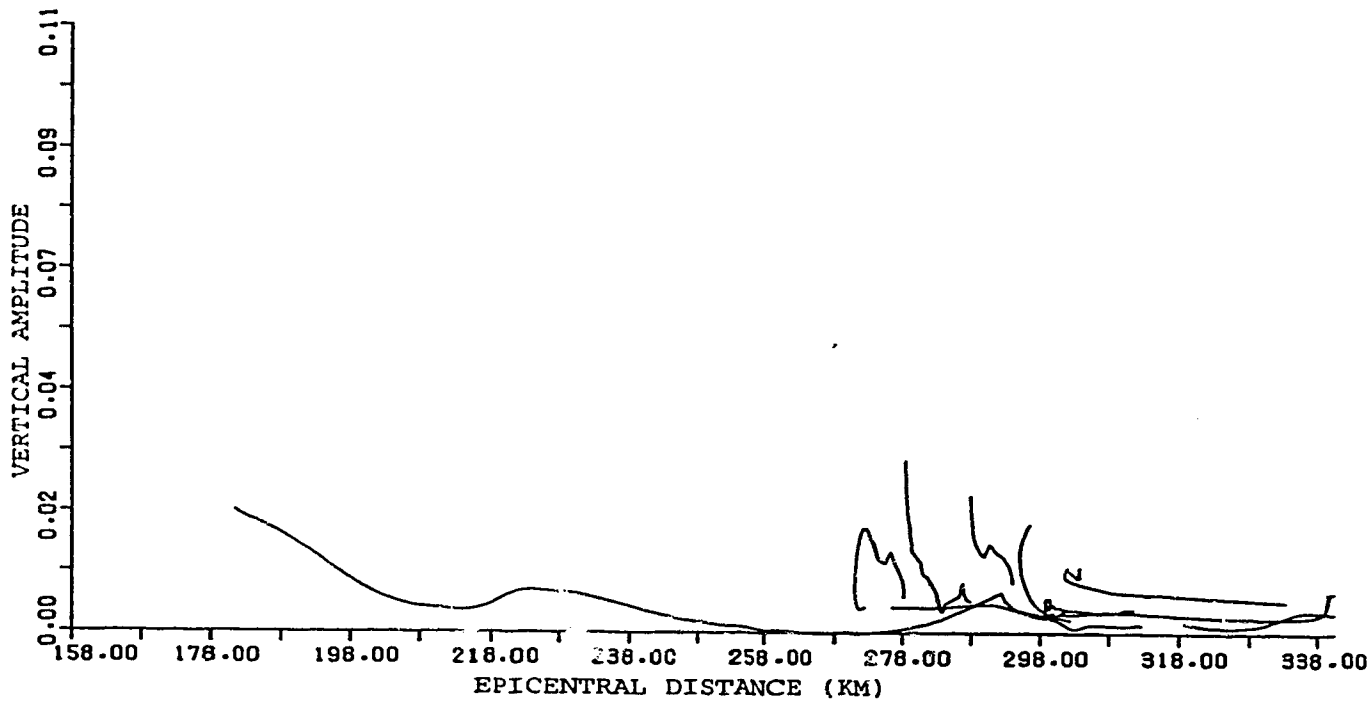


Figure 5.16 Ray amplitude near caustics calculated by modified Airy approximation

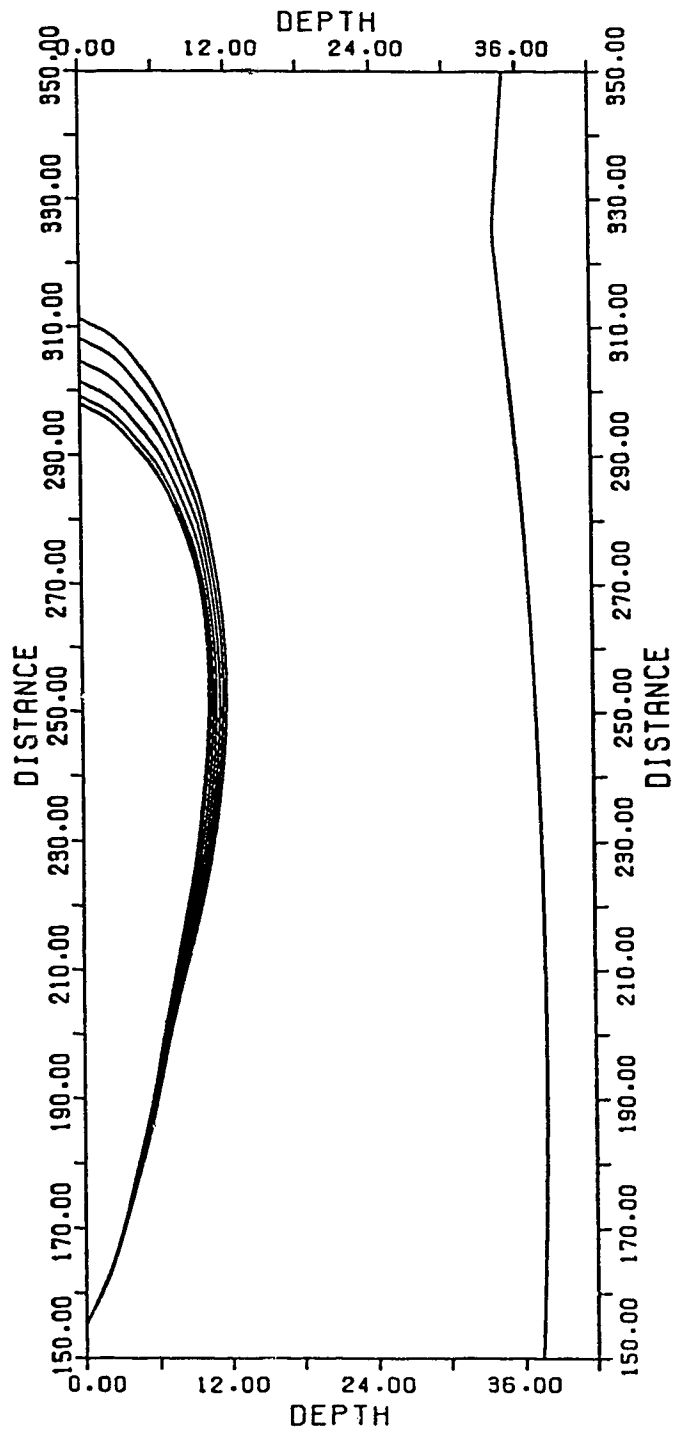


Figure 5.17 One ray branch with negative $\frac{dr}{d\theta}$ for one of the caustics located at 297.8 km

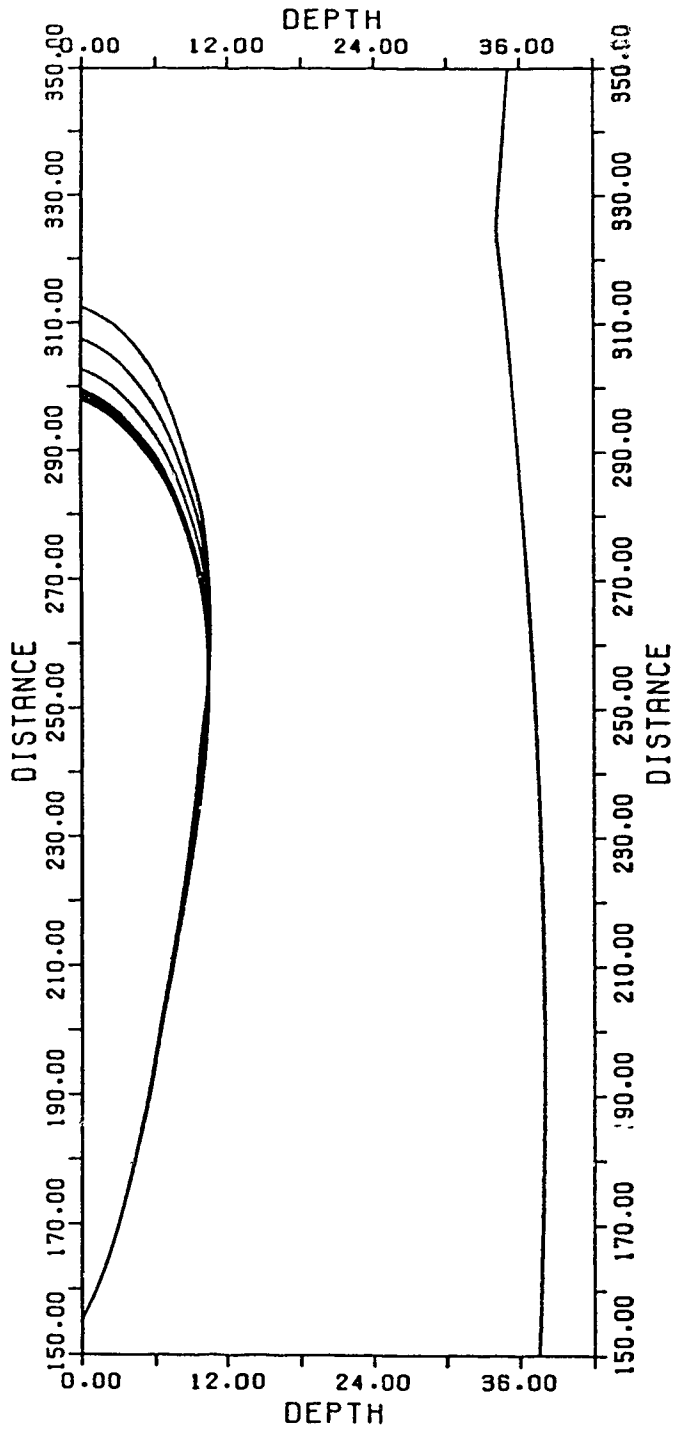


Figure 5.18 Another ray branch with positive $\frac{dr}{d\theta}$ for the caustic located at 297.8 km

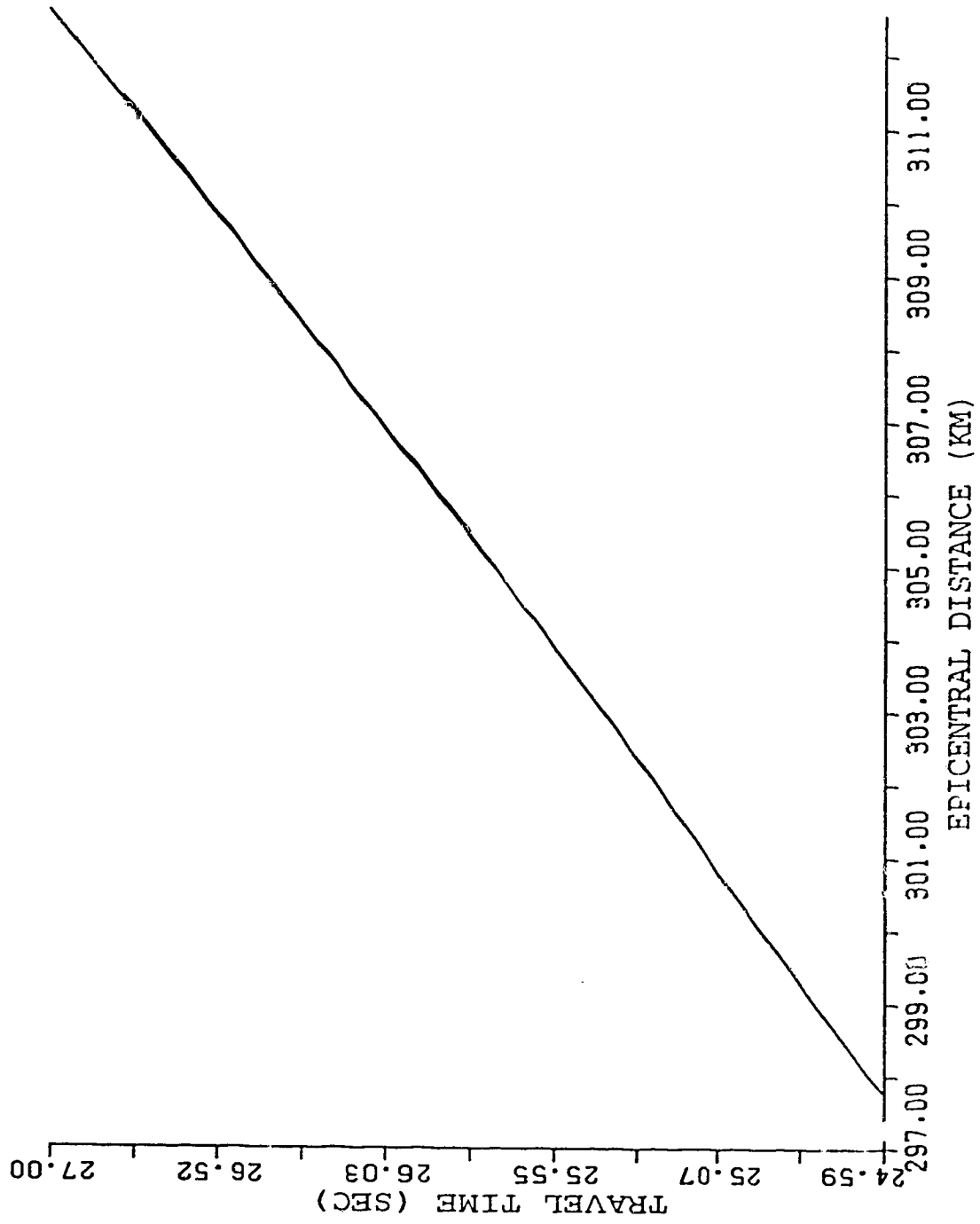


Figure 5.10 Travel time - distance curve of the caustic located at 297.8 km

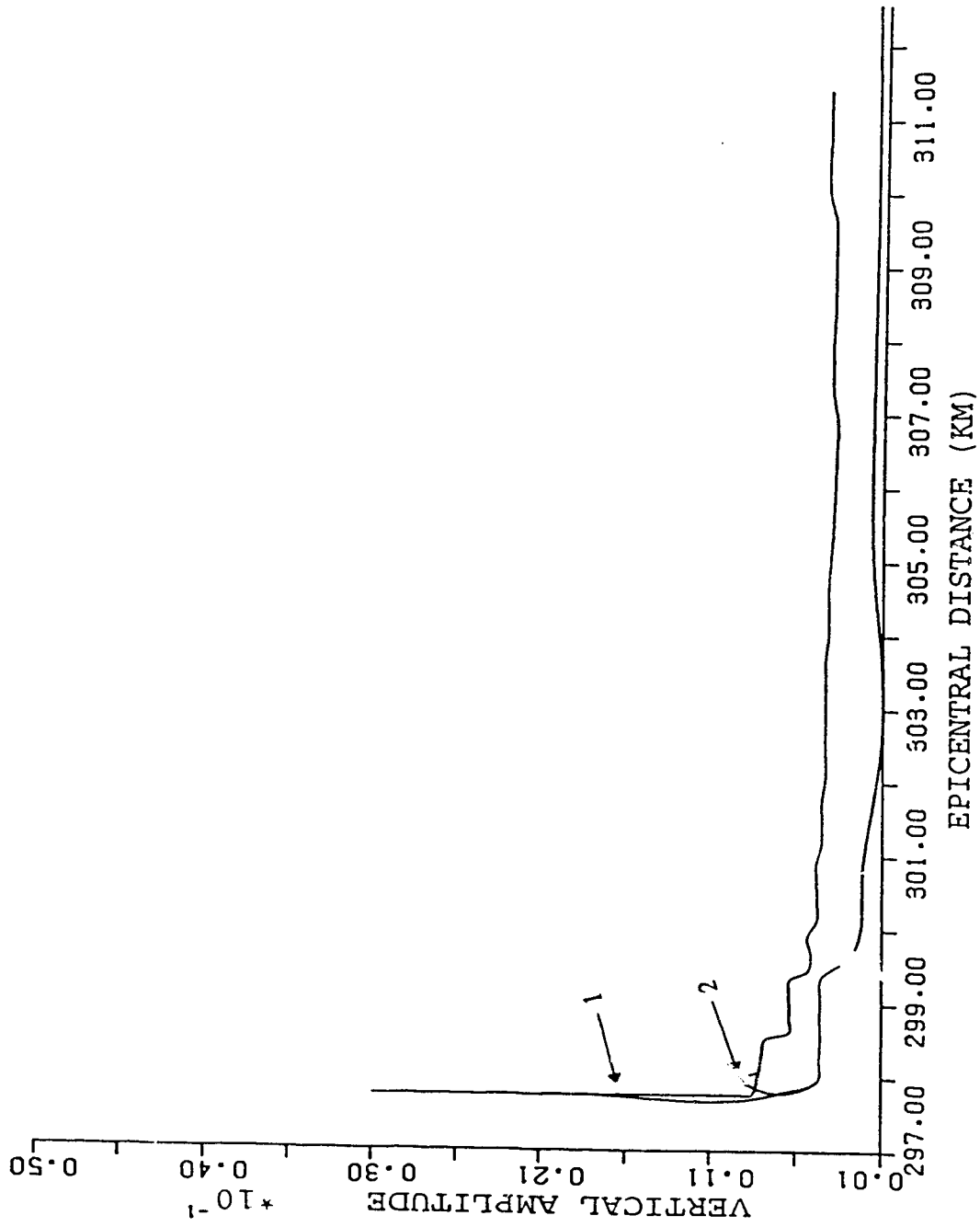


Figure 5.20 Amplitude - distance curve calculated by (1) the ray method and (2) the modified Airy approximation

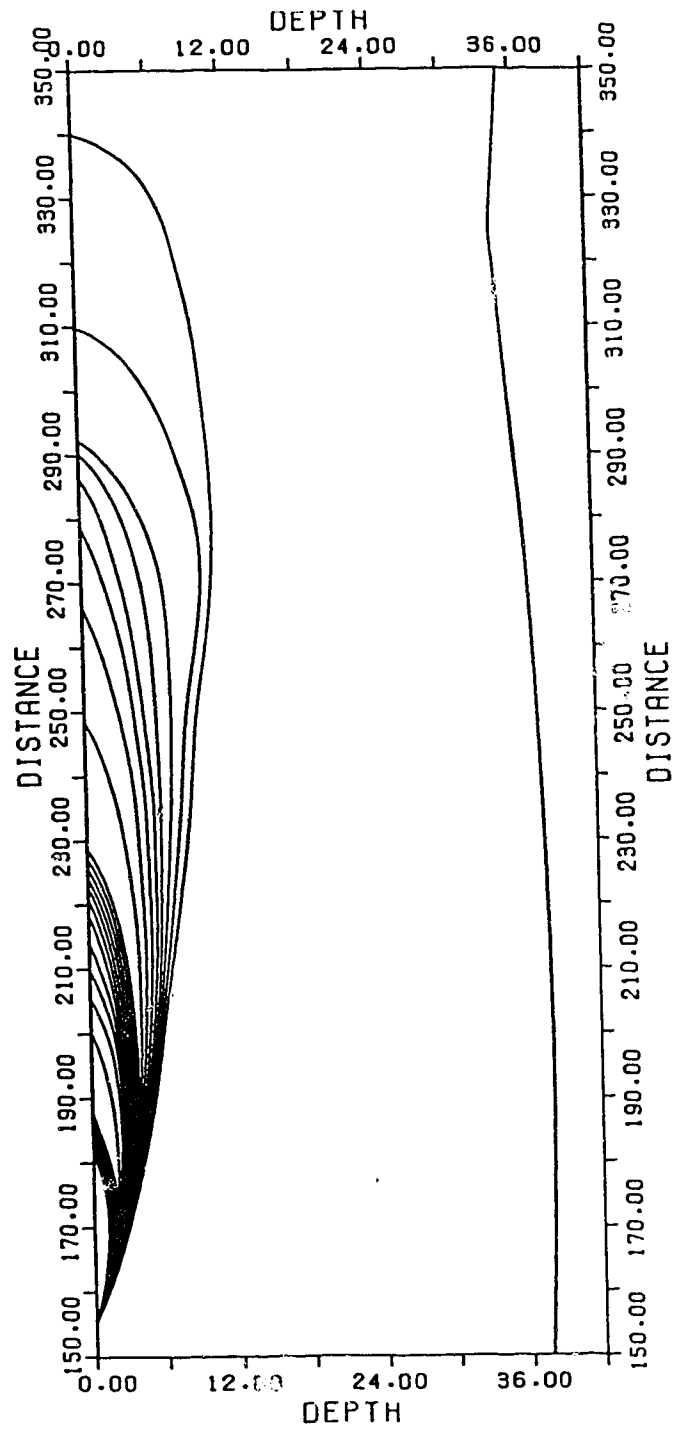


Figure S.21 Ray diagram with the take-off angle ranging from 74.60° to 81°

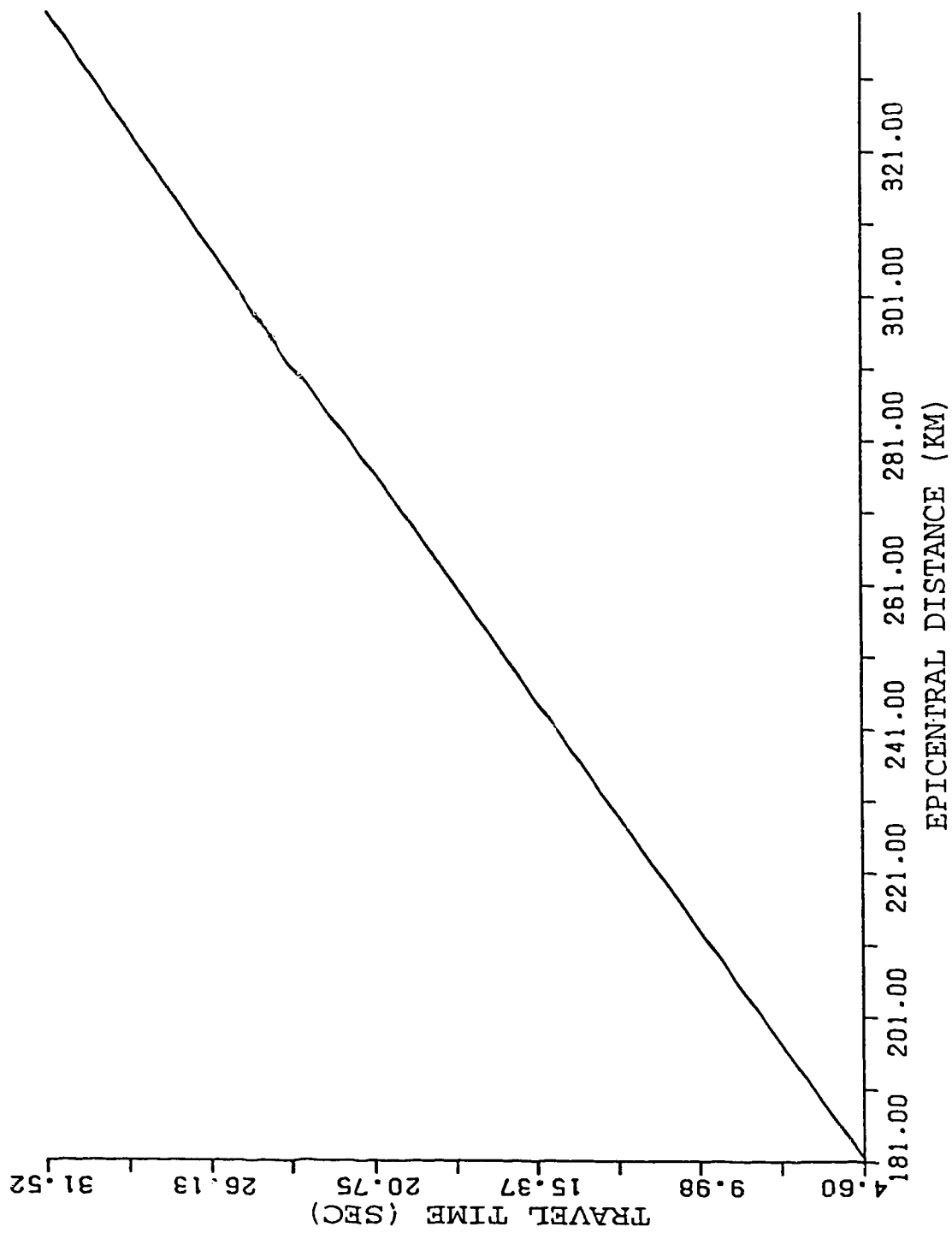


Figure 5.22 Travel time -distance curve for ray between 74.60° to 81°

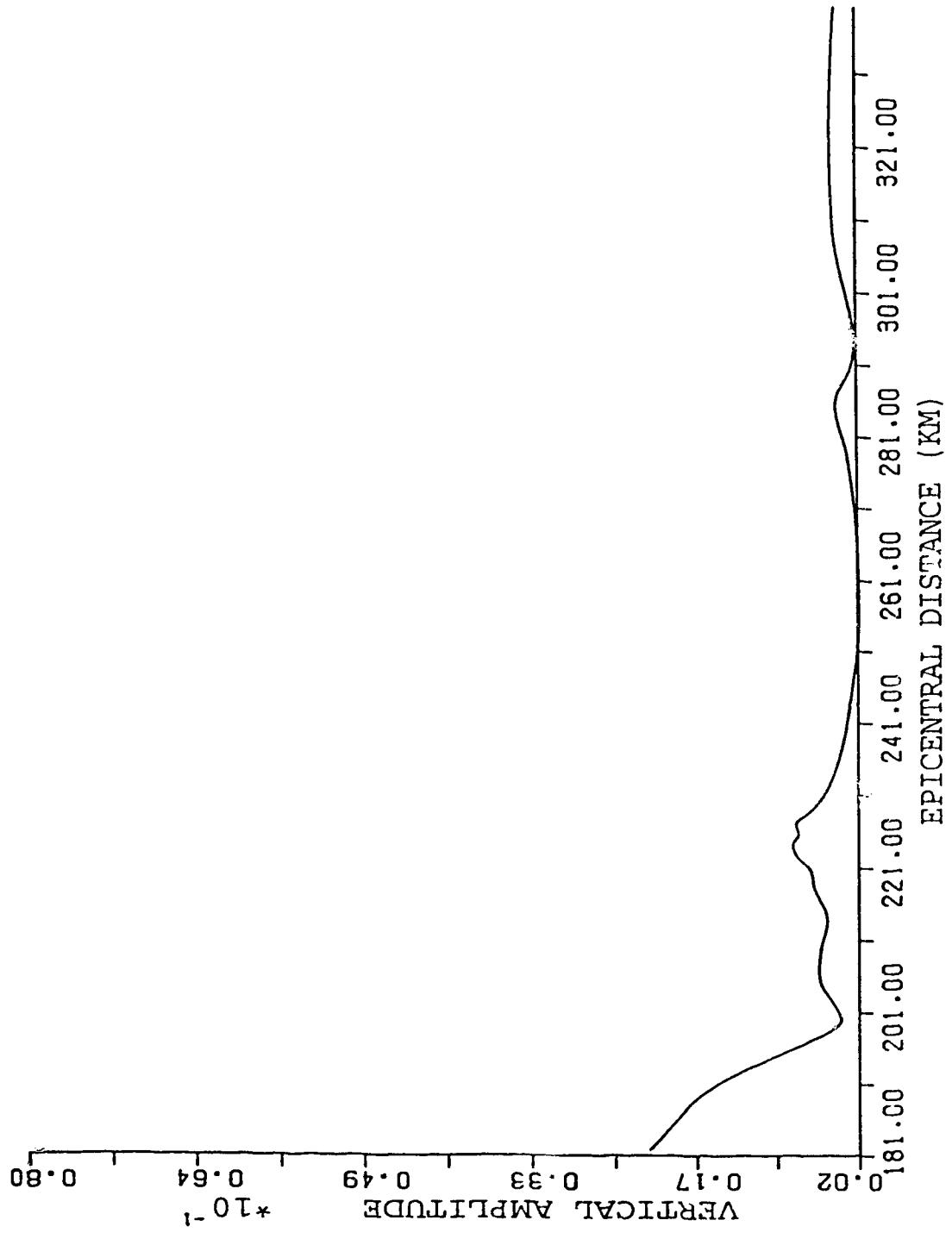


Figure 5.23 Amplitude - distance curve calculated by our ray method

5.5 Conclusions

From the discussion of previous chapters, the influence of different mesh sizes is reasonably small. The travel time found by this method is accurate for vertical inhomogeneous media and is reasonable well for inhomogeneous media compared with other methods. However, this method needs much less CPU time than other methods. The ray amplitude is also obtained using this method no matter there are caustics or not. Hence, the technique of circular approximation appears to be a reasonable accurate and efficient ray tracing method.

Although developed in two-dimensional media, it can be easily extended to three-dimensional media.

Reference

- Abramowitz, M. and Stegun, I., 1965, Handbook of mathematical functions: New York, Dover Publications.
- Asakawa, E. and Kawanaka, T., 1993, Seismic ray tracing using linear traveltimes interpolation, Geophysical Prospecting, V. 41, pp. 99-111
- Aki, K. and Richards, P. G., 1980, Quantitative Seismology: Theory and methods W. H. Freeman and Co.
- Alekseev, A. and Gel'chinskiy, B., 1959, On the ray method of computation of wave fields for inhomogeneous media with curved interfaces: Problems in the dynamic theory of propagation of seismic waves, Leningrad University, V. 3, pp. 107-160.
- Aric, K. and Gutdeutsch, R., 1978, Travel times and ways of elastic waves in a medium of two-dimensional velocity distribution: Pure and Applied Geophys.
- Babich, V. and Alekseev, A., 1958, Ray method of computing wave front intensities: Izvestiya, Academy of Sciences, USSR, Geophysics Series, V. 1, pp. 9-15.
- Brekhovskikh, L., 1990, Waves in layered media: New York, Academic Press.
- Cambridge University Press. Numerical recipes in FORTRAN, Cambridge Univ. Press.
- Cerveny, V. and Ravindra, R., 1971, Theory of seismic head waves, Toronto, University of Toronto Press.
- Cerveny, V. and Zahradnik, J., 1972, Amplitude - distance curves of seismic body waves in the neighborhood of critical points and caustics: Z. für Geophysik, V. 38, p. 9-19.
- Cerveny, V., Langer, J. and Psencik, I., 1974, Computation of geometrical spreading of seismic body waves in laterally inhomogeneous media with curved interfaces Geophys. J. R. astr. Soc. V. 38., pp. 9-19

- Cerveny, V., Molotkov, I. and Psencik, I., 1977, Ray method in seismology: Prague. Charles University Press.
- Cerveny, V. and Psencik, I., 1979, Ray amplitude of seismic body waves in laterally inhomogeneous media, *Geophys. J. R. astr. Soc.*, V. 57, pp. 97-106
- Cerveny, V. and Hron, F., 1980, The ray series method and dynamic ray tracing system for three dimensional inhomogeneous media, *B.S.S.A.* V. 70, pp.47-77.
- Cerveny, V. and Soares, J.,1992, Fresnel volume ray tracing,*Geophys.*,V.57,pp.902-915
- Chapman, C., 1978, Anew method for computing synthetic seismograms: *Geoph. J. R. Astr. Soc.*, V. 54, pp. 481-518.
- Chapman, C. and Drummond, R., 1982, Body-wave seismograms in inhomogeneous media using Maslov asymptotic theory, *BSSA*, V. 72, S227-S317.
- Chaman, C., 1985, Ray theory and its extensions: WKBJ and Maslov seismograms *J. Geophys.*, V. 57, pp. 27-43.
- Chen, K. and Ludwig, D., 1972, Calculation of wave amplitudes by ray tracing:*J. Acoust. Soc. Am.*, V. 54, pp. 431-436.
- Choi, A., and Hron, F., 1981, Amplitude and phase shift due to caustics: *B.S.S.A.* V. 71, pp. 1445-1461.
- Choy, G. and Richards, P., 1975, Pulse distortion and Hilbert transformation in multiply reflected and refracted body waves: *BSSA*, V. 65, pp. 55-70.
- Clarke, T. J., 1993, The complete ordered ray expansion-I calculation of synthetic seismograms, *Geophys. J. Int.*, V. 115, pp. 421-434.
- Daley, P. and Hron, F., 1992, Application of the ray-reflectivity method to multilayered thin bed structure, *BSSA*, V. 82, pp. 914-933.
- de Boor, Carl, 1978, A practical guide to splines, Springer-Verlag.

- Forsythe, G., Malcolm, M. and Moler, C., 1977, Computer methods for mathematical computations, Prentice-Hall.
- Fuchs, K. and Muller, G., 1971, Comparison of synthetic seismograms with the reflectivity method and comparison with observers, Geophys. J. R. astr. Soc. V. 23, pp. 417-433.
- Gardner, G., Gardner, L. and Gregory, A., 1974, Formation velocity and density: The diagnostic basis for stratigraphic traps: Geophysics, V. 39, pp.770-780.
- Gel'chinskiy, B. Y., 1961, Expression for the spreading function, Problems in the dynamic theory of seismic wave propagation, V. 5, Leningrad Univ. Press.
- Gilbert, F. and Backus, G., 1966, Propagator matrices in elastic wave and vibration problems, Geophys., V. 31, pp. 326-332.
- Green, A., 1976, Ray paths and relative intensities in one and two-dimensional models B.S.S.A., V. 66, pp. 1581-1607.
- Helmberger, D. and Harkrider, D., 1978, Modelling earthquakes with generalized ray theory, Modern problem in wave propagation, pp. 499-518, New York
- Hron, F. and Kanasevich, E.R. (1971), Synthetic seismograms for deep seismic sounding studies using asymptotic ray theory, BSSA, V. 61, PP. 1169-1200
- Hron, F., 1972, Numerical methods of ray generation in multilayered media: methods in computational physics, V. 12, pp. 1-34.
- Hron, F., 1973, A numerical ray generation and its application to the computation of synthetic seismograms for complex layered media: Geophys. J. R. astr. Soc. V. 35, pp. 345-349.
- Hron, M. and Chapman, C.H., 1973, Seismograms from Epstein transition zones, Geophys., J.R. astr. Soc., V. 37, pp. 305-322

- Hubral, P., 1979, A wave front curvature approach to the computing of ray amplitudes in inhomogeneous media with curved interfaces, *Studia Geophys., Geodaet., Ceskoslov* V. 23, pp.131-137
- Julian, B. Gubbins, D., 1977, Three-dimensional ray tracing: *J. Geophys., V.43*, pp. 95-113.
- Karal, F. and Keller, J., 1959, Elastic wave propagation in homogeneous and inhomogeneous media: *J. Acoust. Soc. Am.*, V. 31, pp. 694-705.
- Kim, W. and Cormier, V., 1990, Vicinity ray tracing: an alternative to dynamic ray tracing *Geophys. J. Int.*, V. 103, pp. 639-655.
- Kline, M. and Kay, I., 1965, *Electromagnetic theory and geometrical optics*: New York, Intersciences Publishers.
- Ludwig, D., 1966, Uniform asymptotic expansions at a caustic: *Comm. Pure Appl. Math.* V. 19, pp. 215-250.
- Marcinovskaya, N. and Krasavin, V., 1968, Algorithm for the calculation of reflected waves in media with curvilinear interfaces: problems in the dynamic theory of propagation of seismic waves, *Leningrad University*, V. 9, pp. 135-144.
- Marks, L. and Hron, F., 1978a, Ray tracing in complex media: Presented at the Workshop Meeting on Seismic Waves in Laterally Inhomogeneous Media, Liblice, Czechoslovakia
- Marks, L., 1980, Computational topics in ray seismology, Ph.D Thesis, University of Alberta
- Nettleton, L., 1940, *Geophysical prospecting for oil*: New York, McGraw - Hill.
- Sachs, D.A. and Silbiger, A. 1970, Focusing and refraction of harmonic sound and transient pulses in stratified media, *J. Acoust. Soc. Amer.*, V. 49, pp. 824-840

Sato, R., 1969, Amplitude of body waves in a heterogeneous sphere. Comparison of wave theory and ray theory: *Geophys. J. R. astr. Soc.*, V. 17, pp. 527-544.

Vidale, J., 1988, Finite-difference calculation of travel times, *BSSA*, V.78, pp. 2062-2076

Wesson, R., 1971, Travel-time inversion for laterally inhomogeneous crustal velocity models: *BSSA*, V. 61, pp. 307-316.

White, D., 1978, Ray theory for a wide class of sound speed profiles with two-dimensional variation: *J. Acoust. Soc. Am.*, V. 63, pp. 405-419.

Zhu, T. and Chun, K. Y., 1994, Understanding finite-frequency wave phenomena: phase-ray formulation and inhomogeneity scattering. *Geophys. J. Int.*, V. 119 pp. 78-90.

Appendix A

Approximation of interfaces by Parabolic Spline

A method of piecewise approximation of curvilinear interfaces by a group of smoothly linked parabolae was first suggested by Marciovskaya and Krasavin (1968). We shall present a modified form devised by Hron (personal communication) and used in his programs since 1973. It'll be presented briefly in this appendix.

Suppose that a set of M discrete points, Specified by their two-dimensional Cartesian coordinates $N_m = [\xi_m, \zeta_m]$, $m=1, \dots, M$, are given as points lying on a curvilinear interface. We may approximate this interface with the help of I parabolae

$$z(x) = (a_i x_i + b_i)x_i + c_i, \quad i=1, \dots, I \quad (\text{A.1})$$

each of them being defined over the interval $x \in [x_i, x_{i+1}]$. As continuity conditions, we impose

$$\begin{aligned} z_i(x_{i+1}) &= z_{i+1}(x_{i+1}) \\ \left. \frac{dz_i}{dx} \right|_{x_{i+1}} &= \left. \frac{dz_{i+1}}{dx} \right|_{x_{i+1}} \end{aligned}$$

The continuity of the curve that passes through all M points could be realized by solving the following linear system for the $(i+1)$ -th parabola given the i -th one:

$$\begin{bmatrix} x_{i+1}^2 & x_i & 1 \\ \xi_m^2 & \xi_m & 1 \\ 2x_{i+1} & 1 & 0 \end{bmatrix} \begin{bmatrix} a_{i+1} \\ b_{i+1} \\ c_{i+1} \end{bmatrix} = \begin{bmatrix} z_i(x_{i+1}) \\ \zeta_m \\ (2a_i + b_i)x_{i+1} \end{bmatrix} \quad (\text{A.2})$$

where $[\xi_m, \zeta_m]$ are coordinates of the closest input point for which $x_{i+2} = \xi_m > x_{i+1}$. However, if this system were solved for all $M-1$ pairs of adjacent points, considerable CPU time would be consumed and the surface would have a corrugated nature for some types of input data. The problem can be settled by allowing the curve to fall short of some input points by an arbitrarily specified distance. For this purpose, equation C.2 may be solved for some more distant points (iteratively, beginning with point M) and the $(i+1)$ -th parabola will be accepted if for any ε

$$\left| \frac{(a_{i+1}\xi_j + b_{i+1})\xi_j + c_{i+1} - \zeta_j}{\text{Max}(\zeta_j) - \text{Min}(\zeta_j)} \right| \leq \varepsilon$$

for

$$x_{i+1} < \xi_j < \xi_m$$

This method failed if the ζ_i are scattered over a large interval compared to the ξ_i interval. This will bring about the undesirable corrugated surface. In order to avoid this, we must modify the approach. First, a parabola is found that passes through N_i, N_{i+1}, N_{i+2} by solving the usual set of three linear equations for the coefficients $a_{i+1}, b_{i+1}, c_{i+1}$. Then the two predetermined parabolae $(a_{i\pm 1}, b_{i\pm 1}, c_{i\pm 1})$ will be united by an inserted parabola (a_i, b_i, c_i) . The right bound of the interval of definition of the i -th parabola is termed x_{i+1} and its left bound is $x_i = \xi_i - \Delta x$. The value Δx is selected iteratively to make the relation

$$x_i < \xi_i < x_{i+1} < \xi_{i+1}$$

to hold. The coefficients

$$\begin{aligned} a_i &= \frac{-2a_{i-1}x_i + 2a_{i+1}x_{i+1} - b_{i-1} + b_{i+1}}{2(x_{i+1} - x_i)} \\ b_i &= 2(a_{i+1} - a_i)x_{i+1} + b_{i+1} \\ c_i &= -(a_{i+1} - a_i)x_{i+1}^2 + c_{i+1} \end{aligned} \tag{A.3}$$

and the right bound

$$x_{i+1} = \frac{2(c_{i+1} - c_{i-1}) + (b_{i+1} - b_{i-1})x_i}{2(a_{i-1} - a_{i+1})x_i + (b_{i-1} - b_{i+1})} \quad (\text{A.4})$$

are the solutions of the following system algebraic equations (with x_i as a parameter)

$$a_{i-1}x_i^2 + b_{i-1}x_i + c_{i-1} = a_i x_i^2 + b_i x_i + c_i$$

$$2a_{i-1}x_i + b_{i-1} = 2a_i x_i + b_i$$

$$a_i x_{i+1}^2 + b_i x_{i+1} + c_i = a_{i+1} x_{i+1}^2 + b_{i+1} x_{i+1} + c_{i+1}$$

$$2a_i x_{i+1} + b_i = 2a_{i+1} x_{i+1} + b_{i+1}$$

Appendix B

Ray amplitude by wave method

We consider a perfectly elastic, isotropic medium in which the wave velocities and density are functions only of the vertical coordinate z . For symmetry in the solution, we consider an explosive source located at the point with cylindrical coordinate $(r, z, \phi) = (0, z_0, 0)$ and described by the following source function

$$P(r, z, t) = P_0(t) \frac{\delta(z - z_0) \delta(r)}{2\pi r}$$

Since the ray path in a vertically inhomogeneous medium is a plane curve, the azimuthal angle ϕ can be ignored. Within the medium, the equations of motion are

$$\nabla \cdot \bar{\bar{\sigma}} = \rho \frac{\partial^2 \bar{u}}{\partial t^2} - \bar{f} \quad (\text{B.1})$$

where the body force per unit volume is

$$\bar{f}(r, z, t) = -\nabla P(r, z, t)$$

and the stress dyadic $\bar{\bar{\sigma}}$ is

$$\bar{\bar{\sigma}} = (\lambda \nabla \cdot \bar{u}) \bar{\bar{I}} + \mu [\nabla \bar{u} + (\bar{u} \nabla)^T]$$

$\bar{\bar{I}}$ is unit dyadic and the superscript T indicates a transpose.

Equation B.1 can be considerably simplified if transformed coordinates are used.

We'll use the Fourier transform in time defined by

$$\begin{aligned} \bar{u}(r, z, \omega) &= \int_{-\infty}^{\infty} \bar{u}(r, z, t) e^{-i\omega t} dt \\ \bar{u}(r, z, t) &= \frac{1}{2\pi} \int_{-\infty}^{\infty} \bar{u}(r, z, \omega) e^{i\omega t} d\omega \end{aligned} \quad (\text{B.2})$$

and the zeroth-order Hankel transform in the cylindrical radius r defined by

$$\bar{u}(p, z, \omega) = \int_0^{\infty} \bar{u}(r, z, \omega) r J_0(\omega p r) dr$$

$$\bar{u}(r, z, \omega) = \omega^2 \int_0^{\infty} \bar{u}(p, z, \omega) p J_0(\omega p r) dp$$

With these transformations, the equations of motion and constitutive equations are reduced to a system of first order ordinary differential equations

$$\frac{d\bar{V}}{dz} = i\omega \bar{\bar{A}} \bar{V} + \bar{w} \quad (B.3)$$

where

$$\bar{V}^T = \left[\frac{-1}{pr} \frac{\partial(ru_r)}{\partial r}, \sigma_{zz}, i\omega u_z, \frac{-1}{i\omega pr} \frac{\partial(r\sigma_{rz})}{\partial r} \right] \quad (B.4)$$

are doubly transformed components of displacement and stress;

$$\bar{w}(p, z, \omega) = \left[0, -f_z, 0, \frac{1}{i\omega pr} \frac{\partial(rf_r)}{\partial r} \right] \quad (B.5)$$

are the doubly transformed force function; and the matrix $\bar{\bar{A}}$ is given by

$$\bar{\bar{A}} = \begin{bmatrix} 0 & 0 & p & \frac{1}{\mu} \\ 0 & 0 & \rho & p \\ \frac{p\lambda}{\lambda + 2\mu} & \frac{1}{\lambda + 2\mu} & 0 & 0 \\ \rho - \frac{4p^2\mu(\lambda + \mu)}{\lambda + 2\mu} & \frac{p\lambda}{\lambda + 2\mu} & 0 & 0 \end{bmatrix}$$

After Gilbert and Backus (1966), we will call the non-singular matrix $\bar{\bar{V}}$ a fundamental matrix of the differential system B.3, if it is a solution of the homogeneous form of the system, i.e. if each of its columns satisfies

$$\frac{d\dot{\mathbf{V}}}{dz} = i\omega\bar{\bar{\mathbf{A}}}\dot{\mathbf{V}} \quad (\text{B.6})$$

The propagator can be constructed from any fundamental matrix by

$$\bar{\bar{\mathbf{P}}}(z; z_0) = \bar{\bar{\mathbf{V}}}_f(z)\bar{\bar{\mathbf{V}}}_f^{-1}(z_0) \quad (\text{B.7})$$

Using the propagators, the solution of the homogeneous system B.6 can be easily expressed as

$$\dot{\mathbf{V}}(p, z, \omega) = \bar{\bar{\mathbf{P}}}(z; z_0)\dot{\mathbf{V}}(p, z_0, \omega) \quad (\text{B.8})$$

while that for the inhomogeneous system B.3 is

$$\dot{\mathbf{V}}(p, z, \omega) = \bar{\bar{\mathbf{P}}}(z; z_0)\dot{\mathbf{V}}(p, z_0, \omega) + \int_{z_0}^z \bar{\bar{\mathbf{P}}}(z; \xi)\bar{\mathbf{w}}(p, \xi, \omega)d\xi \quad (\text{B.9})$$

Thus we see that the basic problem in solving the equation B.1 is to find a fundamental matrix $\bar{\bar{\mathbf{V}}}_f$.

The matrix $\bar{\bar{\mathbf{A}}}$ has eigenvalues $\pm q_p$ and $\pm q_s$ where

$$q_p = \left(\frac{1}{v_p^2} - p^2 \right)^{\frac{1}{2}}; \quad q_s = \left(\frac{1}{v_s^2} - p^2 \right)^{\frac{1}{2}}$$

Then the corresponding normalized eigenvectors are

$$\dot{\mathbf{V}}_{\pm p}^{\Gamma} = \frac{1}{(2\rho q_p)^{\frac{1}{2}}} (-p, \mu\Gamma, \mp q_p, \pm 2\mu p q_p)$$

$$\dot{\mathbf{V}}_{\pm s}^{\Gamma} = \frac{i}{(2\rho q_s)^{\frac{1}{2}}} (\pm q_s, \pm 2\mu p q_s, -p, -\mu\Gamma)$$

where $\Gamma = q_s^2 - p^2$ and $i = (-1)^{\frac{1}{2}}$.

Let matrix $\bar{\bar{\mathbf{N}}} = \{ \bar{\mathbf{V}}_{+p}, \bar{\mathbf{V}}_{-p}, \bar{\mathbf{V}}_{+s}, \bar{\mathbf{V}}_{-s} \}$ and we can obtain

$$\overline{\overline{Q}} = \overline{\overline{N}}^{-1} \overline{\overline{A}} \overline{\overline{N}} = \begin{bmatrix} -q_p & 0 & 0 & 0 \\ 0 & q_p & 0 & 0 \\ 0 & 0 & -q_s & 0 \\ 0 & 0 & 0 & q_s \end{bmatrix}$$

Thus it follows that

$$\overline{\overline{N}}^{-1} \overline{\overline{A}} = \overline{\overline{Q}} \overline{\overline{N}}^{-1}$$

Using this relationship, the homogeneous system B.6 can be re-written as

$$\frac{d(\overline{\overline{N}}^{-1} \overline{\overline{V}})}{dz} = i\omega \overline{\overline{Q}} (\overline{\overline{N}}^{-1} \overline{\overline{V}}) + \overline{\overline{B}} (\overline{\overline{N}}^{-1} \overline{\overline{V}})$$

where

$$\overline{\overline{B}} = \frac{d\overline{\overline{N}}^{-1}}{dz} \overline{\overline{N}}^{-1}$$

Note that $\overline{\overline{B}}$ involves the derivatives of the elastic parameters and is one order in frequency lower than $i\omega \overline{\overline{Q}}$. Therefore, if the problem is such that the WKB conditions are satisfied, i.e., if the variations in the elastic parameters of the medium are small over a wavelength and that the solution is not required near turning points where either q_p or q_s vanishes, then we can ignore the term in $\overline{\overline{B}}$ and approximate the homogeneous system B.6 by

$$\frac{d(\overline{\overline{N}}^{-1} \overline{\overline{V}})}{dz} = i\omega \overline{\overline{Q}} (\overline{\overline{N}}^{-1} \overline{\overline{V}})$$

for which $e^{-i\omega \int_{-\infty}^z \overline{\overline{Q}}(\xi) d\xi}$ is a solution matrix.

Therefore, in the WKB approximation, a fundamental matrix of the elastodynamic equations B.3 is

$$\overline{\overline{V}}_f = \overline{\overline{N}} e^{-i\omega \int_{-\infty}^z \overline{\overline{Q}}(\xi) d\xi} \quad (\text{B.10})$$

To compute the synthetic seismograms along a ray, first, we need to calculate the wave in the source region which is regarded as homogeneous. Using B.5, B.7, B.10 and the radiation condition, we can obtain

$$\bar{V}^T(p, M_s, \omega) = \frac{i\omega P_0(\omega) e^{-i\omega \left| \int_{z_0}^{z_s} q_p(\xi) d\xi \right|}}{\pi v_p^2(z_0) (2\rho q_p)_{M_s}^{1/2} (2\rho q_p)_{M_0}^{1/2}} \cdot (p, -\mu\Gamma, -q_p, 2\mu\rho q_p) \quad (\text{B.11})$$

where $M_s = (r_s, z_s)$ denotes a point within the source region.

For the computation of synthetic seismograms, the particle displacement \bar{u} is desired. This can be obtained from the vertical displacement u_z by

$$\bar{u} = \frac{u_z}{(\bar{n} \cdot \bar{n}_z)} \bar{n}$$

where \bar{n}_z is unit vector in positive z direction and \bar{n} may be the direction of P or SV waves. Using this relation and the definition B.4 of \bar{V} , the source wave displacement at $M_s = (r_s, z_s)$ is

$$\bar{u}(p, M_s, \omega) = \frac{S(\omega)}{i\omega q_p(M_0)} \frac{\left[\left(\frac{\rho}{q_p} \right)^{1/2} \cos\theta \right]_{M_0}}{\left[\left(\frac{\rho}{q_p} \right)^{1/2} \cos\theta \right]_M} e^{-i\omega \left| \int_{z_0}^{z_s} q_p(\xi) d\xi \right|} \bar{n}_p \quad (\text{B.12})$$

where θ is the acute angle between \bar{n}_p and \bar{n}_z and

$$S(\omega) = \left[\frac{i\omega P_0(\omega) q_p}{2\pi\rho v_p^2 \cos\theta} \right]_{M_0}$$

is the spectrum of the source pulse.

Outside source region, wave propagation is described by the homogeneous system B.6. At any two points $M_1 = (r_1, z_1)$ and $M_2 = (r_2, z_2)$, the wave solutions are related through the propagator by B.8, i.e.

$$\vec{V}(p, M_2, \omega) = \overline{\overline{N}}(M_2) e^{-i\omega \int_{z_1}^{z_2} \overline{\overline{Q}}(\xi) d\xi} \overline{\overline{N}}^{-1}(M_1) \vec{V}(p, M_1, \omega) \quad (B.13)$$

Again, using the definition B.4 of \vec{V} , for a givening type of wave, say a downgoing P wave in our discussion, the complex amplitudes at the two points are related by

$$u(p, M_2, \omega) = \frac{G(M_1)}{G(M_2)} e^{-i\omega \int_{z_1}^{z_2} q_p(\xi) d\xi} u(p, M_1, \omega) \quad (B.14)$$

where

$$G = \left(\frac{\rho}{q_p} \right)^{1/2} \cos \theta \quad (B.15)$$

From B.11 and B.14, we can finally obtain the amplitude of a ray from source to receiver.

If there is a turning point, its effect can be represented by the reflection coefficient $e^{i\frac{\pi}{2}}$, i.e., B.14 is multiplied by $e^{i\frac{\pi}{2}}$ (Choi and Hron, 1981).

When a wave is incident upon an interface, it will either be reflected or transmitted and mode conversion can occur. The complex amplitude u_I of incident wave and the complex amplitude u_R of the reflected or transmitted wave are related through the plane wave reflection and transmission coefficients R (as given by Cervený and Ravindra 1971, section 2.3)

$$u_R = R u_I \quad (B.16)$$

Thus, starting with the source wave displacement B.12, the relations B.14, B.16 can be used to construct the particle displacement of an arbitrary ray which has gone through n turning points and suffered k reflections and transmissions at the points O_j , $j=1, \dots, k$, before reaching receiver point M . The particle displacement at M is

$$u(p, M, \omega) = (-1)^r \frac{S(\omega)G(M_0)}{i\omega q_p(M_0)G(M)} e^{-i\omega\psi(p) + i\pi \frac{\pi}{2}} \prod_{j=1}^k \frac{G(O_j^-)}{G(O_j^+)} R(O_j) \quad (\text{B.17})$$

Inverting the Hankel transform and keeping only the first term of the asymptotic expansion for the Hankel function (Abramowitz and Stegun 1965), from B.17, we obtain the solution in the frequency domain

$$u(M, \omega) = (-1)^r S(\omega) \left[\frac{\omega}{2\pi r} \right]^{\frac{1}{2}} e^{i\left(n\frac{\pi}{2} - \frac{\pi}{4}\right)} \int_{-\infty}^{\infty} f(p) e^{-i\omega\tau(p,r)} dp \quad (\text{B.18})$$

where $f(p)$, $\tau(p, r)$ and $\psi(p)$ are defined in Section 4.1.

Equation B.18 is the plane wave approximation of the WKBJ solution for the displacement amplitude of an arbitrary ray.